UNIVERSIDADE FEDERAL DO CEARÁ

CENTRO DE TECNOLOGIA

DEPARTAMENTO DE ENGENHARIA DE TELEINFORMÁTICA

PROGRAMA DE PÓS-GRADUAÇÃO EM ENGENHARIA DE TELEINFORMÁTICA

MESTRADO ACADÊMICO EM ENGENHARIA DE TELEINFORMÁTICA

NÍBIA SOUZA BEZERRA

INTERFERENCE AWARE RESOURCE ALLOCATION WITH QOS GUARANTEES IN MULTISERVICE OFDMA/SC-FDMA SYSTEMS

FORTALEZA

2013

NÍBIA SOUZA BEZERRA

INTERFERENCE AWARE RESOURCE ALLOCATION WITH QOS GUARANTEES IN MULTISERVICE OFDMA/SC-FDMA SYSTEMS

Dissertação apresentada ao Curso de Mestrado Acadêmico em Engenharia de Teleinformática do Programa de Pós-Graduação em Engenharia de Teleinformática do Centro de Tecnologia da Universidade Federal do Ceará, como requisito parcial à obtenção do título de mestre em Engenharia de Teleinformática. Área de Concentração: Sinais e Sistemas

Orientador: Prof. Dr. Tarcisio Ferreira Maciel

Coorientador: Prof. Dr. Vicente Angelo de Sousa Jr.

FORTALEZA

2013

Dados Internacionais de Catalogação na Publicação
Universidade Federal do Ceará
Biblioteca Universitária
Gerada automaticamente pelo módulo Catalog, mediante os dados fornecidos pelo(a) autor(a)

B469i Bezerra, Níbia Souza.
Interference aware resource allocation with QoS guarantees in multiservice OFDMA/SC-FDMA systems / Níbia Souza Bezerra. – 2013.
90 f. : il. color.

Dissertação (mestrado) – Universidade Federal do Ceará, Centro de Tecnologia, Programa de Pós-Graduação em Engenharia de Teleinformática, Fortaleza, 2013.
Orientação: Prof. Dr. Tarcisio Ferreira Maciel.
Coorientação: Prof. Dr. Vicente Angelo de Sousa Jr..

1. Cellular networks. 2. Quality of Service. 3. Radio Resource Allocation. 4. Intercell interference. 5. Resource Block aggregation. I. Título.

CDD 621.38

NÍBIA SOUZA BEZERRA

INTERFERENCE AWARE RESOURCE ALLOCATION WITH QOS GUARANTEES IN MULTISERVICE OFDMA/SC-FDMA SYSTEMS

Dissertation presented to the Academic Master's in Teleinformatics Engineering from the Graduate Program in Teleinformatics Engineering from the Technology Center from the Federal University of Ceará, as a partial requirement to obtain the master's degree in Teleinformatics Engineering. Concentration area: Sygnals and Systems.

Approved on: August 09th, 2013

EXAMINING BOARD

Prof. Dr. Tarcisio Ferreira Maciel (Supervisor)
Federal University of Ceará (UFC)

Prof. Dr. Vicente Angelo de Sousa Jr. (Co-supervisor)
Federal University of Rio Grande do Norte (UFRN)

Prof. Dr. Francisco Rafael Marques Lima
Federal University of Ceará (UFC)

Prof. Dr. André Noll Barreto
Federal University of Brasília (UNB)

Prof. Dr. Emanuel Bezerra Rodrigues
Federal University of Ceará (UFC)

To my father, José Ildegardo Bezerra, whose example led me to become an engineer. I love you dad.

ACKNOWLEDGEMENTS

I would like to thank my advisor, Tarcisio Maciel, for giving me the opportunity to conduct this thesis by him. Your constant support, guidance and patience have made this thesis possible. I also would like to thank my personal friend and co-advisor Vicente Sousa Jr., for the incredible help with the implementation, simulations and discussions about the results presented in this work. Special thanks to Rafael Lima, whose PhD thesis was the basis for the conduction of this thesis, as also for the support and discussions about the algorithms and the simulator. Many thanks also to all members of UFC.30 and UFC.33 projects, whose help and talks contributed immensely for my personal and professional growing. I should also mention my gratitude to Wireless Telecom Research Group (GTEL) and Ericsson Research for the opportunity to work with the most advanced technologies in the field of wireless communications, and for the financial support. Further thanks to FUNCAP for the financial support during the last year.

A special thanks goes to Mairton Jr., Eder Jacques, Juan Medeiros, David Souza, Diego Sousa and Rafael Guimarães for the hours spent studying for the classes, for the leisure time and for all the discussions about technical and not-so-technical problems. Without you guys this journey would have been harder.

Many thanks to my friend Kristofer Sandlund, for helping me reviewing my English and the technical parts of this thesis, as also for all the support during my stay in Luleå.

I would like to specially thank my parents, José and Delma, and my brothers, Ícaro and Petterson, for their blessings, support and being a constant source of inspiration. I also would like to thank them for the comprehension regarding my move to another city.

Last, but not least, a very special thanks to my husband, Benedito. Thanks for the love, care and understanding, mainly in the last few months. You are always here for me, and I'll be always here for you.

RESUMO

Com o aumento do número de assinantes de telefonia móvel em todo o mundo, e sabendo que grande parte desses assinantes possuem smartphones que estão constantemente conectados, novas tecnologias devem ser desenvolvidas de maneira a suprir a demanda por taxas de dados maiores. Para prover um bom serviço a esses usuários, algumas melhorias tecnológicas precisam ser implementadas. Nós podemos citar o desenvolvimento do padrão LTE-Advanced, que pode entregar até 3 Gbps de dados no downlink, e 1.5 Gbps no uplink, como sendo a tecnologia de ponta em relação ao provimento de altas taxas de dados em sistemas móveis de telecomunicação. Nesse novo cenário, o provimento de grandes quantidades de dados não é o único fator dominante. Deve-se também fornecer aos usuários um bom serviço, que pode ser medido por meio de QoS. Alguns esquemas de múltiplo acesso como OFDMA no enlace direto e SC-FDMA no enlace reverso, juntamente com uso de múltiplas antenas no transmissor e/ou no receptor, como MIMO, por exemplo, podem manter a QoS em níveis aceitáveis. Outra funcionalidade que também pode ser adicionada para melhorar o desempenho do sistema é a utilização de algoritmos de RRM. Esses algoritmos são utilizados de maneira a realizar a melhor alocação entre os recursos do sistema e os usuários, de forma que o sistema possa operar nos limites de sua região de capacidade. Seguindo o que foi previamente apresentado, o tema desta dissertação é a avaliação de algoritmos de gerência de recursos de rádio (RRM) – propostos em (LIMA *et al.*, 2012b; LIMA, 2012) e que maximizam a taxa total de um sistema celular enquanto satisfazem restrições de qualidade de serviço – em cenários sujeitos a interferência intercelular bem como sujeitos a novas restrições presentes em sistemas reais, como agregação de recursos de rádio no enlace direto e ajustes de potência de transmissão no enlace reverso. Assim, é nosso objetivo avaliar estes algoritmos de RRM em cenários mais realistas enquanto seu principal objetivo de maximizar a taxa total do sistema sujeito a restrições de qualidade de serviço ainda são atingidos. Em nossas avaliações, foram considerados esquemas com uma e com múltiplas antenas no enlace direto, enquanto esquemas com uma antena foram considerados no enlace reverso. Os resultados obtidos mostram que a interferência, a agregação de recursos e o ajuste de potência podem afetar significativamente o desempenho dos algoritmos de RRM caso não sejam adequadamente levados em consideração. Os resultados também mostram que é possível atenuar parte desse impacto dando aos algoritmos conhecimento adicional sobre a interferência no sistema.

Palavras-chave: Redes celulares. Qualidade de Serviço. Alocação de Recursos de Rádio.

Interferência Intercelular. Agregação de recursos. Ajuste de potência e satisfação

ABSTRACT

With the increasing growth of mobile subscribers all around the world, new technologies should be developed in order to fulfill the demand for higher data rates. Also, a considerable amount of subscribers own smart devices, which are constantly connected to the network, increasing the traffic on mobile networks. In order to provide those users with a good service, some technological improvements should be made. We can cite the development of the Long Term Evolution (LTE)-Advanced standard, which can provide peak data rates of 3 Gbps in the Downlink (DL) and 1.5 Gbps in the Uplink (UL), as one of the leading technologies related to high throughput in mobile networks. In this new scenario, not only it is important to deliver high amounts of data, but also to provide the User Equipments (UEs) with a good service, which can be measured by means of Quality of Service (QoS). Some multiple access schemes like Orthogonal Frequency Division Multiple Access (OFDMA) and Single Carrier - Frequency Division Multiple Access (SC-FDMA) together with multiple antennas techniques like Multiple Input Multiple Output (MIMO) can maintain the QoS at acceptable levels. Another functionality that can be used to improve the system performance is the use of efficient Radio Resource Allocation (RRA) algorithms. Those algorithms are used in order to perform the best possible allocation between the system resources and UEs, in a way that the mobile system can operate in the boundaries of its capacity region. Under the presented conditions, the focus of this thesis is to evaluate the RRA algorithms proposed in (LIMA *et al.*, 2012b; LIMA, 2012), which maximize cellular system total data rate, while satisfying QoS restrictions, in a scenario subject to intercell interference, also facing new restrictions available in real cellular systems, like Resource Block (RB) aggregation for the DL and power adjustment in the UL. Thus, we want to evaluate the Radio Resource Management (RRM) algorithms in a more realistic scenario, as we still want to assure that its main goal will be reached: maximize the system data rate subject to minimum satisfaction constraints per service. We performed the evaluation for the DL using single and multiple antennas schemes, while for the UL we used only the single antenna scheme. As main contributions of this work, we can emphasize modifications in the original Constrained Rate Maximization (CRM) algorithms in order to deal with inter-cell interference, the addition of RB aggregation restriction for the DL and the addition of a more realistic Link Adaptation (LA) and power adjustment in the UL. All those evaluations were performed through computational simulations.

Keywords: Cellular networks. Quality of Service. Radio Resource Allocation. Intercell interference. Resource Block aggregation. Power adjustment and satisfaction.

LIST OF FIGURES

LIST OF TABLES

LIST OF ACRONYMS

3G	3rd Generation
3GPP	3rd Generation Partnership Project
4G	4th Generation
AWGN	Additive White Gaussian Noise
BB	Branch and Bound
BLER	BLock Error Rate
BS	Base Station
CDF	Cumulative Distribution Function
CRM	Constrained Rate Maximization
CSI	Channel State Information
DFT	Discrete Fourier Transform
DL	Downlink
eNB	Enhanced Node B
EPA	Equal Power Allocation
FFT	Fast Fourier Transform
HARQ	Hybrid Automatic Repeat Request
HSPA	High Speed Packet Access
HTTP	HyperText Transfer Protocol
IFFT	Inverse Fast Fourier Transform
IID	Independent and Identically Distributed
ILP	Integer Linear Problem
IMT-A	International Mobile Telecommunications - Advanced
IP	Internet Protocol
ISI	Inter Symbol Interference
LA	Link Adaptation
LTE	Long Term Evolution
LTE-A	LTE - Advanced
MCS	Modulation and Coding Schemes
MIMO	Multiple Input Multiple Output
MISO	Multiple Input Single Output
MMSE	Minimum Mean Square Error
MRC	Maximum Ratio Combining
MRT	Maximum Ratio Transmission

MU-MIMO	Multi-User Multiple Input Multiple Output
MU	Multi-User
OFDM	Orthogonal Frequency Division Multiplexing
OFDMA	Orthogonal Frequency Division Multiple Access
PAPR	Peak-to-Average Power Ratio
PER	Packet Error Rate
QoS	Quality of Service
RB	Resource Block
RBG	Resource Block Group
RRA	Radio Resource Allocation
RRM	Radio Resource Management
SC-FDMA	Single Carrier - Frequency Division Multiple Access
SDO	Standards Development Organization
SINR	Signal to Interference-plus-Noise Ratio
SISO	Single Input Single Output
SIMO	Single Input Multiple Output
SNR	Signal to Noise Ratio
SU	Single-User
SVD	Singular Value Decomposition
TDMA	Time Division Multiple Access
TTI	Transmission Time Interval
UE	User Equipment
UL	Uplink
URM	Unconstrained Rate Maximization
WiMAX	Worldwide Interoperability for Microwave Access
ZMCSCG	Zero Mean Circularly Symmetric Complex Gaussian

CONTENTS

1 INTRODUCTION

This chapter presents the motivation for this thesis in Section 1.1. Section 1.2 brings some important concepts used during the development of this work, while in Section 1.3 we present the state of the art. We finish this chapter presenting the objectives, goals and the scientific production resulting from this thesis in Section 1.4.

1.1 Motivation

With the increase in the availability of new devices which allow wireless communications, the demand for mobile communication services has substantially grown. It is estimated that, in 2013, there are almost as many mobile services subscriptions as people in the world, with the world population estimated in 7.1 billions, as the amount of subscriptions reaches 6.8 billions (ITU, 2013). With this quantity of UEs and the case of wireless network access, metrics as higher data rates and QoS have become key points for the development of new technologies. In order to coordinate this development, the 3rd Generation Partnership Project (3GPP) together with other Standards Development Organizations (SDOs) have been working on the development of new technologies, such as LTE - Advanced (LTE-A) (DAHLMAN *et al.*, 2011; WANNSTROM, 2013), whose focus is on higher system capacity, like the increase in peaks data rates for both DL and UL, higher spectral efficiency, among others. All those features should be compliant with what was defined by the International Mobile Telecommunications - Advanced (IMT-A) (ITU-R, 2008).

As the system load constantly increases, it is also necessary to maintain the service at good level. With more UEs in the system, the data traffic increases, which can affect considerably the QoS, presented to the UE as higher transmission data rates, drop call rates, mobile device usage time and service integration. All these QoS characteristics can be mapped into important performance metrics, necessary to assure the viability of a communication system, such as channel capacity, BLER, UE satisfaction, Peak-to-Average Power Ratio (PAPR), SINR and so on. The provisioning of good values for these performance metrics is one of the concerns of the mobile operators, and also of the telecommunications industry as a whole.

In order to provide the system with better QoS, some actions were taken by different standardization groups, like changes in the network core, with the adoption of an all-Internet Protocol (IP)-based core network, capable of supporting high data throughput (BHALERO, 2010).

This architecture utilizes a packet-switched network technology, which uses available capacity much more efficiently and minimizes the risk of possible problems, such as disconnection, and is also compliant with any IP-based device available in the market (GHADERI; BOUTABA, 2007).

Another action taken in order to enhance the network capabilities was done in the radio layer. The adoption of advanced multiple access techniques is one of those improvements. Orthogonal Frequency Division Multiplexing (OFDM) is a multicarrier modulation firstly presented as patent (NOKIA BELL LABS, 1970), where an orthogonal set of multicarriers is selected, achieving high spectral efficiency due to their spectrum overlap. From this technique, the OFDMA was defined. OFDMA is a multiple access scheme which allocates an orthogonal subcarriers subset per UE, allowing multiuser diversity and simplifying the processing at the receiver. This scheme is nowadays used in the 4^{th} Generation (4G) systems, like LTE/LTE-A (PARKVALL *et al.*, 2011) and Worldwide Interoperability for Microwave Access (WiMAX) (GHOSH *et al.*, 2005). However, the use of OFDMA in the UL is not recommended, because it can lead to a possible frequency shift between the subcarriers, which can cancel the orthogonality as also increase the signal fluctuations, incurring in high PAPR levels. To overcome those issues, the SC-FDMA was adopted to be used in LTE/LTE-A UL. SC-FDMA pre-process the transmitted signal, allocating contiguous groups of subcarriers to the UEs, thus reducing the PAPR (MYUNG *et al.*, 2006).

Together with the multiple access techniques, it is also possible to use multiple antennas at both receiver and transmitter. The use of multiple antennas, like MIMO is mandatory for the 4G systems. MIMO allows the exploitation of the spatial dimension, improving the system spectral efficiency (SESIA *et al.*, 2011), and it can also improve the robustness of wireless links.

Although the use of multiple access techniques together with MIMO can improve the system efficiency, it is also necessary a mechanism that can allocate the available resources in a efficient way. RRA algorithms are responsible for the assignment of frequency/time resources in the most efficient way, in order to guarantee that the system will operate in the boundaries of its capacity region (ZHANG *et al.*, 2006). By doing that, these algorithms can maintain QoS metrics at acceptable levels, allowing the UEs to have their satisfaction constraints fulfilled.

Even using a combination of different techniques in order to increase the system capacity in a scenario with multiple cells, it is common that some kind of interference occurs. The interference can degrade the system performance, and also can cause losses in the data that

has been exchanged between the transmitter and the receiver. To overcome this negative impact caused by interference, one solution would be to make the RRA algorithm aware of it. Giving this knowledge to the RRA algorithm can allow it to handle the interference before the allocation process, thus mitigating any damage due to it (ALMALFOUH; STUBER, 2011).

1.2 Background

We will present some of the important concepts used during the writing of this thesis. In the following sections we will present the multiple antennas techniques, as also an explanation about OFDMA and SC-FDMA, QoS, RRA and interference in wireless systems.

1.2.1 Multiple Antennas Techniques

The invention of MIMO systems occurred in the mids 1990s (PAULRAJ; KAILATH, 1994), but it was only in the last years that most of the progress related to this technique took place.

The first standard to adopt MIMO in a cellular mobile network was the High Speed Packet Access (HSPA) Release 7 (HOLMA *et al.*, 2007). This opened opportunities for the development of new technologies, among which we can mention LTE, which was the first mobile network whose standard has MIMO as one of the key points to its development.

While with SISO we can only exploit time and frequency dimensions, the adoption of multiple antennas at the transmitter and/or receiver opens an extra dimension to signal transmission, the space dimension, which can increase the gains in throughput as also in some other system metrics.

Due to the different amount of possible antennas at the transmitter/receiver sides, we can classify the multiple antennas schemes in three different types:

- Single Input Multiple Output (SIMO), where the transmitter has a single antenna and the receiver has multiple antennas;
- Multiple Input Single Output (MISO), where the receiver has a single antenna and the transmitter has multiple antennas;
- Multiple Input Multiple Output (MIMO), where both transmitter and receiver have multiple antennas.

Among those methods, MIMO is the one which presents three main advantages over

SISO: diversity gain, which is the mitigation of the multipath effect; array gain, which is the spatial version of the matched-filter gain in time domain receivers, and spatial multiplexing gain, which is the ability to send multiple data streams in parallel and to separate them based on their spatial signature.

All the aforementioned multiple antennas techniques can be combined with some multiple access methods in order to increase system performance. We present some of those multiple access methods in the next section.

1.2.2 Multiple Access Methods

Multiple access methods are used together with multiple antennas techniques, allowing an increase in the system performance. For the DL, we used OFDMA, which is introduced in Section 1.2.2.1 , while for the UL we adopt SC-FDMA, explained in Section 1.2.2.2.

1.2.2.1 OFDMA

Regarding multiple access methods, OFDMA is the one being largely used in the newer mobile cellular systems, as it achieves higher transmission data rates and mitigates multipath fading effects in the channel. OFDMA derives from OFDM, which splits the frequency band into several subcarriers, by the use of Inverse Fast Fourier Transform (IFFT), where the spacing between subcarriers makes them orthogonal to each other. However, OFDMA signal presents large fluctuations in the signal envelope, resulting in high PAPR values.

The minimum available resource to be allocated to a UE in LTE is called RB. The RB is composed by a specific number of adjacent subcarriers in the frequency dimension and a number of consecutive OFDM symbols in time dimension (3GPP, 2013). In Single-User (SU) systems that employ OFDMA, a RB can only be allocated to a UE at time. Figure 1 shows the frequency-time resource grid for OFDMA.

1.2.2.2 SC-FDMA

Due to the high PAPR values resulting from OFDMA, SC-FDMA was the choice to be used in the UL for LTE. SC-FDMA is a pre-coded version of OFDMA, because a Discrete Fourier Transform (DFT) is executed before the IFFT performed for OFDMA, and has a lower PAPR in comparison to OFDM, which results in a reduction of battery consumption, requires a

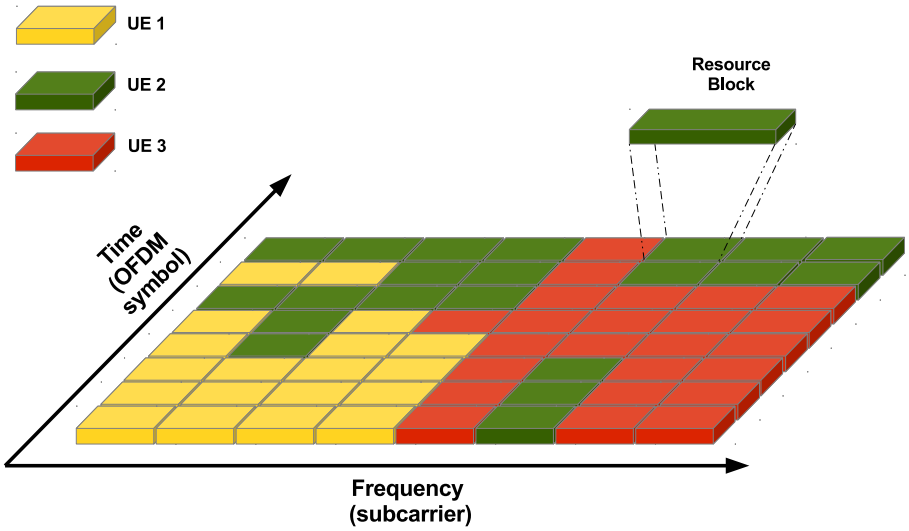

Figure 1 – OFDMA frequency-time representation.

simpler amplifier design and improves uplink coverage and cell-edge performance (MYUNG *et al.*, 2006).

Different from OFDMA, SC-FDMA performs the transmission only on consecutive subcarriers. This means that the RBs must be assigned in a consecutive way in the frequency domain to the UEs. Figure 2 shows an example of the RB allocation in SC-FDMA.

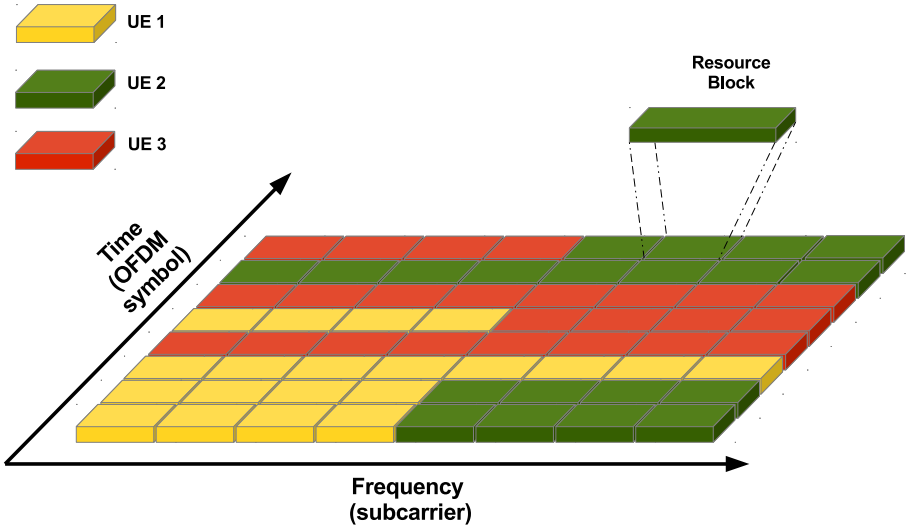

Figure 2 – SC-FDMA frequency-time representation.

1.2.3 QoS and UE Satisfaction

As the load of the cellular networks increases, the service providers must guarantee QoS for their UEs. Metrics as data rate, latency and Packet Error Rate (PER), the fulfillment of the required data rate of a specific amount of UEs can be taken as QoS indicators (3GPP, 2013).

The main goal of QoS is to allow the network to deliver predictable results (CALABRESE, 2009) and in order to maintain the system QoS at acceptable levels, the service providers should have some mechanism capable of constantly monitoring the system performance. This could be named as QoS management feature, which is responsible for constantly keeping track of the system QoS.

As previously said, fulfilling the data rate requirement of a specific amount of UEs can be taken as a QoS indicator. In (LIMA *et al.*, 2012b) this was the author's metric to be used as the QoS indicator. He proposed an algorithm that allocates resources to the UEs while it guarantees that those UEs will be served with a specific minimum data rate.

1.2.4 Radio Resource Allocation

RRA is the operation responsible for the allocation of the available resources in the network to the UE on it. A resource can be defined as frequency bandwidth, power, time slots or any other asset available to be allocated to the UEs.

Most of the available RRA algorithms try to solve the allocation problem restricted to some constraints related to data rate, for example, in order to maintain UEs' QoS. In current communications systems, the use a good RRA algorithm can mean an efficient RRA, which can increase the system capacity.

1.2.5 Interference in Wireless Systems

Cellular system capacity is essentially limited by interference, not by noise. Also, the interference depends on the amount of UEs in the cells, and it is time varying. Network coverage and data throughput can be severely impacted by interference.

Figure 3 presents a scenario where a UE is subject to interference in the DL direction. We can see in this picture that the UE of interest (inside the dark shaded cell) is subjected to interference coming from the the Base Stations (BSs) in the interfering cells (light shaded ones). This is caused by the frequency reuse within the cluster, and it can cause losses in the data

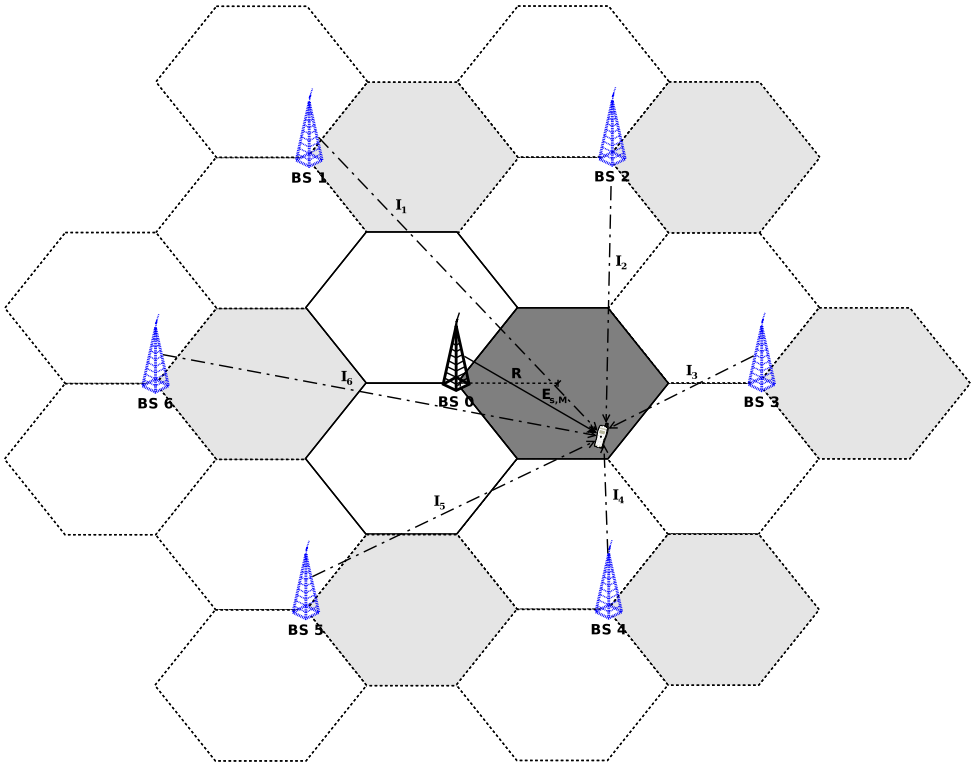

Figure 3 – Interference in a single antenna cellular network, for the DL direction.

transmission.

In order to mitigate the interference, some techniques can be employed, like the use of spatial diversity and linear spatial filtering with the employment of multiple antennas. If it is possible, providing both communication ends with perfect Channel State Information (CSI) can also contributes with the interference mitigation.

1.3 State of the Art

Interference in multi-cellular networks has been a subject of great interest in the last 15 years.

Performing evaluations for the DL, in (LÓPEZ-PÉREZ *et al.*, 2012) the authors proposed a dynamic frequency and power allocation algorithm for the DL of OFDMA-based networks, whose goal was to minimize the total DL transmission power, while the UEs data rate requirements were maintained at acceptable levels. The same authors proposed in (LÓPEZ-PÉREZ *et al.*, 2013) a distributed and coordinated RRA algorithm capable of the use of frequency reuse patterns in a way that the inter-cell interference could be mitigated, as also the DL transmit power could be minimized. They executed that by performing an intelligent and self-adaptable power allocation in each RB assigned to a UE.

Still in the DL, (YU *et al.*, 2013) proposed a RRA algorithm capable of maximizing the overall throughput of UEs at the cell border, while maintaining the required throughput for the UEs in the center of the cell, in a scenario subject to inter-cell interference.

Studying inter-cell interference coordination, in (KOSTA *et al.*, 2013) the authors present an overview of interference avoidance through inter-cell interference coordination. They presented a set of mechanisms used to deal with inter-cell interference. In (RAHMAN; YANIKOMEROGLU, 2010) the problem of inter-cell interference coordination is also studied, but the authors formulated the interference coordination problem as an Integer Linear Problem (ILP).

Regarding the UL, the authors in (FRANK *et al.*, 2010) proposed an interference-aware joint scheduling scheme based on proportional fairness for LTE, while (HOSEIN, 2010) investigates the issues of power allocation and interference management for the LTE UL with applications that must maintain a certain QoS level to the UEs. In (LI *et al.*, 2011) an investigation of power control and resource allocation for the UL is performed and (FAN *et al.*, 2012) presents a distributed joint optimal algorithm which maximizes the system weighted throughput, while avoiding the inter-cell interference in the system. In (DECHENE; SHAMI, 2011) an energy-efficient resource allocation for the UL with synchronous Hybrid Automatic Repeat Request (HARQ) constraints is proposed.

In (WESEMANN *et al.*, 2012) the authors developed a decentralized inter-cell interference coordination method in order to perform a fair resource allocation in large-scale networks. In this work, they performed evaluations in the UL direction, where their inter-cell interference coordination scheme objective was to provide the greatest possible fairness among the UEs, by allowing that all UEs acquire the same data rate.

In (LIMA *et al.*, 2012b; LIMA *et al.*, 2012a; LIMA, 2012), the authors presented RRA algorithms for both DL and UL directions, and they compared their approach to solutions available in literature. However, in those works, the authors simulated a single cell scenario, thus without inter-cell interference.

In this thesis we will evaluate the algorithms presented in (LIMA *et al.*, 2012b; LIMA *et al.*, 2012a; LIMA, 2012) in a scenario subject to interference, when the algorithms are and when they are not aware of the interference in the system. We also decided to evaluate the DL solution when there is RB aggregation, as also the UL solution subject to some power limitations. Those evaluations were not done by the authors in (LIMA *et al.*, 2012b; LIMA *et al.*,

2012a; LIMA, 2012).

Although in (LIMA, 2012) the author proposed RRA algorithms for the DL for both SU and Multi-User (MU) cases, in this work we decided to evaluate only the solutions proposed to the SU case.

1.4 Objectives, Contributions and Scientific Production

We present the objectives, contributions and the organization of the thesis in section 1.4.1, and the scientific production resulting from this thesis in section 1.4.2.

1.4.1 Objectives, Contributions and Thesis Organization

As main contributions of this work, we can emphasize:

- Modifications in the original CRM algorithms in order to deal with inter-cell interference,
- The addition of RB aggregation restriction for the DL,
- The addition of a more realistic LA and power adjustment in the UL.

In Chapter 2 we present the system model adopted during the development of this work. In this same chapter we introduce the CRM problem and we present a general suboptimal framework used to solve this problem. We also show how we modeled the interference and we present the different types of RB aggregation available in the 3GPP standard. The objectives of this chapter are to present the scenarios in which we performed our simulations, as also to explain some of the issues we want to investigate together with the RRA algorithms presented in (LIMA *et al.*, 2012b; LIMA, 2012).

Chapter 3 presents the suboptimal algorithm for the CRM problem for the DL. The main objective of this chapter is to show how we modified the RRA algorithm for the DL presented in (LIMA *et al.*, 2012b; LIMA, 2012) in order to deal with interference and evaluate those algorithms in a scenario subject to interference and RB aggregation, for the cases when the algorithm has and has not knowledge about the interference in the system.

Chapter 4 presents the suboptimal algorithm for the CRM problem for the UL. The main objective of this chapter is to show how we modified the RRA algorithm for the UL presented in (LIMA *et al.*, 2012b; LIMA, 2012) and to evaluate the proposed suboptimal algorithm in a scenario subject to interference, for the cases when the algorithm has and has not knowledge about the interference in the system. As contributions of this chapter we can

mention the addition of LA in our UL scenario, thus allowing the performance evaluation in a more realistic scenario, as also the addition of a very simple power limitation, instead of using Equal Power Allocation (EPA).

In Chapter 5 we pinpoint the main conclusions obtained during the development of this work. We also present some aspects that can be further modeled and investigated together with the suboptimal solution for the CRM problem for both DL and UL.

1.4.2 Scientific Production

Some of the results presented in Chapter 3 were published as follows:

- Lima, F. R. M.; **Bezerra, N. S.**; dos Santos, R. B.; Maciel, T. F.; Freitas, W. C.; Cavalcanti, F. R. P., "*Maximizing Spectral Efficiency with Acceptable Service Provision in Multiple Antennas Scenarios*". European Wireless Conference, 2012.
- *Method and Apparatus for Resource Allocation Achieving Minimum Required Data Rate Guarantees in SC-FDMA Uplink*, US Patent application supported by Ericsson.

At the time of writing, we are working in the publication of the contents in Chapters 3 and 4.

During the Master's course, initiated on the second semester of 2011, the author published some other works also related to wireless cellular networks. They are listed in the following:

- Abinader Jr., F. M.; Sousa Jr., V. A.; Fernandes, A. S. B.; D'Assunção, A. G.; **Bezerra, N. S.**; Lozada G.; Orava, P., "*Evaluation of Joint Sleep and Idle Mode in IEEE 802.16e WiMAX*". International Journal of Computer Science Issues, Vol. 9, Issue 2, 2012.
- Abinader Jr., F. M ; Sousa Jr., V.A. ; D'assunção, A. G. ; Fernandes, A. B. ; **Bezerra, N. S.**; Lozada, G.; Orava P., "*Performance of Power Saving Modes in IEEE 802.16e System*". The 76th IEEE Vehicular Technology Conference, 3-6 September, 2012, Quebec.
- Cavalcante, A. M.; Souza, E. B.; Bazzo, J. J.; **Bezerra, N. S.**; Pontes, A.; Vieira, R. D., "*A Pedometer-Based System for Real-time Indoor Tracking on Mobile Devices*". XXIX Simpósio Brasileiro de Telecomunicações, 2011.

2 SYSTEM MODELING, GENERAL PROBLEM AND FRAMEWORK FOR SOLUTION

This chapter presents the system modeling and the main characteristics of this work. In Section 2.1 we present the system model and the main parameters used along this work. Section 2.2 introduces the suboptimal solution used to solve the CRM problem, while Section 2.3 shows the interference model considered in this work. Section 2.4 presents the RB aggregation procedure.

2.1 System Modeling

We consider a multiuser system composed by B sectored cells, as shown in Figure 4. As it can be seen, we have tri-sectored cells where the BS $b = 1$ is the BS of interest, i.e., the BS that serves all the UEs in the system and $b = 2, \cdots, 7$ represent the interfering BSs. The darker shaded sector represented in the figure is modeled in the system as the sector of interest, where all the UEs are positioned and which is subject to interference.

The UEs are uniformly distributed within the darker shaded sector presented in Figure 4, and are served by the BS $b = 1$. The UEs set is represented by $\mathscr{J}$, where $j = 1, \cdots, J$ are the UEs in the system.

The other BSs are virtual BSs, as also their interfering sectors (the lighter shaded ones). These sectors are only modeled to account for interference, and the sectors in white are not modeled in our system. This system model tries to follow the 3GPP's Case 1 and Case 3 scenarios (3GPP, 2006; 3GPP, 2010a), thus, we have a LTE-like system.

We consider downlink and uplink directions, as also single and multiple antenna scenarios. For downlink, we consider the system working with OFDMA and Time Division Multiple Access (TDMA) and for the uplink the system employs SC-FDMA and TDMA.

For the downlink case, OFDMA has been chosen by most 4G wireless systems, such as the 3GPP systems, due to its high performance and flexibility. OFDMA allows to allocate a subset of orthogonal subcarriers for each UE and so to exploit multiuser diversity. Moreover, due to the high granularity of the subcarriers, services with different rates can be accommodated by allocating different number of resources to each UE.

For the uplink, OFDMA is not a good choice due to the possible frequency deviations among subcarriers, which can ruin the orthogonality, as well as it can present high signal fluctuations among subcarriers leading to an increase in the PAPR levels. High PAPR values con-

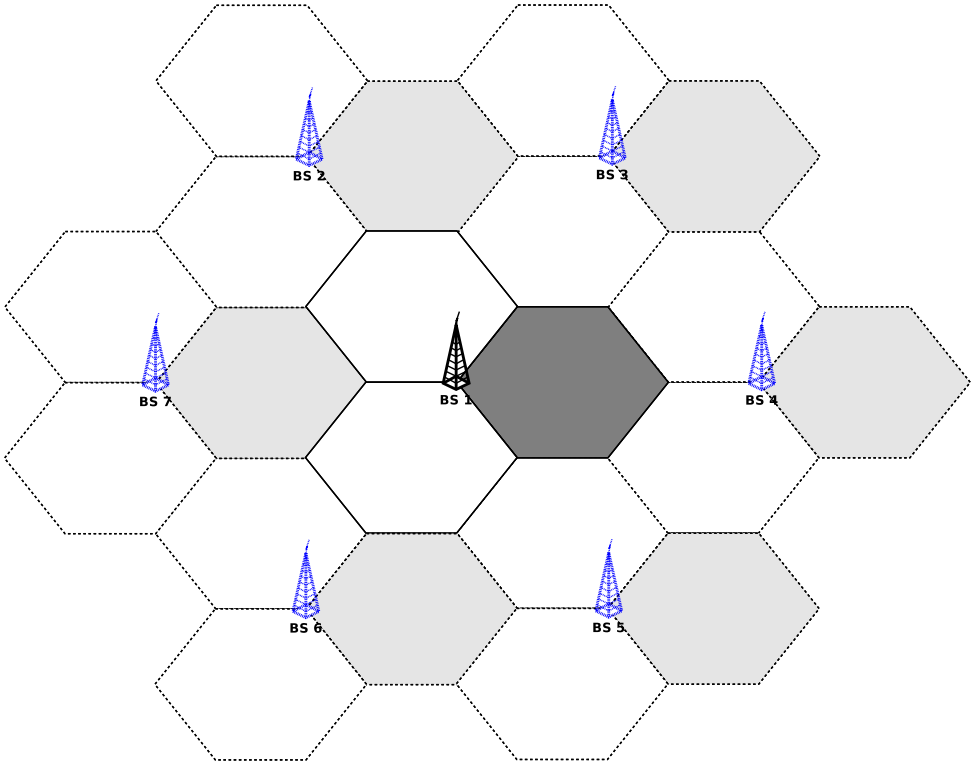

Figure 4 – Cellular network.

siderably difficult the project of amplifiers for the UEs. To overcome these issues, some schemes derived from OFDMA were implemented, among them the one known as SC-FDMA (MYUNG *et al.*, 2006). SC-FDMA performs a pre-processing of the transmitted signal using a DFT and allocates contiguous groups of subcarriers to each UEs, leading to lower PAPR and simplifying the amplifiers' design for the UEs. This scheme is adopted by the 3GPP systems in the uplink direction. Since 3GPP systems are consolidating their path among the 3rd Generation (3G) and 4G systems, we decided to try to follow 3GPP's scenarios during our simulations.

Both OFDMA and SC-FDMA schemes are based on OFDM, which can be efficiently implemented by using the Fast Fourier Transform (FFT).

The minimum available resource to be allocated to a UE is called RB. The RB is composed by a specific number s of adjacent subcarriers ($s \in \{1, \cdots, S\}$) in the frequency dimension and a number o of consecutive OFDM symbols in time dimension, where $o \in \{1, \cdots, O\}$, which correspond to a Transmission Time Interval (TTI). In the system the RBs are identified by the index $r \in \{1, \cdots, R\}$, which is determined by the system and subcarrier bandwidths (3GPP, 2012).

The propagation model in our system includes a distance-dependent path loss model, a log-normal shadowing component and a fast fading component.

The path-loss follows the model proposed in (PARKVALL *et al.*, 2008) for macrocell

system simulation. Considering $F = 2$ GHz as the carrier frequency, the path-loss equation L_p in dB as a function of the distance d in meters is presented as follows:

$$L_p = 35.3 + 37.6 \log_{10}(d). \tag{2.1}$$

The slow fading (shadowing) follows a log-normal distribution, with mean equal to zero and standard deviation equal to σ_s according to the model in (3GPP, 2007). No spatial correlation for shadowing is considered in the system. The fast-fading component of the MIMO channel is the classical Independent and Identically Distributed (IID) Zero Mean Circularly Symmetric Complex Gaussian (ZMCSCG) fading model (PAULRAJ *et al.*, 2003).

Regarding the channel, we consider a MIMO channel subject to interference with B co-channel links where each link involves M_T transmit and M_R receive antennas. The channel matrix for a link of interest u between a receiver i and a transmitter j is denoted by $\mathbf{H}_{i,j}$, which is an $M_R \times M_T$ matrix whose elements $h_{a,b}$ consist in the channel transfer function between the receiver antenna a and transmit antenna b of the MIMO link in the r-th RB. Before transmission, the signals sent through the link u by the transmitter j are precoded by a transmit matrix $\mathbf{M}_j$ with dimension $M_T \times c_j$. The precoded signals traverse the channel $\mathbf{H}_{i,j}$, suffer from interference and noise and, at the receiver, are decoded by a receive matrix $\mathbf{D}_i$ with dimension $c_j \times M_R$. For both $\mathbf{D}_i$ and $\mathbf{M}_j$, c_j denotes the number of transmitted signals (or streams) and $c_j \leq \min(M_T, M_R, \nu)$, where ν is the rank of the channel matrix $\mathbf{H}_{i,j}$. Based on these definitions, the input-output relation for the MIMO channel for a certain link is given by

$$\tilde{\mathbf{y}}_i = \mathbf{D}_i \mathbf{y}_i = \mathbf{D}_i \left(\mathbf{H}_{i,j} \mathbf{M}_j \mathbf{x}_j + \sum_{\forall k \neq j} \mathbf{H}_{i,k} \mathbf{M}_k \mathbf{x}_k + \sigma_i \right), \tag{2.2}$$

where $\mathbf{y}_i$ and $\tilde{\mathbf{y}}_i$ are the prior-filtering received signal vector and the post-filtering received signal vector with dimension $c_j \times 1$, $\mathbf{x}_j$ is the transmit signal vector sent from transmitter j with dimension $c_j \times 1$ and σ_i is the $M_R \times 1$ white ZMCSCG noise vector at the receiver i, whose entries have average power σ_r^2.

It is worth to mention that the matrix $\mathbf{H}_{i,j}$ includes the effects of path-loss, shadowing, and fast fading. We also assume that the channel of interest is perfectly known at the transmitter and receiver while we consider that the interference in the system may or may not be known at the receiver. In the development of (2.2), we omitted the resource index r for simplicity of notation. Moreover, for each resource block, we assume that $h_{a,b}$ are obtained by considering the middle subcarrier among the S ones that compose the RB.

In the following, we index by u the links of interest between a transmitter j and a receiver i for simplicity of notation. Therefore, we might refer, for example, to $\mathbf{H}_{i,j}$, $\mathbf{D}_i$, $\mathbf{M}_j$, and c_j in (2.2) simply as $\mathbf{H}_u$, $\mathbf{D}_u$, $\mathbf{M}_u$, and c_u, respectively, in the developments that follow.

The aforementioned Multi-User Multiple Input Multiple Output (MU-MIMO) interference channel represents a general case for the different antenna configurations considered in this work. Indeed, we perform evaluations considering the following antenna configurations:

- SISO, where both transmitter and receiver have only one antenna;
- SIMO, where the transmitter has a single antenna and the receiver has multiple antennas;
- MISO, where the transmitter has multiple antennas while the receiver has a single antenna;
- MIMO, where both transmitter and receiver have multiple antennas.

The antenna configurations patterns are illustrated in Figure 5. When we increase the number of antennas in the system we also increase the number of streams c_j. With the addition of multiple antennas at the transmitter/receiver, we can exploit spatial diversity, as well as experience an increase in the reliability of wireless links (TSE; VISWANATH, 2005). For all the aforementioned antenna arrangements, we considered SU transmission, i.e., only one UE can be assigned to a specific RB within a TTI. When considering the downlink, transmitters will correspond to the Enhanced Node Bs (eNBs) and receivers to UEs while in the uplink transmitters are UEs and the eNBs are the receivers.

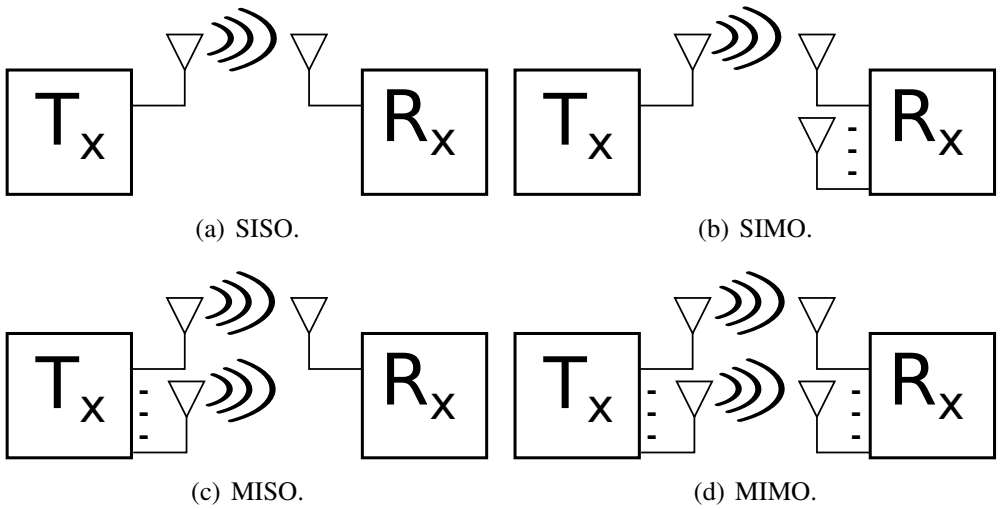

(a) SISO. (b) SIMO.

(c) MISO. (d) MIMO.

Figure 5 – Antenna arrangements patterns.

For the cases in which transmitter and/or receiver have multiple antennas and there is availability of CSI or other information derived therefrom, different multi-antenna transmission schemes can be employed in the system. In particular, we foresee the application of linear spatial

filtering and multiplexing schemes for SU communications. In this context, the following linear precoding schemes will be available for use in the system:

- **Maximum Ratio Combining (MRC)**

  MRC precoding is used to maximize the Signal to Noise Ratio (SNR) in SIMO scenarios (PAULRAJ *et al.*, 2003). The precoding matrix $\mathbf{M}_u$ and the decoding matrix $\mathbf{D}_u$ for the link of interest u between a transmitter j and a receiver i are defined, respectively, as

  $$\mathbf{M}_u = 1, \quad \text{and} \quad \mathbf{D}_u = \frac{\mathbf{H}_u^H}{\|\mathbf{H}_u\|_2}, \tag{2.3}$$

  where $\mathbf{H}_u$ is the channel matrix and $\|\cdot\|_2$ represents the 2-norm of a vector.

- **Maximum Ratio Transmission (MRT)**

  The MRT precoding is designed to maximize the transmitter SNR for MISO scenarios (PAULRAJ *et al.*, 2003). The precoding matrix $\mathbf{M}_u$ and the decoding matrix $\mathbf{D}_u$ for the link of interest u between a transmitter j and a receiver i are defined, respectively, as

  $$\mathbf{M}_u = \frac{\mathbf{H}_u^H}{\|\mathbf{H}_u\|_2}, \quad \text{and} \quad \mathbf{D}_u = 1, \tag{2.4}$$

  where $\mathbf{H}_u$ is the channel matrix.

- **Singular Value Decomposition (SVD)**

  The SVD precoding turns a MIMO channel into a set of decoupled equivalent SISO channels that do not interfere with each other (PAULRAJ *et al.*, 2007). For the link of interest u between a transmitter j and a receiver i, the SVD of the channel matrix $\mathbf{H}_u = \mathbf{U}_u \Sigma_u \mathbf{V}_u^H$ provides unitary right and left singular vector matrices $\mathbf{V}_u$ and $\mathbf{U}_u$, respectively. The precoding matrix $\mathbf{M}_u$ and the decoding matrix $\mathbf{D}_u$ are defined, respectively, as

  $$\mathbf{M}_u = \mathbf{V}_u, \text{ and } \mathbf{D}_u = \mathbf{U}_u^H. \tag{2.5}$$

Another parameter that has to be taken into account is the transmission power. For the downlink, this power refers to the total BS power, and it is known as P^{DL}. For the uplink, the total UE transmission power is known as P^{UL}. Having the power and precoding matrices as parameters, we can measure the channel quality for a stream by means of its SNR, when there is no interference in the system, and by its SINR, when there is interference in the system. The SNR of stream l of link of interest u on a given RB is given by

$$\gamma_{u,l} = \frac{p_{u,l} \cdot |\mathbf{d}_{u,l} \cdot \mathbf{H}_u \cdot \mathbf{m}_{u,l}|^2}{\underbrace{\sum_{m \neq l} p_{u,m} |\mathbf{d}_{u,l} \cdot \mathbf{H}_u \cdot \mathbf{m}_{u,m}|^2}_{\text{intra-cell interference}} + \underbrace{\tilde{\sigma}^2}_{\text{noise}}} \tag{2.6}$$

where $p_{u,l}$ is the power of stream l of link u, $\mathbf{d}_{u,l}$ is the decoding filter vector of stream l of link u, $\mathbf{m}_{u,l}$ is the precoding filter vector of stream l of link u, and $\tilde{\sigma}^2$ is the filtered receive noise power. Analogously, the SINR is defined as

$$\tilde{\gamma}_{u,l} = \frac{p_{u,l} \cdot |\mathbf{d}_{u,l} \cdot \mathbf{H}_u \cdot \mathbf{m}_{u,l}|^2}{\underbrace{\sum_{m \neq l} p_{u,m} |\mathbf{d}_{u,l} \cdot \mathbf{H}_u \cdot \mathbf{m}_{u,m}|^2}_{\text{intra-cell interference}} + \underbrace{\sum_{j \neq u} \sum_{n} p_{j,n} |\mathbf{d}_{u,l} \cdot \mathbf{H}_j \cdot \mathbf{m}_{j,n}|^2}_{\text{inter-cell interference}} + \underbrace{\tilde{\sigma}^2}_{\text{noise}}} \tag{2.7}$$

where $\mathbf{H}_j$ is the channel matrix between an interfering node j and a receiving node i.

Since we are dealing with wireless transmissions, there is a probability of errors occurring during a transmission. Although there are many approaches to deal with those errors, we consider the usage of a link adaptation functionality. Link adaptation allows the adaptation of the transmit data rate according to the current channel state. In order to change the transmit data rate, we assume that the modulation and channel coding rates are changed according to the channel state. We assume that there are some Modulation and Coding Schemes (MCS), each one with different performance regarding the BLER. The BLER performance curves used in this work for the downlink analyses were obtained from (MEHLFÜHRER *et al.*, 2009) and are presented in Figure 6(a). In order to generate equivalent curves for the uplink, we resorted to the simulator presented in (BLUMENSTEIN *et al.*, 2011), and available in (TU WIEN,), with which we performed simulations for 15 different MCSs whose resulting BLER curves are shown in Figure 6(b). The parameters used for the generation of the curves presented in Figure 6(b) are shown in Table 1. Similar results can be found in (UBISSE; VENTURA, 2011), although the authors used a slightly different configuration than the one we used to generate our curves.

Table 1 – LTE system parameters used for generation of uplink BLER curves.

Parameter	**Value**
System bandwidth	5 Mhz
Subcarrier spacing	15 kHz
Subframe duration	1 ms
Number of UEs	1
Number of eNodeBs	1
Antenna scheme	SISO
Cyclic prefix length	'normal' (3GPP, 2010b)
Channel	AWGNs
Modulation and Coding Schemes	4-QAM, ECR $\in \{78, 120, 193, 308, 449, 602\}$ 16QAM, ECR $\in \{378, 490, 616\}$ 64QAM, ECR $\in \{446, 567, 666, 772, 873, 938\}$

As stated in Chapter 1, we want to evaluate the performance of the suboptimal solution used to solve the CRM problem in a system subject to interference, as also in a system

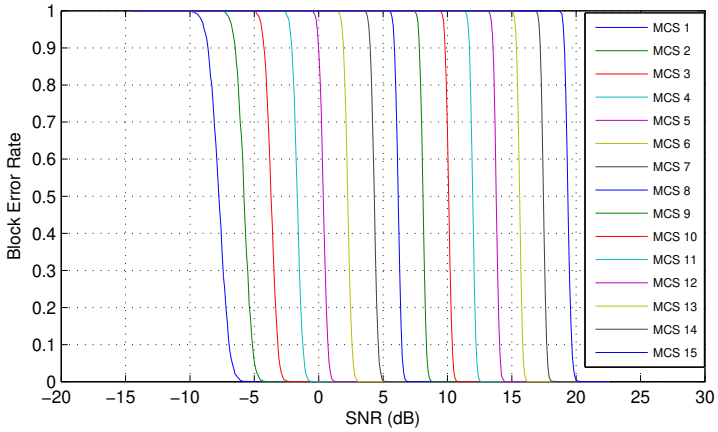

(a) Downlink.

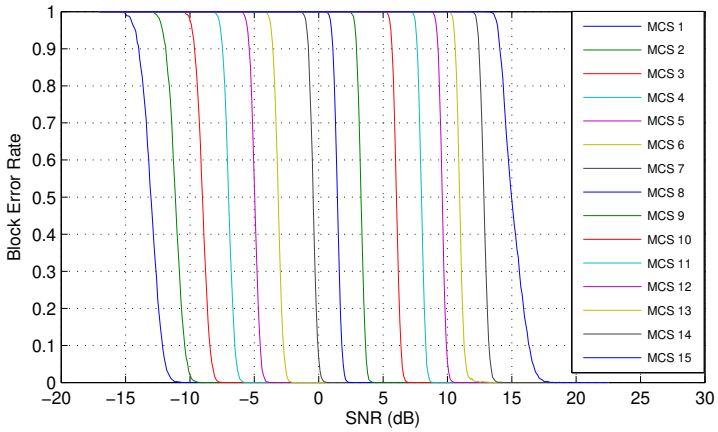

(b) Uplink.

Figure 6 – BLER curves.

where the RBs are grouped before the allocation process. In the further sections we will detail the aforementioned aspects.

2.2 Suboptimal Solution for the CRM problem

The suboptimal solution for the CRM problem was firstly described in (LIMA *et al.*, 2012b; LIMA *et al.*, 2012a) and it is better explained in (LIMA, 2012). The CRM problem consists in a resource allocation problem, where an association between UEs and RBs should respect some requirements related to the multiple access, as also related to minimum satisfaction aspects. Those requirements include:

- A RB can only be used for a UE at a time, i.e., we will have only SU mode. It is necessary to assure that the frequency resources will remain orthogonal to each other.
- A specific amount of UEs in a service must be served with a minimum required data rate.

Those requirements are common for both directions, DL and UL. However, for the

UL, we have one more requirement, due to the use of SC-FDMA: we need to assure that the UEs have only contiguously RBs assigned to them as stated in 1.2.2.2.

In order to perform the RB allocation and to assure that the aforementioned requirements will be fulfilled, a suboptimal framework for the CRM problem was developed. This solution is presented in details in (LIMA, 2012), and it is composed by two parts: **Unconstrained Maximization** and **Reallocation**.

In the **Unconstrained Maximization** part, the main idea is to have a good initial assignment between RBs and UEs that is on the boundary of the capacity region for the problem solution. This means that we allocate RBs to the UEs in order to increase the total cell throughput, regardless of the minimum satisfaction constraints.

In the **Reallocation** part, we basically switch RBs between the UEs, in order to fulfill the minimum satisfaction constraints imposed by the CRM problem. In the end of this part, we will have a suitable assignment between RBs and UEs, which guarantees that the minimum satisfaction constraints were fulfilled.

Figure 7 presents the main aspects of the suboptimal framework for the CRM problem. In this example, we have two UEs, each one requiring a data rate of 300 kbps, and we want to satisfy both. x and y axes present the acquired data rates for UE 1 and UE 2, respectively. As we can see in the figure, the region that fulfills the imposed satisfaction constraints is the one that is above the 300 kbps in both axes, represented by the square in the upper right corner in the figure. Thus, in the first part of the framework, we find a solution that maximizes the system data rate, without fulfilling the QoS guarantees. This is represented in Figure 7 as the point A. After the first phase, we then switch RBs between the UEs in order to fulfill the satisfaction constraints, which leads to a feasible solution to the problem, represented in the figure as the point B. The path between point A and point B (the reallocations done in the process) are also shown in the figure. Point C, that is shown in the figure, is the one acquired through the optimum solution for the CRM problem, and it is shown only for comparison purposes.

There are some cases where the CRM problem is too hard to solve, such as cases where we have many UEs in the system, and they require a high data rate. When the algorithm employed to solve those problems is not able to find a feasible solution, we say that we have an outage event.

In (LIMA, 2012), the suboptimal solution for the CRM problem was evaluated in an interference-free scenario. Therein, the objectives were to devise the optimum solution and

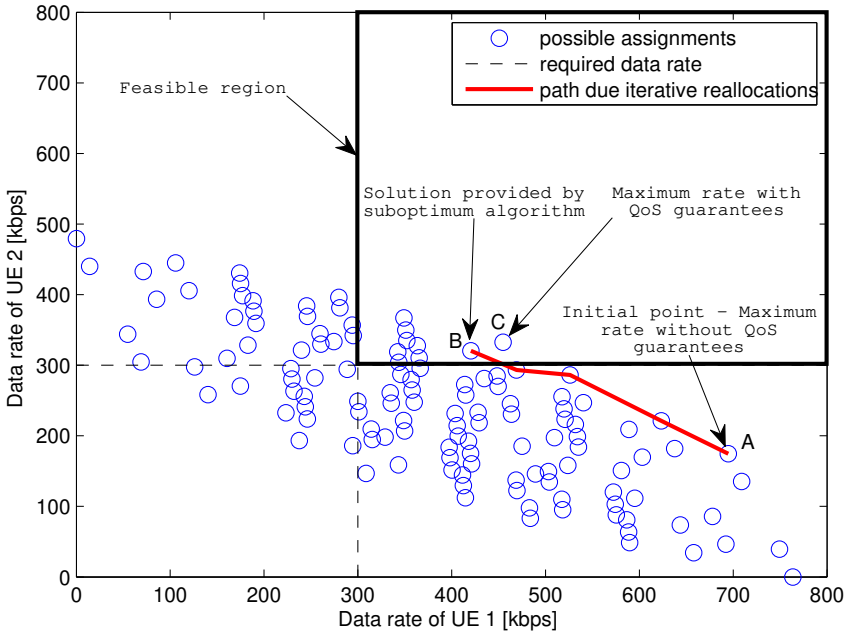

Figure 7 – Suboptimal solution for the CRM problem (LIMA, 2012).

compare it to a proposed suboptimal one in order to assure that the CRM problem could be solved through a suboptimal solution with near-optimal performance.

In order to complement the work done in (LIMA, 2012), we decided to evaluate the suboptimal solution to the CRM problem in a scenario with inter-cell interference and so get insight on the solution behavior when it has or does not have knowledge of the interference levels in the system. In the next section we will explain in the details how the interference was modeled.

2.3 Interference Modeling

The system topology used during our simulations is described in Section 2.1. Regarding the interference model used in this work, it is a computational model that was implemented for single and multiple antenna cases for the DL direction, and for the single antenna case (SISO) for the UL. It is a simplified model designed by us, in order to get insights about the interference impact in the CRM algorithms presented in (LIMA, 2012).

In this interference model, we perform the calculation for all the interfering gains using a λ parameter, which is the probability that the r-th RB will be selected by the b-th BS for allocation. This parameter is used in order to randomly select which RBs were set as active (i.e., are generating interference) by the b-th BS in order to account for the interfering links.

For example, if we set λ parameter in 50%, each BS will select approximately 50% of the RBs available in the pool of RBs. After that, we inspect the RBs selected by the virtual BSs to see if they are the same as the RBs selected by the user of interest. If so, we consider them as the interfering links. We then use the interfering links to evaluate the interference impact in the SINR according to (2.7).

For the DL direction, after defining which RBs are interfering with the selected RB in the BS of interest, we randomly select a UE among all the UEs in the system, and we position this UE in the interfering BS. We then use this UE channel gain in this BS and in this RB in order to account for the interference. Figure 8(a) illustrates the DL scenario used during our simulations. The darker shaded sector represented in the figure is modeled in the system as the sector of interest, where all the users are positioned and which is subject to interference. The cell radius is represented by the dotted line, and it is named as the variable R. The other BSs are virtual BSs, as also their interfering sectors (the lighter shaded ones). These sectors are only modeled to account for interference, and the sectors in white are not modeled in our system. Although in Figure 8(a) we only represent 2 interfering BSs (BS2 and BS5) we have a total of 6 interfering BSs in our system and the other BSs are hidden in the figure for sake of simplicity.

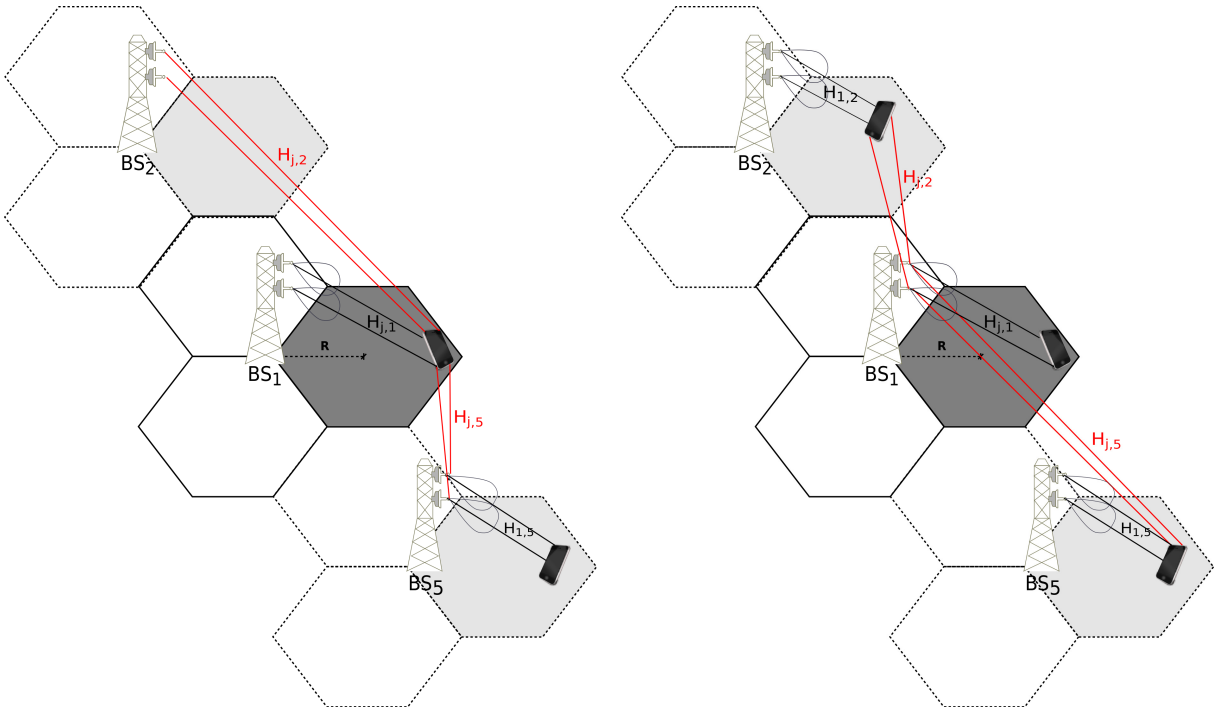

(a) Downlink. (b) Uplink.

Figure 8 – Interference modeling.

For the UL direction, since we are using SC-FDMA and this scheme requires that

the RBs are contiguously assigned to a UE (which makes the simulation computationally costly), the interference is modeled in a different way than in the DL direction. In the UL, we use as interference pattern the one generated by the allocation done by the suboptimal framework in past TTIs. Thus, we do not have interference in the first TTI, and in the second one we have interference pattern for just one interfering BS. We only have a full interference pattern (for all the interfering BSs) after the 7^{th} TTI. Because of this behavior, we disregard the 200 initial TTIs, in order to maintain a statistical reliability in the interference modeling. The choice of the interfering UEs in each interfering BS per RB is done in the same way as it is in the DL direction. Figure 8(b) shows the UL scenario used during our simulations. Although in the figure we only show one interfering UE per BS as also only two interfering BSs, in our simulations the number of interfering UEs is defined by the λ parameter (as explained above), and our grid is composed by 7 BSs in total, but they were hidden in the figure for sake of simplicity.

As stated previously, there is also another factor to be taken in consideration during our work. This is related to the RB aggregation, which is described in (3GPP, 2010c) and it will be detailed in the next section.

2.4 RB aggregation

RB aggregation is a practical limitation of LTE systems imposed by the 3GPP consortium. It consists in the grouping of two or more RBs in order to form a RBG. This aggregation procedure is described in (3GPP, 2010c), where the existing resource allocation types for the DL and UL channels are detailed. There are three allocation types for the DL and one for the UL, and each one of them is depicted in the following.

The first allocation type for the DL is resource allocation type 0, where the resources are allocated to the scheduled users according to Table 2

Table 2 – Type 0 Resource Allocation: RBG Size vs. Number of RBs on DL.

# of RBs (N_{RB}^{DL})	$\leqslant 10$	11 - 26	27 - 64	65 - 110
RBG Size (P)	1	2	3	4

The total number of RBGs per number of RBs in the system is given by:

$$N_{RBG} = \lceil N_{RB}^{DL}/P \rceil \tag{2.8}$$

where P RBGs have the size of $\lfloor N_{RB}^{DL}/P \rfloor$ and if $N_{RB}^{DL} \mod P > 0$, then one of the RBGs will

have the size of $N_{RB}^{DL} - P \cdot \lfloor N_{RB}^{DL}/P \rfloor$. The RBGs are numbered from 0 to $N_{RBG} - 1$. Figure 9(a) presents an example of resource allocation type 0, for a system composed by 28 RBs.

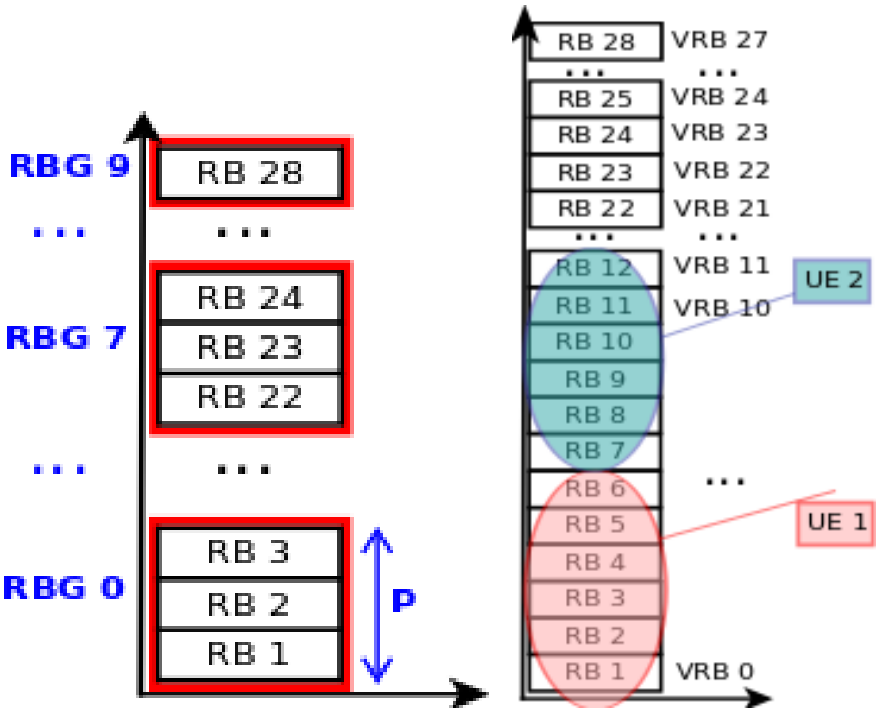

(a) Resource allocation type 0 for the DL.

(b) Resource allocation type 2 for the DL and virtual resource block allocation for the UL.

Figure 9 – Resource allocation types.

As it can be seen in the figure, we have 10 RBGs, where 9 RBGs have the size of P (3 in this case, according to table 2) and one of them has the size of 1, as explained above.

The second allocation type for the DL is resource allocation type 1. Since this is not in use in our work, we will not explain this type here. For further information about this allocation type, see in (3GPP, 2010c).

The third allocation type for the DL is resource allocation type 2. For this case, the RBs are contiguously allocated to the UEs in the form of virtual resource blocks or distributed virtual resource blocks. Figure 9(b) presents this type of allocation.

The resource allocation defined for the UL is a virtual resource block allocation, similar to allocation type 2 for the DL. Figure 9(b) also illustrates this kind of allocation.

In this work we chose the resource allocation type 0 to perform our evaluations for the DL, and the virtual resource block allocation for the UL. The study of the other resource allocation types is left for future work.

All the aforementioned resource allocation types are explained in more details

in (3GPP, 2010c).

3 INTERFERENCE IMPACT FOR THE DOWNLINK CASE

In this chapter we present the CRM problem for the DL case, as also a suboptimal algorithm to solve this problem. We evaluate this suboptimal algorithm in three different scenarios: with interference in the system, with RB aggregation and with interference plus RB aggregation. In Section 3.1 we describe the CRM problem and we present the suboptimal solution to solve this problem in Section 3.2. Section 3.3 brings the results and the main performance analyses of the suboptimal algorithm. We finish this chapter presenting some conclusions in Section 3.4.

3.1 Description of the CRM Problem for the Downlink Case

Resource assignment is an important matter during UEs scheduling. In order to address this matter, we can write it as an optimization problem, as it was previously described in (LIMA *et al.*, 2012b; LIMA, 2012). We firstly start describing some of the variables used to compose the optimization problem. Since we are interested in allocating resources to UEs at the same time we aim to maintain a minimum satisfaction constraint, which is a minimum rate per UE, we need to determine the UEs data rate. The transmit data rate of UE j in RB r is defined as:

$$q_j = \begin{cases} \sum_{l}^{c_j} f(\gamma_l), & \text{if there is no interference in the system} \\ \sum_{l}^{c_j} f(\tilde{\gamma}_l), & \text{if there is interference in the system} \end{cases} \tag{3.1}$$

where c_j is the number of streams as defined in (2.2), γ and $\tilde{\gamma}$ are the SNR and SINR, as defined in Chapter 2, and $f(\cdot)$ represents a function that maps the SNR/SINR values to the transmit data rate. It must be noticed that we omitted the resource index r for sake of notation simplicity.

We define $\mathbf{X}^{\mathrm{DL}}$ as a $J \times R$ assignment matrix with elements $x_{j,r}^{\mathrm{DL}}$ that are valued as 1 if the RB $r \in \mathscr{R}$ is assigned to the UE $j \in \mathscr{J}$ and 0 otherwise. We can also define t_j as the data rate requirement from UE j in the current TTI, $\mathscr{S}$ as the set of services in the system, where k_s is the minimum number of UEs from service $s \in \mathscr{S}$ that must be satisfied.

With the definitions above, we can now write the CRM problem in its standard form:

$$\max_{\mathbf{X}^{\mathrm{DL}}} \left(\sum_{j \in \mathscr{J}} \sum_{r \in \mathscr{R}} q_{j,r}^{\mathrm{DL}} \cdot x_{j,r}^{\mathrm{DL}} \right), \tag{3.2a}$$

subject to

$$\sum_{j \in \mathscr{J}} x_{j,r}^{\mathrm{DL}} = 1,\ \forall r \in \mathscr{R}, \tag{3.2b}$$

$$x_{j,r}^{\mathrm{DL}} \in \{0,1\},\ \forall j \in \mathscr{J} \text{ and } \forall r \in \mathscr{R}, \tag{3.2c}$$

$$\sum_{j \in \mathscr{J}_s} u\left(\sum_{r \in \mathscr{R}} q_{j,r}^{\mathrm{DL}} \cdot x_{j,r}^{\mathrm{DL}},\ t_j \right) \geq k_s,\ \forall s \in \mathscr{S}. \tag{3.2d}$$

Due to constraint (3.2d), which is non-linear, the optimal solution can have a high computational complexity, thus preventing us from using it. However, this problem can be converted into an ILP problem by the use of some algebraic methods, as shown in (LIMA, 2012), and as such can be solved by standard methods like the Branch and Bound (BB) algorithm (NEMHAUSER; WOSLEY, 1999).

In (LIMA, 2012), the optimal solution for this problem is also showed. In that work, the optimal solution has been compared to the suboptimal solution. As showed in (LIMA *et al.*, 2012b; LIMA, 2012), the suboptimal solution presents a good performance and complexity, with its results being close to those of the optimal solution. Since in here we are interested in investigating how the suboptimal solution behaves in scenarios subject to inter-cell interference, we will not present the optimal solution.

In the next section we will present the suboptimal solution proposed by the authors of (LIMA *et al.*, 2012b; LIMA, 2012) to the CRM problem, and we will describe its parts in details.

3.2 Low-Complexity Suboptimal Solution for the CRM Problem

The suboptimal algorithm described herein was firstly described in (LIMA *et al.*, 2012b). This algorithm tries to allocate RBs to UEs in an OFDMA-based system subject to a minimum number of UEs that must be satisfied per service and where a minimum rate is required per UE to satisfy it. The algorithm is divided into two parts: **Unconstrained Maximization** and **Reallocation**. These parts are depicted in Figure 10 and Figure 11, respectively.

In the following, we describe both parts where the provided information has been adapted from (LIMA *et al.*, 2012b; LIMA, 2012). In the **Unconstrained Maximization** part, the main idea is to have an initial assignment which achieves the highest possible data rate in the system. The algorithm is started by defining the auxiliary ($\mathscr{B}$) and available ($\mathscr{G}$) UE sets and they are initialized with the set of all UEs ($\mathscr{J}$). Then the maximum rate allocation (BOHGE *et*

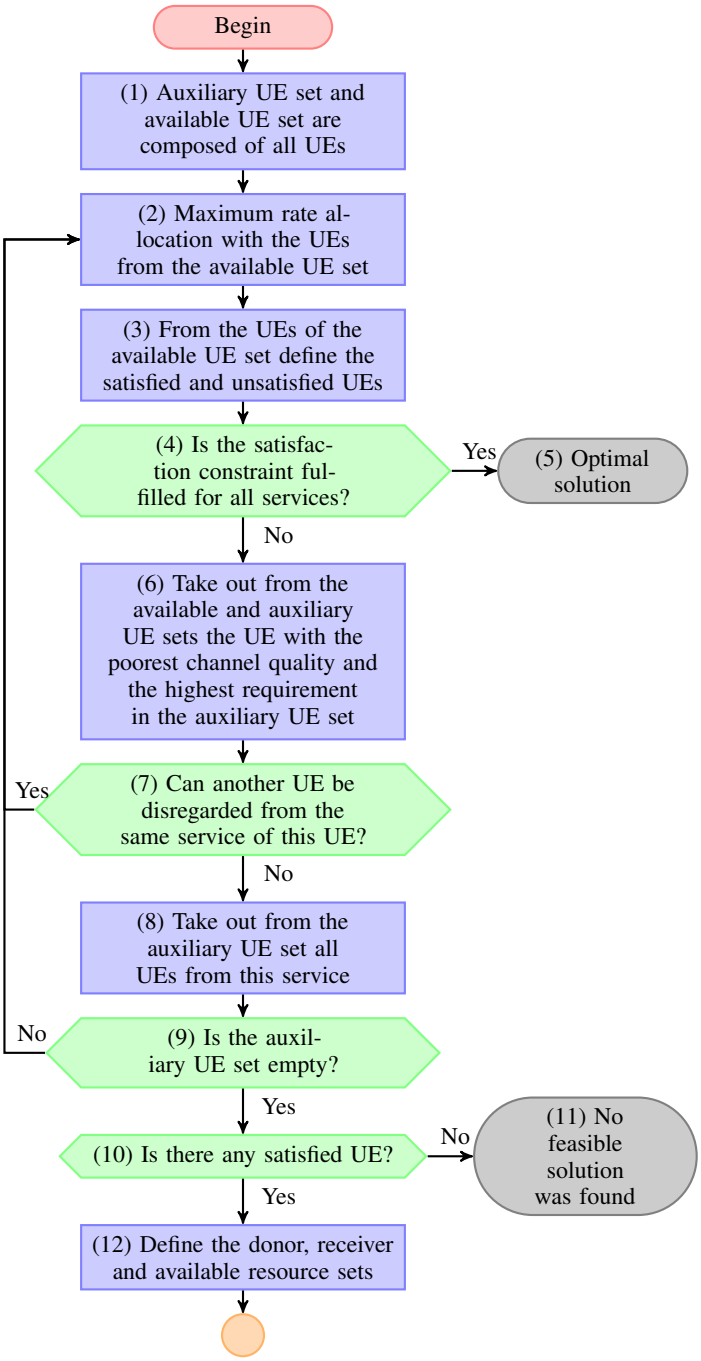

Figure 10 – Flowchart of the first part of the suboptimal framework: Unconstrained Maximization (adapted from (LIMA, 2012)).

al., 2007; LIU; LI, 2005) is solved with the UEs from the available UE set. The maximum rate allocation basically assigns each available resource from the resource set ($\mathscr{R}$) to the UE with highest rate on it. After that, the UEs that have the data rate requirement fulfilled are defined as the satisfied UEs and the remaining ones as the unsatisfied UEs. If the minimum required number k_s of satisfied UEs of each service s is achieved, an optimum solution was found. However, note that this is an uncommon situation due to the distribution of the UEs within the cell. In general,

few UEs will get most of the available resources.

If the satisfaction constraint for any service is not fulfilled, a UE of the auxiliary UE set ($\mathscr{B}$) will not receive resources at the current TTI, thus it will be ignored. The criterion to select the UE $j^\star$ that will not receive any resources is given by

$$j^\star = \arg\min_{j \in \mathscr{B}} \frac{\left(\frac{1}{R} \sum_{r \in \mathscr{R}} q_{j,r} \right)}{t_j}, \tag{3.3}$$

where $\mathscr{B}$ is the auxiliary UE set as defined before with the UEs of the services that still can be ignored, $\mathscr{R}$ is the resource set of size R, $q_{j,r}$ is the rate of UE j at resource r, and t_j is the target rate of UE j in the current TTI. With this criterion the ignored UEs are the ones that require, in average, more RBs to be satisfied. The selected UE is removed from the available and auxiliary UE sets.

The next step is to check whether the service of the ignored UE can have another UE ignored without infringing its minimum satisfaction constraints. If this is not possible, all the UEs from this service are removed from the auxiliary UE set ($\mathscr{B}$). In this case, no UE from that service will be ignored anymore. All this procedure is repeated until either an optimum solution is found or no UE can be ignored, i.e., the auxiliary UE set is empty. In the former case, where the auxiliary UE set ($\mathscr{B}$) in not empty, the maximum rate allocation if performed again with the remaining UEs in the available UE set. In the latter case, it is checked if at least one UE is satisfied. If so, from the available UE set ($\mathscr{G}$) and the RB set ($\mathscr{R}$) three new sets are defined: the donor ($\mathscr{D}$) and receiver UE sets ($\mathscr{N}$), and the available resource set ($\mathscr{P}$). The donor UE set is composed of the satisfied UEs in the available UE set and can donate RBs to the unsatisfied UEs. The receiver UE set is composed of the unsatisfied UEs from the available UE set and need to receive RBs from the donors to have fulfilled their rate requirements. Finally, the available resource set is composed by all the resources from the UEs in the donor UE set, i.e., the resources that can be donated to the unsatisfied UEs (receiver UEs). In case there is no satisfied UE after executing the first part, the suboptimal algorithm is not able to find a feasible solution, i.e., that comply with the minimum satisfaction constraints.

In the **Reallocation** part the basic idea consists in reallocating RBs from the donors to the receivers. It starts by choosing the UE from the receiver UE set ($\mathscr{N}$) with the worst channel quality to get resources until its data rate requirement is fulfilled. This is done in order to assign the minimum number of RBs to the UEs in bad channel conditions as to get them satisfied and assign the remaining RBs to the UEs with better channel quality, thus increasing the total

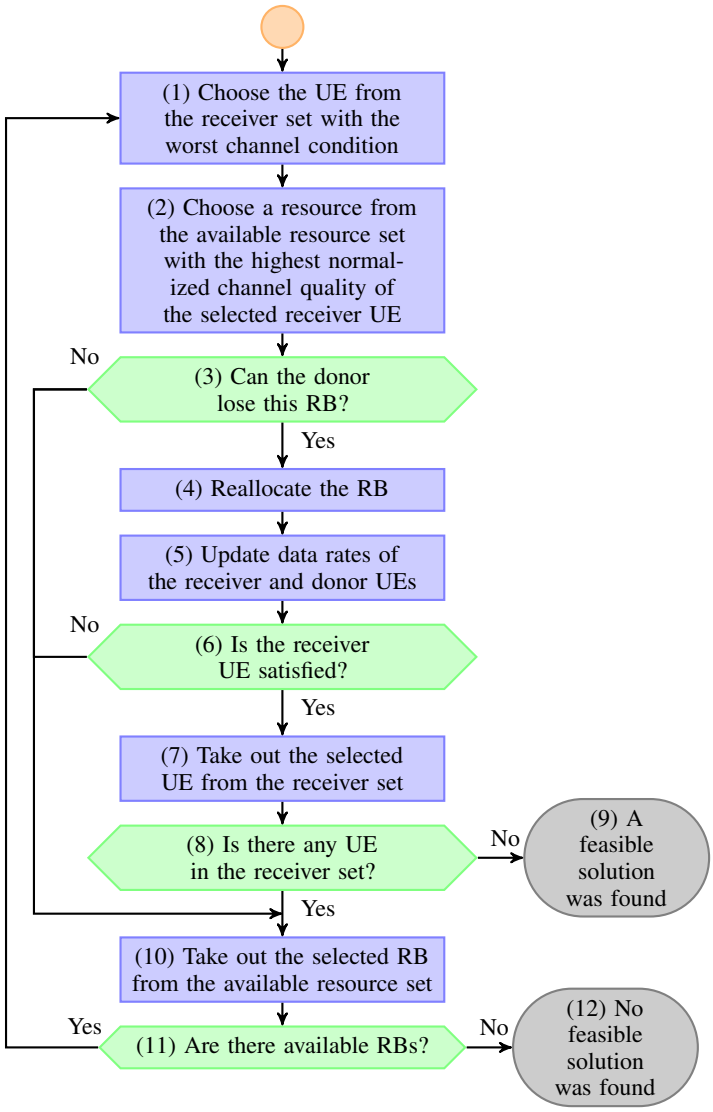

Figure 11 – Flowchart of the second part of the suboptimal framework: Reallocation (adapted from (LIMA, 2012)).

cell throughput. Then, a resource $r^\star$ is selected from the available resource set to the receiver UE $j^\star$ based on the following criterion

$$r^\star = \arg\max_{r \in \mathscr{P}} \frac{q_{j^\star,r}}{q_{j^+,r}}, \tag{3.4}$$

where j^+ is the UE from the donor UE set ($\mathscr{D}$) that has got assigned the resource n in the first part of the suboptimal algorithm. Note that, if the reallocation of the selected RB will leave the donor UE unsatisfied, the selected RB is not reallocated. In fact, this RB is taken out of the available resource set ($\mathscr{P}$) and another RB is chosen.

If the donor can lose the selected RB, this RB is assigned to the receiver UE and the data rates of the receiver and donor UEs are updated. If after reallocation the receiver UE is satisfied, this UE is removed from the receiver set ($\mathscr{N}$). Otherwise, the receiver will get more

resources according to equation (3.4). This process is repeated until either all the receivers are satisfied or there is no available resource to be reallocated. In the former case, the algorithm has found a feasible solution. In the latter, the algorithm was not able to find a feasible solution.

We have to mention that, for the cases where we have RB aggregation, the RBs allocated in the **Unconstrained Maximization** part and the RBs reallocated in the **Reallocation** part of the suboptimal algorithm correspond to RBGs instead of individual RB, as showed in Section 2.4 from Chapter 2. Since with RB aggregation we treat the RBG as an individual resource, it was not necessary to rewrite the CRM problem.

In the next sections we will show how we proceed our evaluations on the algorithm for different scenarios.

3.3 Performance Evaluation

This section presents the analyses on the performance of the previously described suboptimal solution of the CRM problem for the DL in a scenario with inter-cell interference. We evaluate the UEs' SINRs, outage rates for different values of λ, and the average satisfaction of the UEs in the system. In Section 3.3.1, we present the main simulation assumptions and performance metrics used for comparison. In Section 3.3.2 we show the simulation results.

3.3.1 Simulation Assumptions

In order to evaluate the suboptimal solution of the CRM problem, we consider that there are two different services whose UEs have the same rate requirement. For both services we use the same traffic model, which is a full buffer traffic model. For the all antenna arrangements, we performed simulations for three different scenarios:

- When there is only interference in the system;
- When there is only RB aggregation;
- When there is interference and RB aggregation in the system.

For the first and last scenarios, we realized two kinds of simulation: one, where the algorithm knows the interference present in the system, and it uses those values when performing the scheduling of the UEs; in the second one, the algorithm is not aware of interference, which means that the scheduling procedure will be done without any knowledge about the interference present in the system, i.e., scheduling will be based only on SNR values.

We consider that the channel transfer function of a UE in an RB is defined as the channel transfer function of the central subcarrier that composes the RB, as stated in Chapter 1. Table 3 summarizes the main simulation parameters.

Table 3 – Main simulation parameters.

Parameter	**Value**	**Unit**
Cell radius	334	m
Number of subcarriers per RB	12	-
Number of snapshots	3000	-
Antenna configuration $M_R \times M_T$	1×1 2×1 1×2 2×2	SISO SIMO MISO MIMO
Shadowing standard deviation	8	dB
Path loss	$35.3 + 37.6 \log_{10}(d)$ [a]	dB
Noise spectral density	$3.16 \cdot 10^{-20}$	W/Hz
Total BS power	43	dBm
Power per RB [b]	29.02	dBm
Channel model	Classical IID ZMCSCG	-
Number of services	2	-

For comparison purposes, the first and last scenarios described above were also simulated without interference in the system, and the second scenario was also simulated for the case without RB aggregation.

When the performance metrics are concerned, we consider three main ones: SINR/SNR, outage ratio and satisfaction of the UEs per service.

An outage event happens when the suboptimal solution to the CRM problem can not manage to find a feasible solution. Note that depending on the positions of the UEs within the cell, channel gains and data rate requirements of the UEs, the problem itself can be infeasible and therefore the algorithm would have an outage event. Outage rate is defined as the ratio between the number of snapshots with outage events and the total number of simulated snapshots. Therefore, this performance metric shows the capability of the algorithm in finding a feasible solution to our problem.

Satisfaction of the UEs is measured to all the UEs, independently when there was an outage event or not. It is defined as the ratio between the number of UEs that had their data rate requirement fulfilled and the total number of UEs per service in the system. We present this metric as percentage and averaged over all the simulated system snapshots.

Finally, increments in the offered load are emulated by increasing the rate requirements of the UEs for all the scenarios described above. We also incremented number of RBs

and the cell loading (interference) in the system in order to obtain a better view of the simulated scenarios. All the UEs have the same data rate requirement independently of service type.

3.3.2 Results and Analyses

In this section we will show the results obtained for the suboptimal solution to the CRM problem in the DL in a system subject to inter-cell interference. We investigate three main aspects: the impact of interference, the impact of RB aggregation, and the impact of RB aggregation with interference in the system.

3.3.2.1 Interference Impact

Regarding the impact of the interference in the system, we performed simulations for all the antenna arrangements (SISO, SIMO, MISO and MIMO), varying the cell loading (λ parameter) in the system. Table 4 shows the simulation parameters for the different cases used to evaluate the performance of the suboptimal algorithm for the CRM problem.

Table 4 – Parameters of the considered scenarios.

Parameter	**Value**
Antenna configuration	SISO, SIMO/MISO, MIMO
Number of UEs per service	8 (Service 1), 6 (Service 2)
Required number of satisfied UEs per service	7 (Service 1), 5 (Service 2)
Number of RBs	26
UEs' required rate	[64 kbps:32 kbps:896 kbps]
Cell loading (λ)	25%, 50%, 75%, 100%

Figure 12 presents the CDFs of the SINRs for all the UEs in the system obtained for the SISO antenna case for the required data rate of 480 kbps when the algorithm is aware of interference.

The first conclusion we can take from this figure is that when we increase the cell loading (by increasing the value of λ), the system performance decreases, as expected. We can also see that, even for the highest cell loading value, we have acceptable values of SINR at the 50-th percentile (approximately 10 dB). This happens because once the algorithm knows the interference, it can use this information to perform a better resource assignment for the UEs.

Figure 13 presents the CDFs of the SINRs from the scheduled UEs in the system for the required data rate of 480 kbps and with cell loading λ set to 50%. In this figure we can see three cases: when there is no interference in the system, when there is interference and the

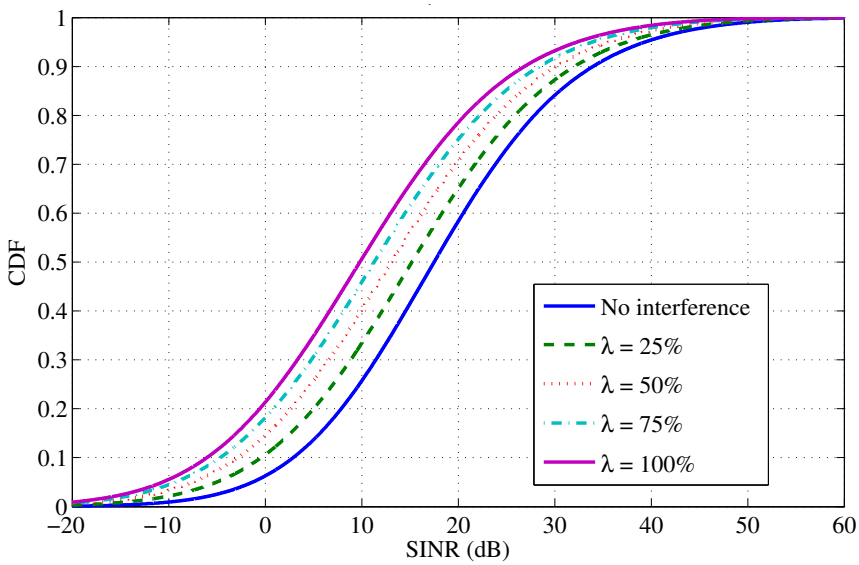

Figure 12 – CDFs of the SINRs of all the UEs in the system. Required data rate: 480 kbps, algorithm aware of interference, SISO.

algorithm is aware of it, and when there is interference but the algorithm is not aware of it. As we can see, the algorithm performs better when it knows the interference, and if we inspect the figure at the 50-th percentile, we noticed that the difference between the case when there is no interference and when the algorithm is aware of interference is of 7.57% and 15.40% when the algorithm does not know interference. In this point of the curve we have a gain in capacity of more than 7.8%, due to interference knowledge by the algorithm. While this gain might not seem very expressive, it can have a considerable impact on the system capacity since the suboptimal algorithms aims at keeping capacity on its edge while respecting the QoS constraints.

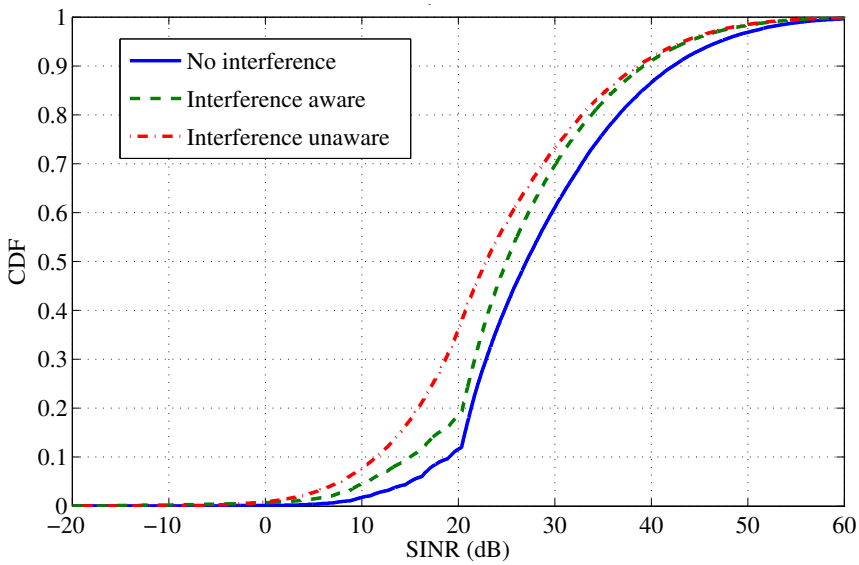

Figure 13 – Comparison of the CDFs of the SINRs of the scheduled UEs in the system. Required data rate: 480 kbps with cell loading of 50%, SISO.

Comparing Figure 12 to Figure 13, we can observe that the SINR values in the latter are higher than the values in the former. This happens because in Figure 13, we only account for the UEs that where scheduled by the algorithm, i.e., the UEs that had their data rate requirement fulfilled, and in Figure 12 we are accounting for every user in the system, even the ones that were in outage situation. Also, in Figure 13 we can see that there is a small "knee" in the curves where there is no interference in the system (represented in blue) and where there is interference and the suboptimal algorithm is aware of it (represented in the green dotted line). This "knee" delimits two conditions: one, on the left side of the "knee", where the users have lower SNR/SINR values, and the other one, on the right, showing users with higher SNR/SINR values. This is a result of the users choice performed by the suboptimal algorithm: it chooses users in a way that all the satisfaction restrictions are fulfilled, and those users on the left side of the "knee" are the ones with worst channel conditions, that, even though, had their requirements fulfilled, while the users on the right side are the ones with better channel conditions (which explains the higher SNR/SINR values).

The next metric that we evaluated is the outage rate. Figures 14 and 15 present the outage rates for SISO case where the algorithm is aware and where it is not aware of interference, respectively. Evaluating Figure 14 we can see that the outage events tend to occur for lower rate requirements as we increase the cell loading, i.e., since we the more we add interference in the system, the more difficult is to the algorithm finding a feasible solution to the scheduling problem. When we compare Figure 14 and Figure 15, it is possible to see that for the case when the algorithm is not aware of interference, the outage rates are really high, even for the lowest rate requirements, as also for the lowest cell loading value. This clearly shows that, if the algorithm can be made aware of interference in the system, it can perform better, which leads to the results presented in Figure 14. More importantly, this result demonstrates that the the algorithm works in the presence of interference as long as it is aware of interference and degrades softly with the increase in the amount of interference of the system, as it would be expected from a well-designed resource allocation algorithms. Therefore, we have shown that the suboptimal algorithm can be applied efficiently to scenarios with inter-cell interference.

The other metric used for our analyses is the satisfaction of the UEs. When the algorithm has the perfect knowledge of the interference, it can estimate the SINR for each link, and thus can use this value to calculate the UEs' data rates and, based on that, perform the resource allocations. According to Table 4, we want to satisfy 87.5% of the UEs from service 1

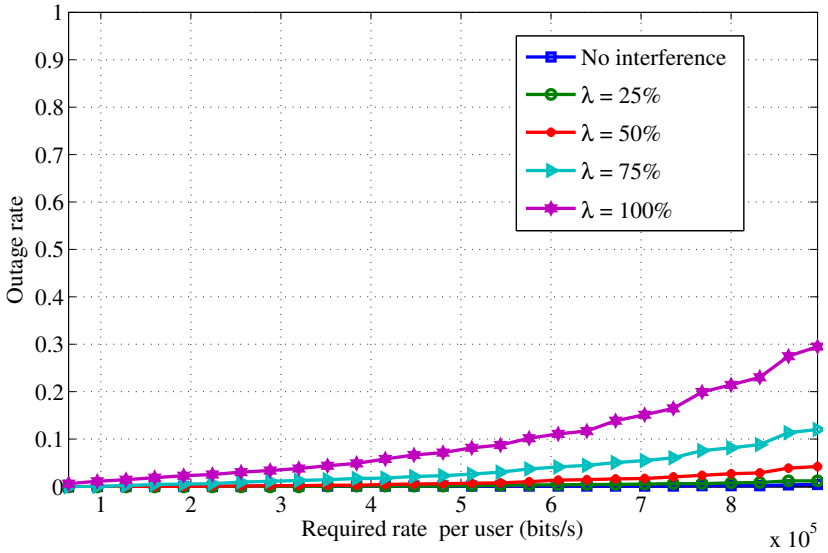

Figure 14 – Comparison of the outage rates for the case where the algorithm is aware of interference versus interference disabled, SISO.

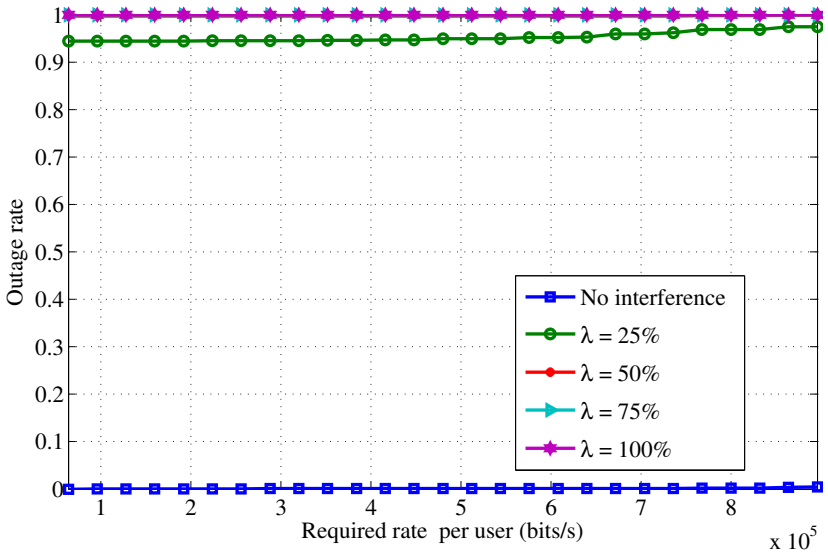

Figure 15 – Comparison of the outage rates for the case where the algorithm is not aware of interference versus interference disabled, SISO.

(7 UEs from a group of 8) and 83.33% of UEs from service 2 (5 UEs from a group of 6).

Figure 16 shows the satisfaction results per service for the case when the algorithm is aware of interference in the system.

In this figure, we can see that until the required rate of 576 kbps, for the cell loadings of 25% and 50%, the satisfaction of the UEs for the case when there is no interference and when there is interference and the algorithm is aware of it is almost the same for both cases in all the services. This means that, once the algorithm has perfect knowledge about the interference, it can maintain the satisfaction of the UEs at relatively high levels. However, when we increase the data rate requirements and the interference in the cell, we notice that the satisfaction of the

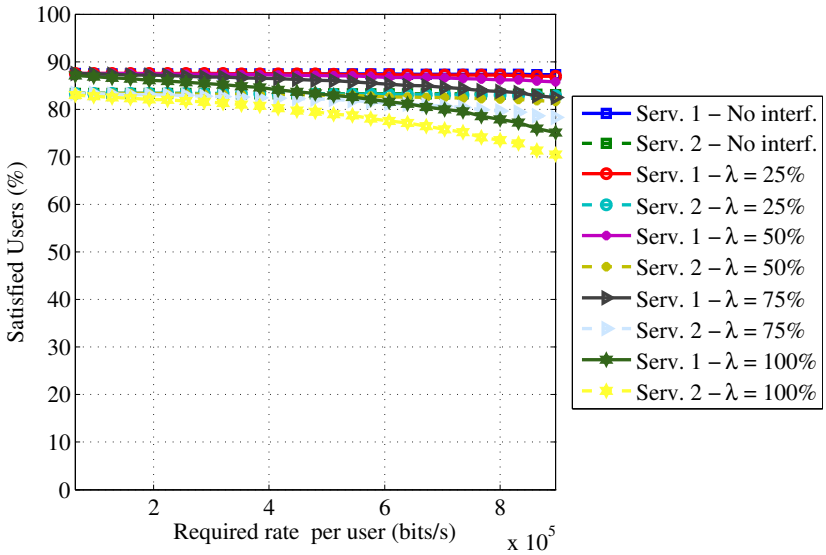

Figure 16 – Comparison of the percentage of satisfied UEs for the case where the algorithm is aware of interference, SISO.

UEs decreases, and this is reflected in the outage rates showed in Figure 14. For these cases, the suboptimal algorithm is not able to allocate the available resources in a good way, because the UEs data rates (calculated based on the SINR values) are minimized by the high interference levels in the system.

Regarding the case where the algorithm is not aware of interference, which is showed in Figure 17, it is notable that the satisfaction of the UEs is at considerably lower levels than the ones required by the services. This means that, for those situations, the algorithm is never able to find a feasible solution to the allocation problem. As happened for the aforementioned case, these lower satisfaction levels are reflected in the outage rates showed in Figure 15.

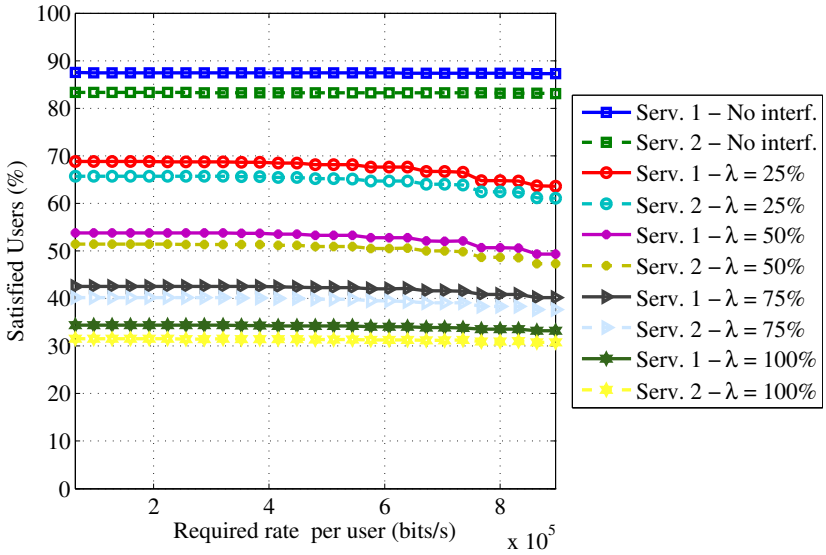

Figure 17 – Comparison of the percentage of satisfied UEs for the case where the algorithm is not aware of interference, SISO.

The further evaluations in the suboptimal algorithm were performed for the multi-antenna case. We simulated the SU case for MISO, SIMO and MIMO antenna arrangements, and the number of antennas used in our simulations can be found in Table 3.

Figure 18 shows a comparison between the cases without interference for all the antenna arrangements. The first thing to be noticed is that the y-axis is set from 0 to 0.1, showing that, in the absence of interference, the outage rates remain practically at zero for all the simulated cases, which means that the suboptimal algorithm was able to solve the allocation problem in all cases. We will use this as the reference case.

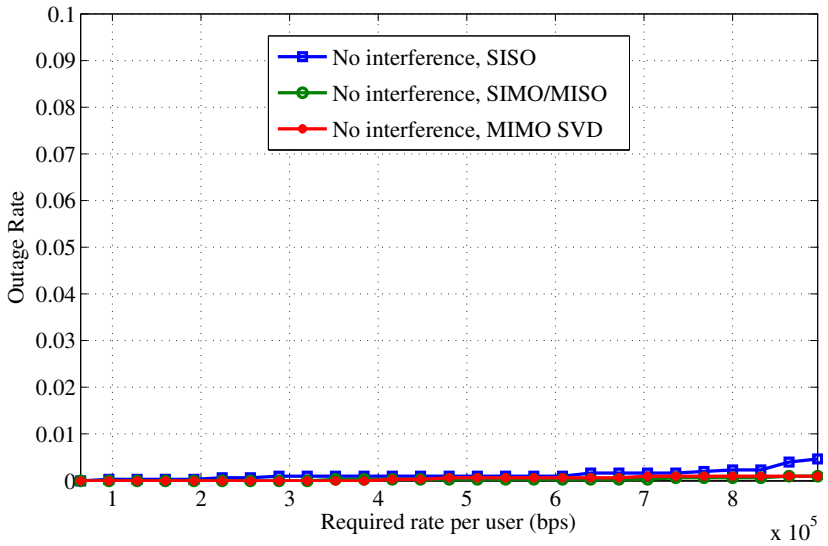

Figure 18 – Comparison of the outage rates for the case where there is no interference in the system, for all antenna arrangements.

Figure 19 presents a comparison of outage rates for all the antenna arrangements where the interference level (λ parameter) is set to 25%, where the suboptimal algorithm is and is not aware of interference.

For the first case, when the suboptimal algorithm knows the interference, we can see that the outage rates only increase for high required data rates, and mainly for the SISO case. This happens because when we add more antennas in the system, we can take advantage of the spatial dimension to improve the system performance, which contributes to lower outage rates. Evaluating the latter case (without interference knowledge), we can notice that the outage rates for all cases is over 90%. In this case, the suboptimal algorithm could not find a feasible solution for the allocation problem in most of the simulated snapshots, an issue that occurs due to the absence of knowledge about the interference in the system. For both cases we can notice that SIMO and MISO results are superimposed. This happens because the performance of MRC and

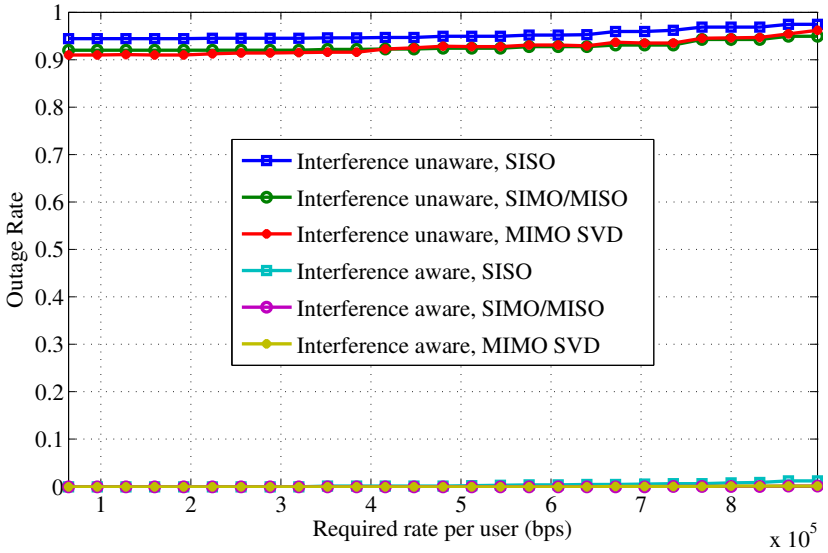

Figure 19 – Comparison of the outage rates for the case where there is interference in the system, for all antenna arrangements, with a cell loading (λ) of 25%.

MRT filters are equivalent, since we assume perfect CSI at both communicating ends.

Figure 20 also shows a comparison of outage rates for all the antenna arrangements, but with the interference level set to 75%. When the suboptimal algorithm is aware of interference we can notice that SISO outage rates are the ones with higher values, as explained before. For the highest data rate requirement (896 kbps), SISO outage rate is at 12%, while at the same point the outage rate for the MIMO case is at 3.6%. For the case where the suboptimal algorithm is not aware of interference, and for all antenna arrangements, the outage rates are almost at 100%. For this case, the suboptimal algorithm never finds a solution for the allocation problem.

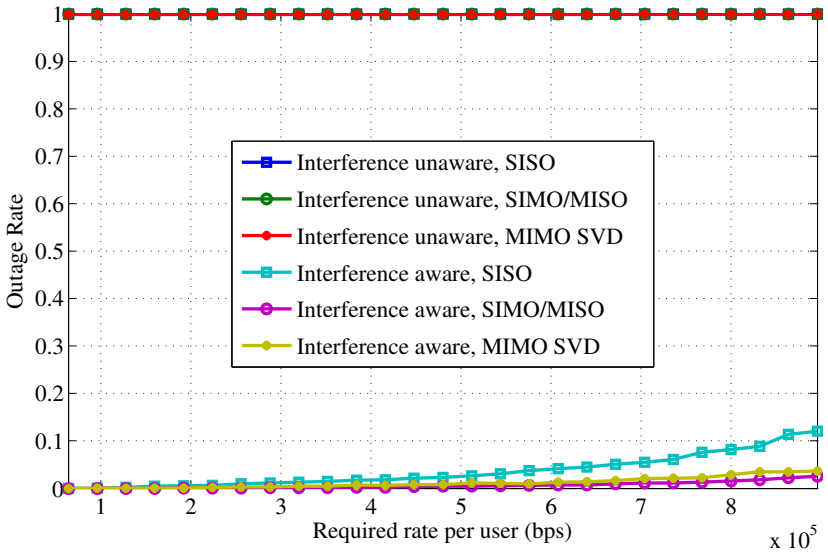

Figure 20 – Comparison of the outage rates for the case where there is interference in the system, for all antenna arrangements, with a cell loading (λ) of 75%.

For all the cases mentioned above we can clearly see how important it is for the suboptimal algorithm to know the interference in the system. It can take better decisions regarding the resource allocation when it knows the interference to which the UEs are subjected to. Also, when we increase the number of antennas in both communicating ends, we can take advantage of the spatial dimension, allowing the algorithm to improve its performance, even when the cell loading is set to higher values. Although, as the results presented in Figure 20 showed, we can see that the SIMO/MISO antenna arrangement has a slightly better result when compared to the MIMO arrangement, for the case where the algorithm is aware of interference. This happens because, for the MIMO arrangement, we have two streams on both transmitter and receiver, and both streams are subject to interference, while for the SIMO/MISO arrangement we only have one stream subject to interference. At the highest data rate requirement (896 kbps), the difference in outage between SIMO/MISO and MIMO is of 1%, as explained before.

Besides the interference impact, we also evaluate the suboptimal algorithm for the case when there is RB aggregation (3GPP, 2010c). This case is explained in details in the next section.

3.3.2.2 Impact of RB aggregation

Another evaluation performed during our studies was about the RB aggregation. The RB aggregation consists in the grouping of two or more RBs in order to form a RBG, described in (3GPP, 2010c) and previously explained in Chapter 2, Section 2.4.

Table 5 presents the simulation parameters for the different cases used to evaluate the performance of the suboptimal algorithm for the CRM problem in the presence of RB aggregation in the system.

Table 5 – Parameters of the considered scenarios for the downlink.

Parameter	**Value**
Antenna configuration	SISO, SIMO/MISO, MIMO
Number of UEs per service	8 (Service 1), 6 (Service 2)
Required number of satisfied UEs per service	7 (Service 1), 5 (Service 2)
Number of RBs	26, 45, 88
RBG size	2, 3, 4
UEs' required rate	[64 kbps:32 kbps:896 kbps] (26 RBs) [96 kbps:64 kbps:1.76 Mbps] (45 RBs) [160 kbps:128 kbps:3.488 Mbps] (88 RBs)

We start the evaluation by presenting a comparison for the outage rates for the

scenarios with and without RB aggregation. As it can be seen in Figure 21, the y-axis is set from 0 to 0.2 in order to allow a better visualization of the results.

Taking the SISO configuration as example, presented in Figure 21(a), we can see the outages rates have a difference of 15.34% for 26 RBs, 15.3% for 45 RBs and 8.7% for 88 RBs, between the cases with and without RB aggregation. For the SIMO/MISO and MIMO arrangements, we can also notice the same behavior showed for SISO: the outage rates are higher for the cases when there is RB aggregation. This happens because, in this case, we lose in RB granularity for the resource assignment due to aggregation, i.e., the suboptimal algorithm has to allocate RBs is groups of 2, 3 or 4 (depending on the total number of RBs in the system), instead of assigning each RB individually at a time, which means that, if a user could donate only one RB to another user in order to satisfy it, while maintaining its own satisfaction at acceptable levels, it could not be done, due to the aggregation restriction.

Figure 22 presents the SNRs curves for all the antenna configurations for the cases with and without RB aggregation, for the required data rate of 800 kbps. Inspecting the curves, we will see that the SNRs for the cases with RB aggregation present lower values when compared to the SNRs for the case without RB aggregation for all the antenna configurations. Table 6 brings the losses due to the RB aggregation for all antenna arrangements, as also for all number of RBs at the 50^{th} percentile. We can see that the highest losses are for the case where we have 88 RBs in the system, which means we have groups of 4 RBs to be allocated to each user. Those losses are above 85% for each antenna arrangement, and this behavior is due to the same reason mentioned before: the loss in granularity due to RB aggregation.

Table 6 – Losses due to RB aggregation in the 50^{th} percentile.

	SISO	**SIMO/MISO**	**MIMO**
26 RBs	85.84%	87.09%	72.68%
45 RBs	81.67%	83.97%	70.13%
88 RBs	90.87%	91.09%	85.87%

After the aforementioned evaluations, we decided to combine both in order to see how our system would behave in the presence of RB aggregation plus interference. The findings for this case are presented in the further section.

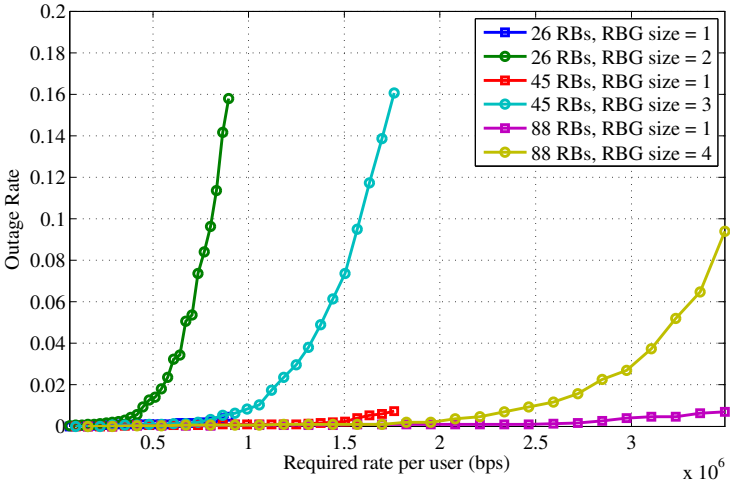

(a) SISO.

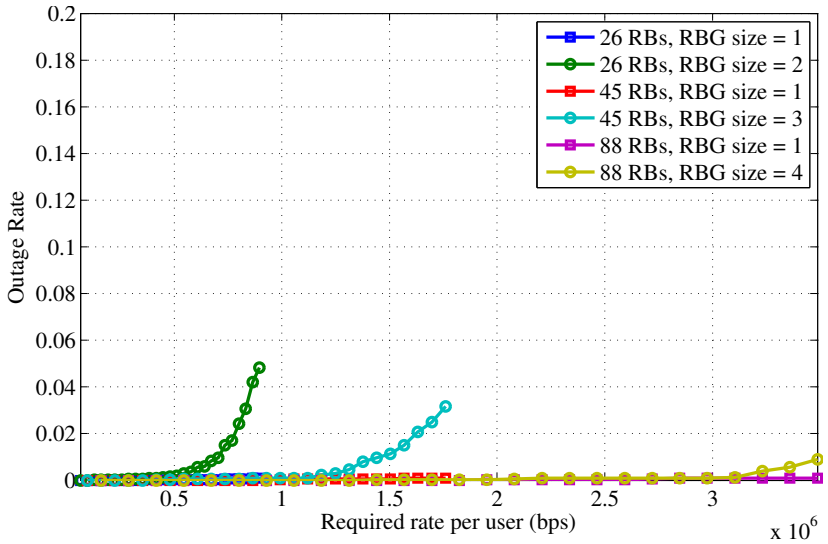

(b) SIMO/MISO.

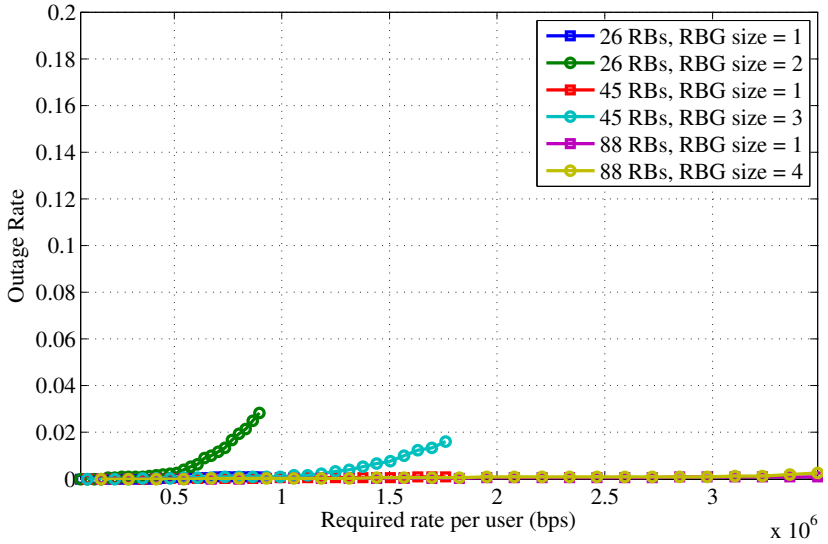

(c) MIMO.

Figure 21 – Comparison of the outage rates for the cases with and without RB aggregation.

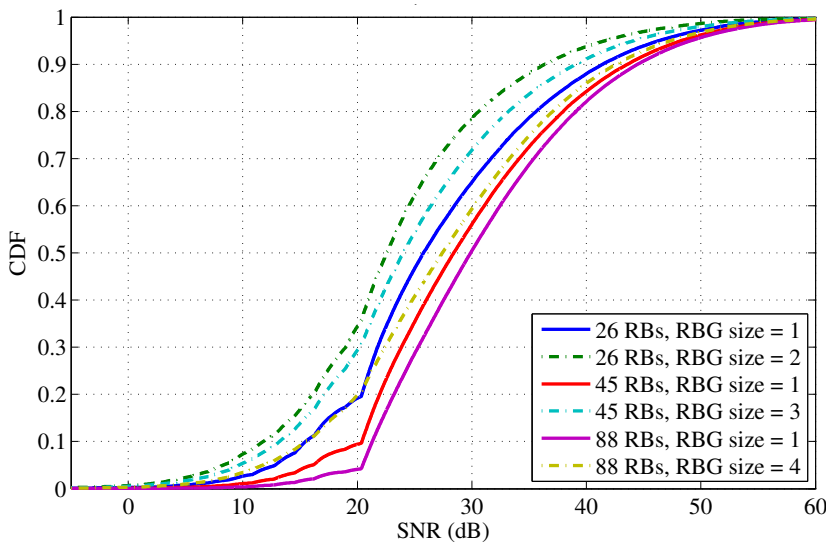

(a) SISO.

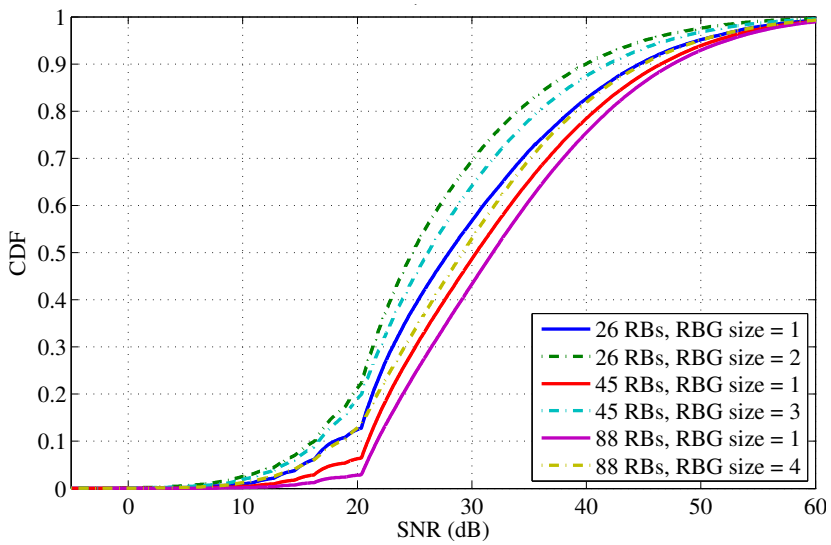

(b) SIMO/MISO.

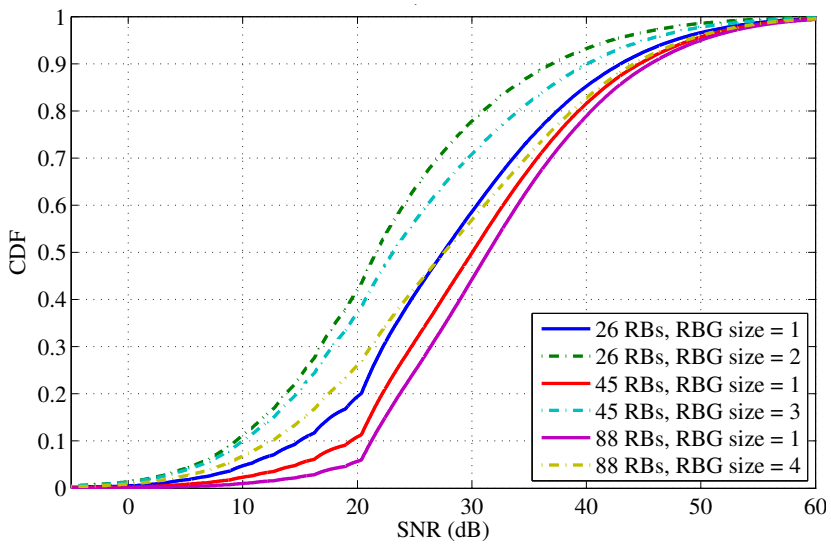

(c) MIMO.

Figure 22 – Comparison of the CDFs of the SNRs of the scheduled UEs in the system with and without RB aggregation. Required data rate: 800 kbps.

3.3.2.3 Impact of RB aggregation with interference in the system

The last evaluation we performed for DL direction was a mix between the two previously presented scenarios: the impact of RB aggregation with interference in the system. Table 7 presents the parameters considered during our evaluations.

Table 7 – Parameters of the considered scenarios.

Parameter	**Value**
Antenna configuration	SISO, SIMO/MISO, MIMO
Number of UEs per service	8 (Service 1), 6 (Service 2)
Required number of satisfied UEs per service	7 (Service 1), 5 (Service 2)
Number of RBs	26, 45, 88
RBG size	2, 3, 4
UEs' required rate	[64 kbps:32 kbps:896 kbps] (26 RBs) [96 kbps:64 kbps:1.76 Mbps] (45 RBs) [160 kbps:128 kbps:3.488 Mbps] (88 RBs)
Cell loading (λ)	25%, 50%, 75%, 100%

Figure 23 shows the outage rates for the SISO arrangement with 26 RBs for the cases with 25% and 75% of interference, respectively. In both figures, we can see three cases: one in which there is no interference in the system; the second, in which there is interference but the suboptimal algorithm is unaware of it, and a third one in which there is interference but the suboptimal algorithm has perfect knowledge about it. For each of these cases, there is also the comparison between the scenario where there is no RB aggregation, i.e., RBG size = 1, and the scenario where there is RB aggregation, i.e., RBG size = 2.

In both figures, we can see that the worst situation happens when the suboptimal algorithm is not aware of interference. This occurs because it does not know the interference levels in the system and, therefore, it assigns resources to the UEs based on wrong (too optimistic) estimates of their achievable data rates on each resource causing the outage events.

This impact of interference on the performance of the suboptimal algorithm can be noticed for both scenarios with and without RB aggregation. However, for the case when there is RB aggregation (when RBG size = 2), we can perceive that the outage rates are considerably higher than the ones for the case without RB aggregation for both figures. This is due to the fact that, when we group RBs, we lose in granularity for the resource assignment, i.e., the suboptimal algorithm has to allocate RBs in pairs in this specific case with 26 RBs (RBG size = 2), instead of assigning each RB individually at a time.

When we compare the cases where the suboptimal algorithm is aware of interference,

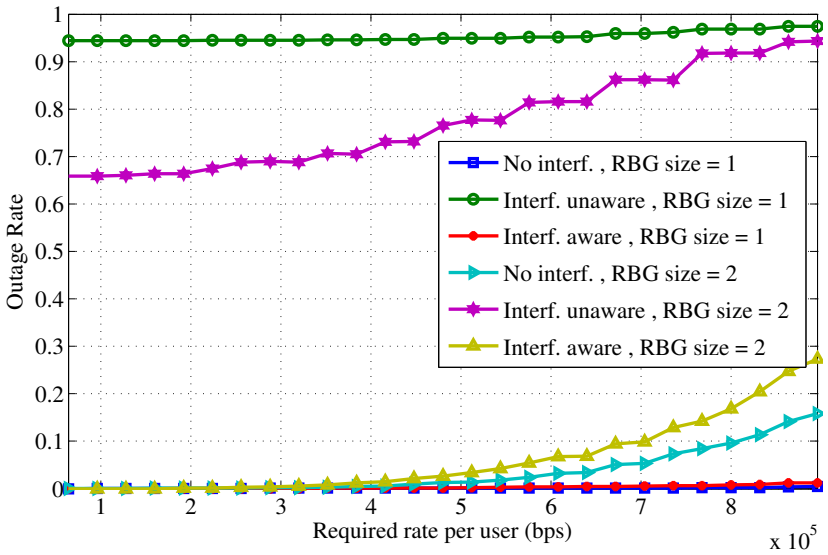

(a) $\lambda = 25\%$.

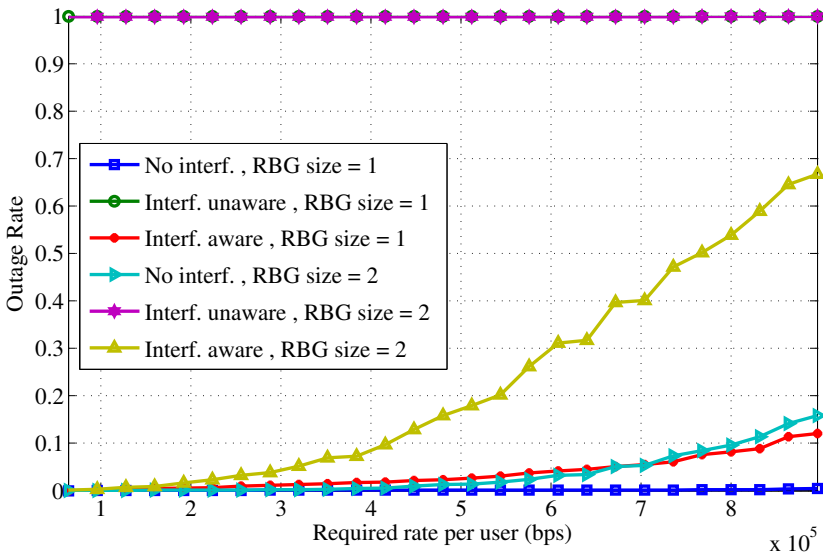

(b) $\lambda = 75\%$.

Figure 23 – Comparison of the outage rates for SISO scenario with 26 RBs with and without RB aggregation in the presence of interference in the system.

we can notice that the case with RB aggregation presents a higher outage rate in comparison with the case where there is no RB aggregation. We can see that for the required rate of 600 kbps, the case with RB aggregation presents an outage of 14%, while for the case without RB aggregation the outage for the same required rate is approximately 1%. As stated before, this increment in the outage is caused by the loss in granularity in the resource assignment.

Comparing the figures to each other, we can see that the worse situation occurs in Figure 23(b), for the case where there is RB aggregation and the suboptimal algorithm is not aware of it. Since we combine two conditions that decrease the system performance, this is exactly the behavior we expected from the algorithm: higher outage rates, which means that the

suboptimal algorithm could not find a feasible solution for the proposed problem.

Figure 24 presents a comparison between the outage rates for the SISO arrangement with 26, 45 and 88 RBs when the suboptimal algorithm is aware of interference, for the cell loading of 50%.

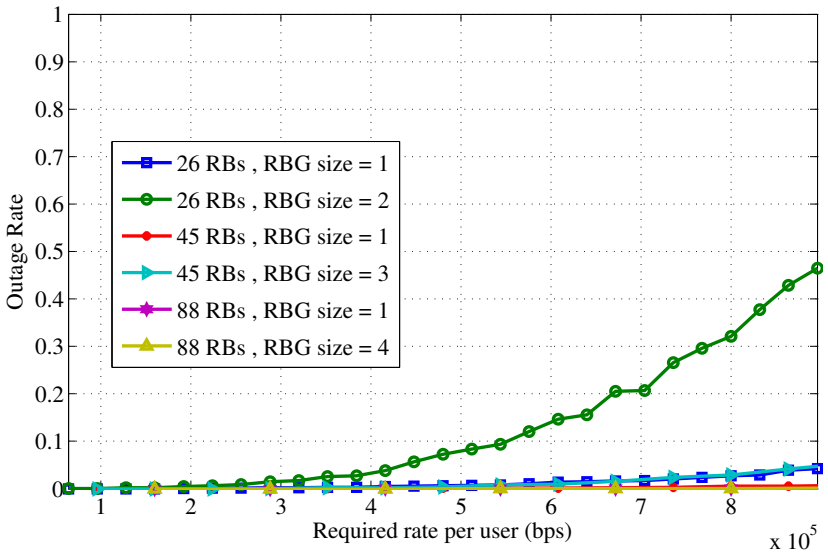

Figure 24 – Comparison of the outage rates for the SISO case with 26, 45 and 88 RBs with and without RB aggregation, with a cell loading (λ) of 50%. Suboptimal algorithm is aware of interference.

We can notice that for the cases in which there is RB aggregation, the outage rates are higher in comparison with the cases in which there is no RB aggregation. The reason for that is the same stated before: the loss of granularity in the resource assignment. Also, we can see that as the number of RBs in a RBG increases, the outage rates also increase. It is worth mentioning that Figure 24 presents only the scenario where the suboptimal algorithm is aware of interference and, as it can be noted in the curves, the algorithm's performance is strictly related to the RB aggregation.

Figure 25 shows the SINR values for SISO arrangement with 45 RBs, for the scenarios without interference and when there is interference and the suboptimal algorithm is aware of it, with and without RB aggregation, for the cell loading of 50%, for the required data rate of 800 kbps.

Looking at the 50th percentile in this figure, we can notice a difference of 18.33% between the case with and without RB aggregation when there is no interference, and a corresponding difference of 23.58% for the case where the suboptimal algorithm is aware of interference. These differences occur due to the loss in granularity caused by RB aggregation,

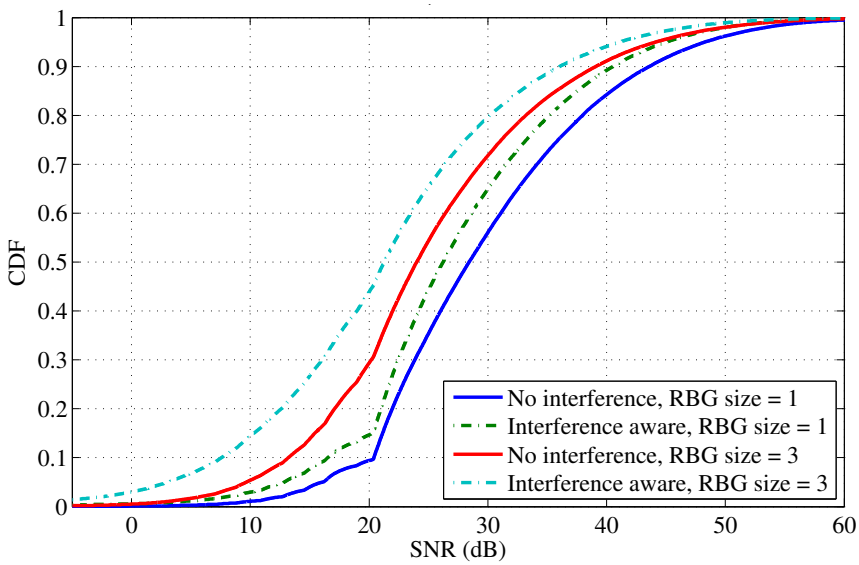

Figure 25 – Comparison of the SINRs for SISO case with 45 RBs, with a cell loading (λ) of 50%. Required rate: 800 kbps.

as explained in Section 3.3.2.2. We can also notice that the difference for the case with interference and the suboptimal algorithm aware of it is higher than the difference in the scenario without interference. This difference is explained by the presence of interference: when there is interference (even if the suboptimal algorithm knows it) the SINRs in the system tends to decrease.

We also compared the differences between the different antenna configurations. Figures 26(a), 26(b) presents a comparison between SISO and SIMO/MISO cases and SISO and MIMO, respectively, in a scenario with 45 RBs, where there is RB aggregation and with a cell loading of 50%.

The first thing to be noted is that SIMO and MISO results are superimposed. This happens because the performance of MRT and MRC are equivalent since we assume perfect CSI at both communicating ends. We can also see that, when we use more antennas in the system we can see almost the same behavior in the outage rates, when we compare SISO without interference and SIMO/MISO aware of interference. This is explained by the fact that, with more antennas the system, we can take advantage of the spatial dimension to improve the system performance.

In the absence of interference, and when there is interference but the suboptimal algorithm is aware of it, the outage values are quite low for the low and medium data rates requirements. This does not happen when there is interference and the suboptimal algorithm is unaware of it. For this case, and for all antenna arrangements, the outage rates are higher than

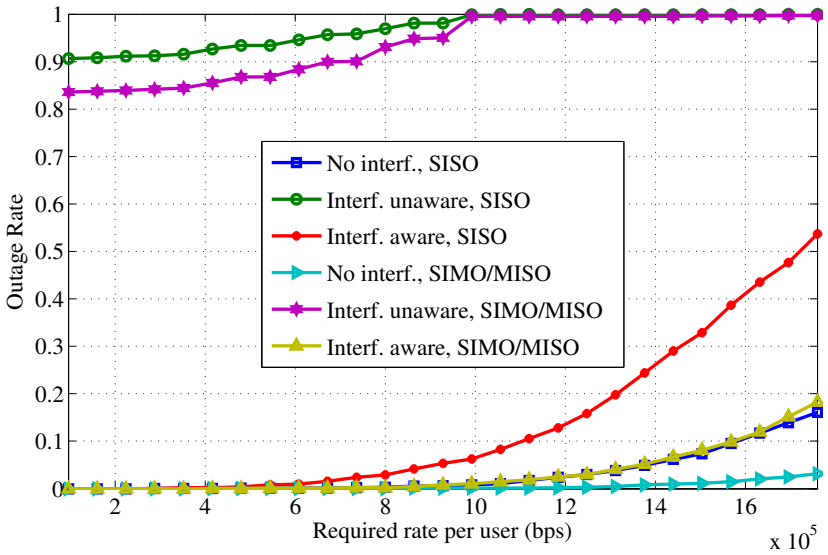

(a) SISO versus SIMO/MISO.

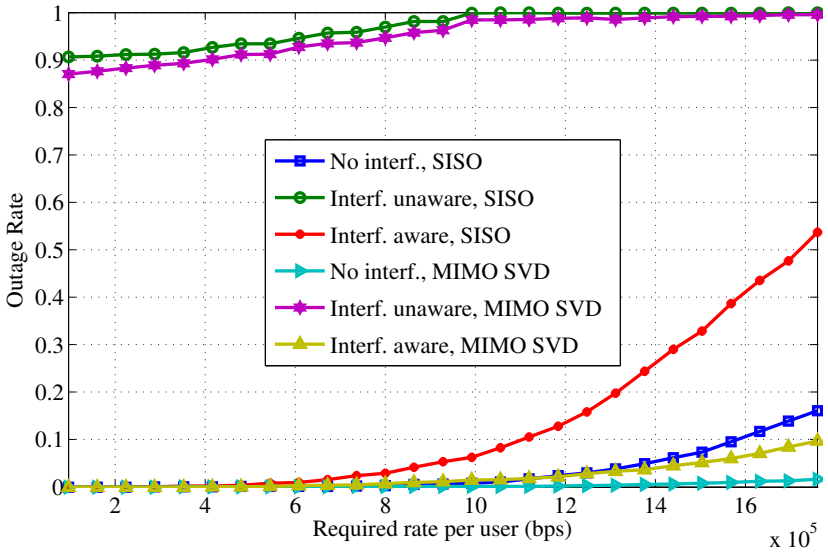

(b) SISO versus MIMO with SVD precoding.

Figure 26 – Comparison of the outage rates for a scenario with 45 RBs with RB aggregation in the presence of interference in the system, with a cell loading of 50%.

90%, as it is possible to see in the figures. This shows that the knowledge of interference can considerably increase the suboptimal algorithm performance. Regarding the antenna arrangements, we can notice that SISO case is the one with worst performance, even for the scenarios without interference. This is expected, since with more antennas the system can take advantage of the spatial dimension, as previously mentioned.

3.4 Partial Conclusions

In this chapter we presented the suboptimal solution to the CRM problem to the DL direction, for SU single and multi antenna arrangements, and also its behavior in the presence

of only interference, only RB aggregation and the combination of both interference and RB aggregation in the system.

The results showed that, as we increase the cell loading (the amount of interfering links in the cell), the system performance decreases. However, we also could see that we can overcome this issue if the suboptimal algorithm is aware of the interference present in the system. Related to the RB aggregation, we could see that the worse performance occurs when the RBs are aggregated. For both cases, we also could see that in the presence of multiple antennas in the transmitter and/or receiver, we have an increase in the system performance, which occurs due to the spatial diversity exploited by the multiple antennas.

When we combined inter-cell interference and RB aggregation, we could see that the system performance also tends to decrease. The worst case happens when there is interference and the suboptimal algorithm is not aware of it, together with RB aggregation. But again, if the suboptimal algorithm has knowledge about the interference, and if there is multiple antennas in the transmitter/receiver, then the system performance stays at good levels.

4 INTERFERENCE IMPACT FOR THE UPLINK CASE

In this chapter we will present how the interference impacts in the suboptimal solution given to the CRM problem to the uplink. We start describing the CRM problem for the uplink in Section 4.1, and we explain the suboptimal solution for this problem in Section 4.2. Section 4.3 is devoted to the performance evaluation of the suboptimal solution, where we show the simulation assumptions and discuss the results. We finish this chapter presenting some conclusions in Section 4.4.

4.1 Description of the CRM Problem for the Uplink Case

For the UL in LTE systems, the 3GPP consortium recommends the use of SC-FDMA, and for this multiple access model we have to deal with two restrictions related to resource allocation: **exclusivity**, where only one UE can be allocated per RB (this is also present in OFDMA) and **adjacency**, where a UE can have multiple RBs assigned to it, since those RBs are adjacent to each other. According to (WONG *et al.*, 2009), the number Υ of possible assignment patterns, dependent of the number R of RBs is given by:

$$\Upsilon = \frac{1}{2}R^2 + \frac{1}{2}R + 1. \tag{4.1}$$

from which we can define $\mathscr{Y} = \{1, \cdots, \Upsilon\}$ as the set of the indices of all possible assignment patterns.

In order to explain how the resource allocation is performed for the SC-FDMA, we can define a binary $R \times \Upsilon$ RB allocation matrix

$$\Omega = \begin{bmatrix} 0 & 1 & 0 & 0 & 0 & 1 & 0 & 0 & 1 & 0 & 1 \\ 0 & 0 & 1 & 0 & 0 & 1 & 1 & 0 & 1 & 1 & 1 \\ 0 & 0 & 0 & 1 & 0 & 0 & 1 & 1 & 1 & 1 & 1 \\ 0 & 0 & 0 & 0 & 1 & 0 & 0 & 1 & 0 & 1 & 1 \end{bmatrix}, \tag{4.2}$$

as seen in (WONG *et al.*, 2009), where each $\omega_{r,\upsilon}$ matrix element is set to 1, when an RB is assigned to a UE, and 0 otherwise. This matrix shows the possible assignment for a case where we have $R = 4$ and $\Upsilon = 11$.

Like we did for the DL, we consider the channel model in the frequency domain. We then define $\mathbf{X}^{\mathrm{UL}}$ as a $J \times \Upsilon$ assignment matrix with elements $x^{\mathrm{UL}}_{j,\upsilon}$, which are set to 1 if the assignment pattern $\upsilon \in \mathscr{Y}$ is assigned to the UE $j \in \mathscr{J}$ and 0 otherwise. The channel transfer

function for the j^{th} UE at the s^{th} subcarrier of the r^{th} RB is defined as $h^{\text{UL}}_{j,s,r}$. Differently from the OFDMA case, for the SC-FDMA case we define the channel transfer function in function of subcarriers, instead of RBs. This was done because we need a frequency domain equalization in SC-FDMA systems (MYUNG *et al.*, 2006), as we will further explain.

In addition to the resource allocation restrictions cited in (WONG *et al.*, 2009), the author also mention three restrictions related to power allocation:

(i) **Total power**, where the total transmission power for each UE should be less than a maximum power level P^{UL};

(ii) **Peak power**, where the peak transmission power for each UE on each subcarrier should be less than some peak power level $\hat{P}^{UL}_s$;

(iii) **Constant power allocation**, where all the subcarriers allocated to a UE must have a constant power.

In our case, we considered $\hat{P}^{UL}_s$ as

$$\hat{P}^{UL}_s = \frac{P^{UL}}{(\alpha * S)}, \tag{4.3}$$

where α represents a specific number of RBs, and S is the total number of subcarriers per RB. The values given for the α parameter will be presented in Section 4.3.

We then define the power each UE can use to transmit in a subcarrier in a RB as

$$\check{p}^{UL}_s = \min\left(\frac{P^{UL}}{S \cdot R}, \hat{P}^{UL}_s\right), \tag{4.4}$$

where R is the total number of RBs in the system.

From (2.6), we can define the SNR experienced by the UE j at the s^{th} subcarrier of the RB r for the case where there is no interference at the system as

$$\gamma^{\text{UL}}_{j,s,r} = \frac{\check{p}^{UL}_s \cdot \alpha^{\text{UL}}_j \cdot |h^{\text{UL}}_{j,s,r}|^2}{\underbrace{\zeta}_{\text{intra-cell interference}} + \left(\sigma^{sub}\right)^2}, \tag{4.5}$$

where α^{UL}_j is the effect of the path loss plus shadowing of the link between UE j and the serving BS, ζ represents the intra-cell interference experienced by UE j and $\left(\sigma^{sub}\right)^2$ is the noise power at the receiver in the bandwidth of a single subcarrier. Analogously, the SINR based in (2.7)

(used in a scenario with inter-cell interference) is defined as

$$\tilde{\gamma}^{\mathrm{UL}}_{j,s,r} = \frac{\check{p}^{UL}_{s} \cdot \alpha^{\mathrm{UL}}_{j} \cdot |h^{\mathrm{UL}}_{j,s,r}|^2}{\underbrace{\zeta}_{\text{intra-cell interference}} + \underbrace{\xi}_{\text{inter-cell interference}} + \left(\sigma^{sub}\right)^2}, \tag{4.6}$$

where ξ represents the inter-cell interference experienced by UE j.

As mentioned before, we need a frequency domain equalization in SC-FDMA systems (MYUNG *et al.*, 2006). This equalizer is used in order to mitigate Inter Symbol Interference (ISI), and in this work, analogously to which was done in (LIMA, 2012), we will use a Minimum Mean Square Error (MMSE) equalizer. With this equalizer, we can calculate the SNR (SHI *et al.*, 2004) of the data delivered by a certain RB set as:

$$\gamma^{\mathrm{UL\,MMSE}}_{j,\upsilon} = \left(\frac{1}{\frac{1}{c \cdot |\mathscr{R}_\upsilon|} \sum\limits_{r \in \mathscr{R}_\upsilon} \sum\limits_{z=1}^{c} \frac{\gamma^{\mathrm{UL}}_{j,z,r}}{\gamma^{\mathrm{UL}}_{j,z,r}+1}} - 1 \right)^{-1}, \tag{4.7}$$

where $\gamma^{\mathrm{UL\,MMSE}}_{j,\upsilon}$ is the effective SNR experienced by the data transmitted by UE j with the RBs present in the assignment pattern υ, c is the number of subcarriers in one RB, and $\mathscr{R}_\upsilon$ is the set of RBs that compose the assignment pattern υ.

From (4.7), we defined the SINR of the data delivered by a certain RB set in a scenario with inter-cell interference as:

$$\tilde{\gamma}^{\mathrm{UL\,MMSE}}_{j,\upsilon} = \left(\frac{1}{\frac{1}{c \cdot |\mathscr{R}_\upsilon|} \sum\limits_{r \in \mathscr{R}_\upsilon} \sum\limits_{z=1}^{c} \frac{\tilde{\gamma}^{\mathrm{UL}}_{j,z,r}}{\tilde{\gamma}^{\mathrm{UL}}_{j,z,r}+1}} - 1 \right)^{-1}, \tag{4.8}$$

where $\tilde{\gamma}^{\mathrm{UL\,MMSE}}_{j,\upsilon}$ is the effective SINR experienced by the data transmitted by UE j with the RBs present in the assignment pattern υ.

An improvement performed in this work compared to the evaluations performed in (LIMA, 2012) was the introduction of a link adaptation function, responsible for mapping the SNR/SINR to the transmit data rate. In order to change the transmit data rate, we assume that the modulation and channel coding rates are changed according to the channel state. We assume that there are some MCS, each one with different performance regarding the BLER. Following this

model, the transmit data rate of UE j when assigned to the assignment pattern υ is defined as:

$$q_{j,\upsilon}^{\mathrm{UL}} = \begin{cases} f(\gamma_{j,\upsilon}^{\mathrm{UL\,MMSE}}), & \text{if there is no interference in the system} \\ f(\tilde{\gamma}_{j,\upsilon}^{\mathrm{UL\,MMSE}}), & \text{if there is interference in the system} \end{cases} \tag{4.9}$$

With the definitions above, we can now write the CRM problem for the UL in its standard form (LIMA, 2012):

$$\max_{\mathbf{X}^{\mathrm{UL}}} \left(\sum_{j \in \mathscr{J}} \sum_{\upsilon \in \mathscr{Y}} q_{j,\upsilon}^{\mathrm{UL}} \cdot x_{j,\upsilon}^{\mathrm{UL}} \right), \tag{4.10a}$$

subject to

$$\sum_{j \in \mathscr{J}} \sum_{\upsilon \in \mathscr{Y}} \omega_{r,\upsilon} \cdot x_{j,\upsilon}^{\mathrm{UL}} = 1, \quad \forall r \in \mathscr{R}, \tag{4.10b}$$

$$\sum_{\upsilon \in \mathscr{Y}} x_{j,\upsilon}^{\mathrm{UL}} = 1, \quad \forall j \in \mathscr{J}, \tag{4.10c}$$

$$x_{j,\upsilon}^{\mathrm{UL}} \in \{0,1\}, \quad \forall j \in \mathscr{J} \text{ and } \forall \upsilon \in \mathscr{Y}, \tag{4.10d}$$

$$\sum_{j \in \mathscr{J}_s} u\left(\sum_{\upsilon \in \mathscr{Y}} q_{j,\upsilon}^{\mathrm{UL}} \cdot x_{j,\upsilon}^{\mathrm{UL}}, t_j \right) \geqslant k_s, \quad \forall s \in \mathscr{S}. \tag{4.10e}$$

In (4.10a) is the objective function, which is the total uplink data rate transmitted by the UEs. To assure that the RBs are not reused within the interest cell, the constraints (4.10b) and (4.10d) were defined. Constraints (4.10c) and (4.10d) guarantee that only one assignment pattern is chosen by each UE. Finally, constraint (4.10e) indicates that a minimum number of UEs should be satisfied for each service.

In (LIMA, 2012), besides the CRM problem, the author also evaluates another one: the Unconstrained Rate Maximization (URM) problem. He proposed a suboptimal solution for this problem, and since this is not part of our studies, we will use this solution in order to cope with the one given for the CRM problem.

4.2 Low-Complexity Suboptimal Solution for the CRM Problem for the Uplink Case

As the suboptimal solution for the CRM problem for the DL case, the solution for the UL case is also split in two parts: **Unconstrained Maximization** and **Reallocation**. These parts are depicted in Figure 27 and Figure 28, respectively. This solution was firstly described in (LIMA, 2012) and the text below is a direct adaptation of that description.

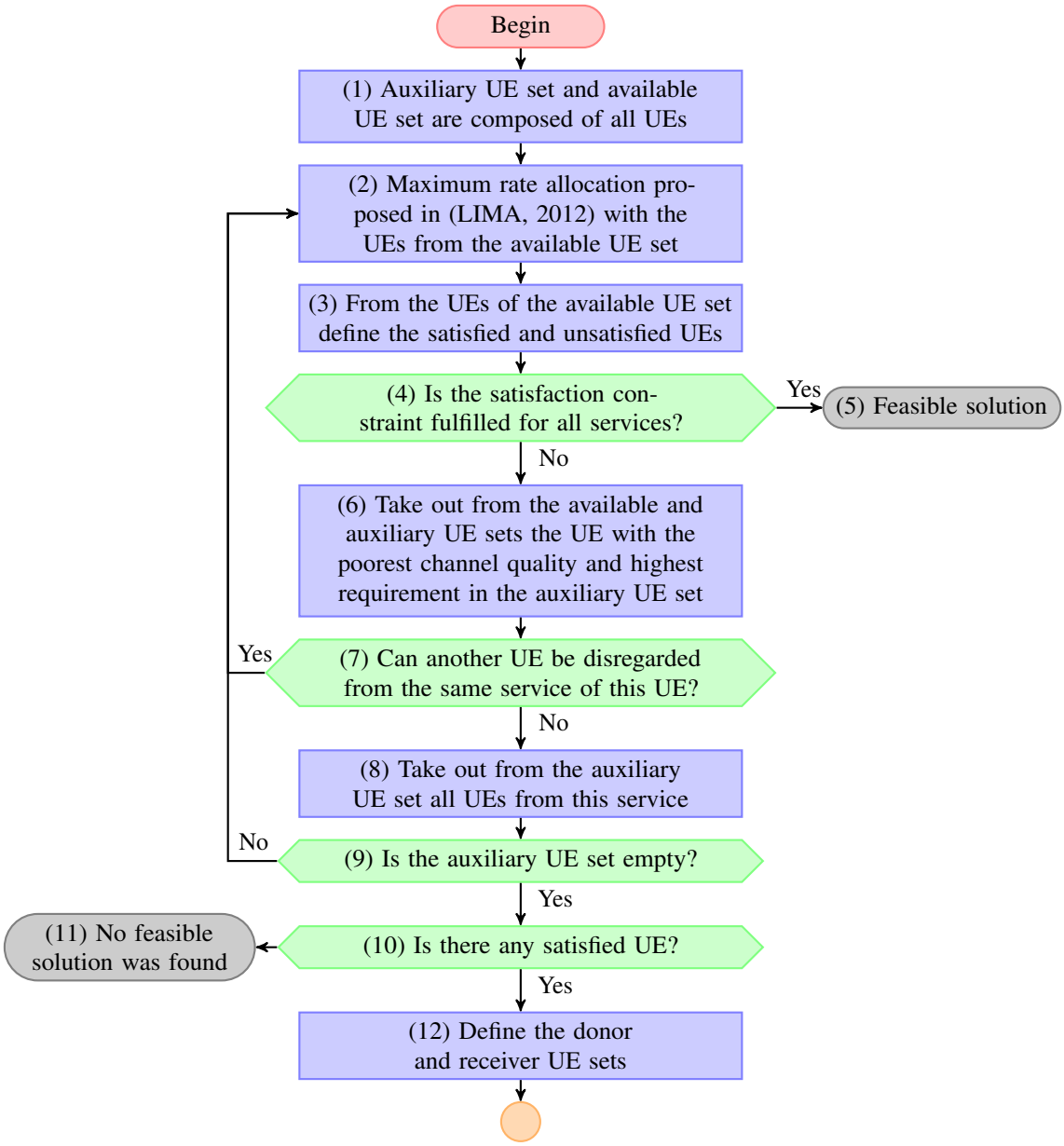

Figure 27 – Flowchart of the first part of the suboptimal framework proposed for the uplink: Unconstrained Maximization (adapted from (LIMA, 2012)).

In the **Unconstrained Maximization** part, the idea is to have an initial assignment which guarantees that the highest possible data rate in the system can be achieved. The algorithm is started (step (1)) by defining the auxiliary ($\mathscr{B}$) and available ($\mathscr{G}$) UE sets and initializing them with the set of all UEs ($\mathscr{J}$). Then in step (2) the maximum rate allocation with the UEs from the available UE set is solved, using the suboptimal solution for the URM problem proposed in (LIMA, 2012). The maximum rate allocation basically assigns each available resource from the resource set ($\mathscr{R}$) to the UE with highest rate on it. After that, on step (3), the UEs that have the data rate requirement fulfilled are defined as the satisfied UEs and the remaining ones as the

unsatisfied UEs. If the minimum required number of satisfied UEs of each service is achieved, as shown in step (4), a feasible solution was found (step (5)). However, note that this is an uncommon situation due to the distribution of the UEs within the cell. In general, few UEs will get most of the available resources.

If the satisfaction constraint for any service is not fulfilled, a UE of the auxiliary UE set ($\mathscr{B}$) will not receive resources at the current TTI, thus it will be ignored. The criterion to select the UE $j^{\star}$ that will not receive any resources for the case without interference in the system is given by

$$j^{*} = \arg\min_{j \in \mathscr{B}} \frac{\frac{1}{c \cdot R} \sum_{r \in \mathscr{R}} \sum_{z=1}^{c} \gamma_{j,z,r}^{\mathrm{UL}}}{q_j}, \tag{4.11}$$

and for the case where there is interference in the system the same criterion is given by

$$j^{*} = \arg\min_{j \in \mathscr{B}} \frac{\frac{1}{c \cdot R} \sum_{r \in \mathscr{R}} \sum_{z=1}^{c} \tilde{\gamma}_{j,z,r}^{\mathrm{UL}}}{q_j}, \tag{4.12}$$

With this criterion the UE that requires, in average, more RBs to be satisfied is ignored. The selected UE is removed from the available and auxiliary UE sets, as showed in step (6).

The next step is to check whether the service of the ignored UE can have another UE ignored without infringing its minimum satisfaction constraints (step (7)). If this is not possible, all the UEs from this service are removed from the auxiliary UE $\mathscr{B}$ set (step(8)) . In this case, no UE from that service will be ignored anymore. All this procedure is repeated until either a feasible solution is found or no UE can be ignored, i.e., the auxiliary UE set is empty. In the former case, where the auxiliary UE set ($\mathscr{B}$) in not empty (step (9)), the maximum rate allocation is performed again with the remaining UEs in the available UE set. In the latter case, it is checked if at least one UE is satisfied (step (10)). If so, in step (12) from the available UE set ($\mathscr{G}$) two new sets are defined: the donor ($\mathscr{D}$) and receiver UE sets ($\mathscr{N}$). The donor UE set is composed of the satisfied UEs in the available UE set and can donate RBs to the unsatisfied UEs. The receiver UE set is composed of the unsatisfied UEs from the available UE set and need to receive RBs from the donors to have fulfilled their rate requirements. In case there is no satisfied

UE after executing the first part, the suboptimal algorithm is not able to find a feasible solution (step (11)), i.e., that comply with the minimum satisfaction constraints.

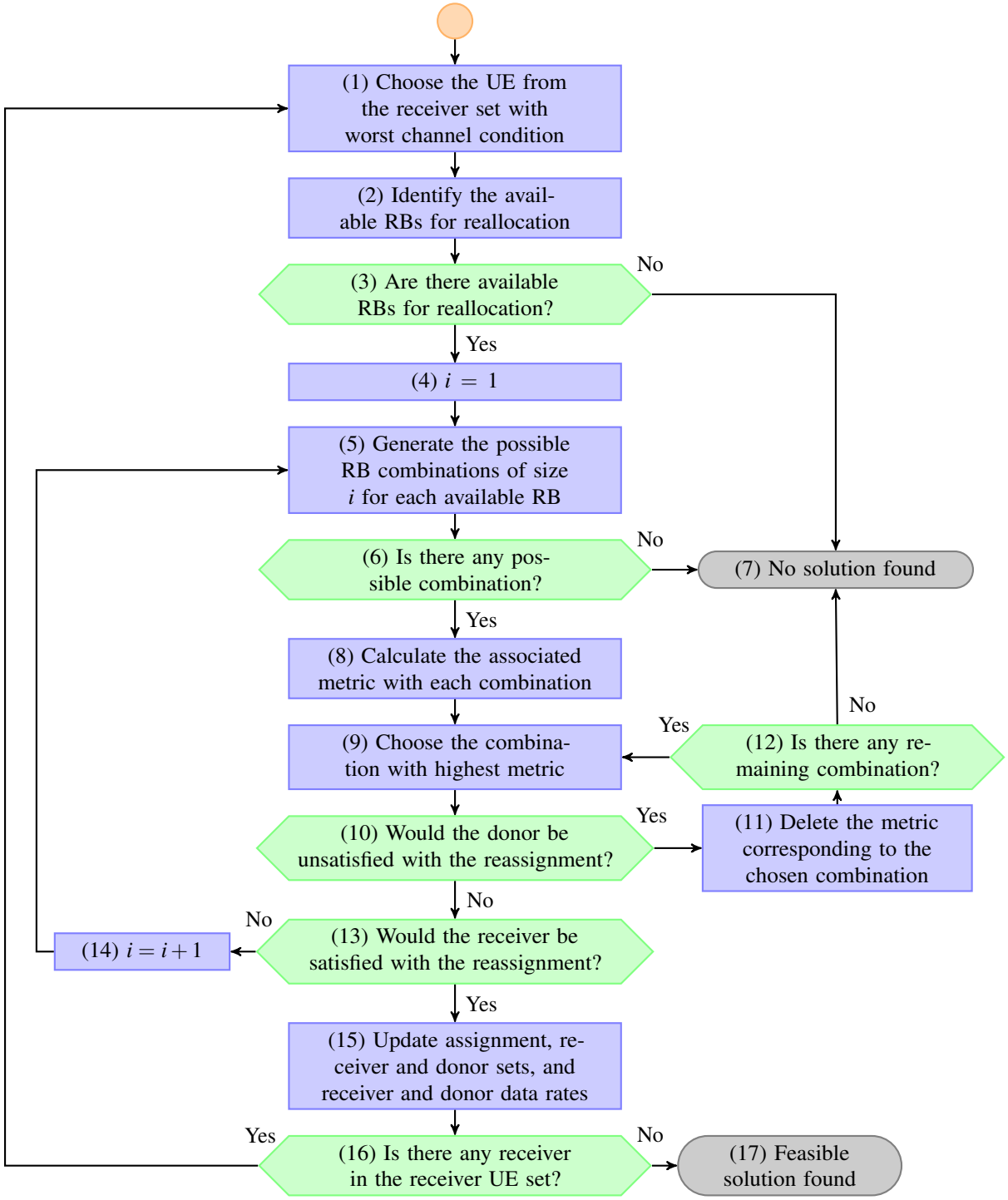

Figure 28 – Flowchart of the second part of the suboptimal framework proposed for the uplink: Reallocation (adapted from (LIMA, 2012)).

In the **Reallocation** part, presented in Figure 28, RBs are reallocated from the donors to the receivers. In step (1) a UE from the receiver UE set ($\mathcal{N}$) is chosen, and it is the one with

the worst channel quality to get resources until its data rate requirement is fulfilled. This is done in order to assign the minimum number of RBs to the UEs in bad channel conditions as to get them satisfied and assign the remaining RBs to the UEs with better channel quality, thus increasing the total cell throughput. In step (2), the RBs that can be reassigned to the selected receiver UE are chosen. There are two possibilities here, as seen in (LIMA, 2012):

1. A RB or a block of RBs was assigned to the receiver UE in the first part of the algorithm: Stating that the selected UE has got assigned the block of RBs from r' to r'' with $r' \leq r''$ and $r' \neq 1$ and $r'' \neq R$. In this case, the RBs available for reassignment are $r' - 1$ and $r'' + 1$. It should be noticed that if $r' = 1$ or RB $r' - 1$ is assigned to another receiver UE, the RB $r' - 1$ is not available for reallocation. Similarly, if $r'' = R$ or RB $r'' + 1$ is assigned to another receiver UE, the RB $r'' + 1$ is not available for reallocation.
2. Receiver UE was not assigned to any RB in the first part: In this case, the available RBs for reallocation are the first and the last RBs of the blocks assigned to each donor UE in the first part of the proposed framework.

For the case **i**, when the receiver UE already got some RBs, the RB selected to reallocation are the ones adjacent the to the receiver UE, in order to not to break the adjacency constraint. For the case **ii**, we select a RB to be reallocate in a way that it does not break the adjacency constraint on the RBs assigned to the donor UEs.

Figure 29 presents a possible assignment for the first part of the algorithm. In this figure, we have 10 RBs, as also 4 UEs, with UEs 1 and 4 being donors, and UEs 2 and 3 being receivers. In all presented examples we selected UEs 2 to receive the selected RBs (represented by the dashed line). Examples 1 to 3 show the case **i**, while example 4 shows the case **ii**.

The next step ((3)) is to check whether there is at least one RB for reallocation. If there is not any, the algorithm is not able to find a feasible solution. Then, in step (4), the variable i is initialized, and the algorithm proceeds to step (5) where the possible contiguous RB combinations of size i for each available RB selected in step (2) are generated, according to (LIMA, 2012).

In step (6) it is verified if there is at least one RB group able to be reallocated without infringing any constraint. If there is not (step (7)), the algorithm did not find a feasible solution. If there is, the algorithm proceeds to step (8), where the efficiency metric associated with each

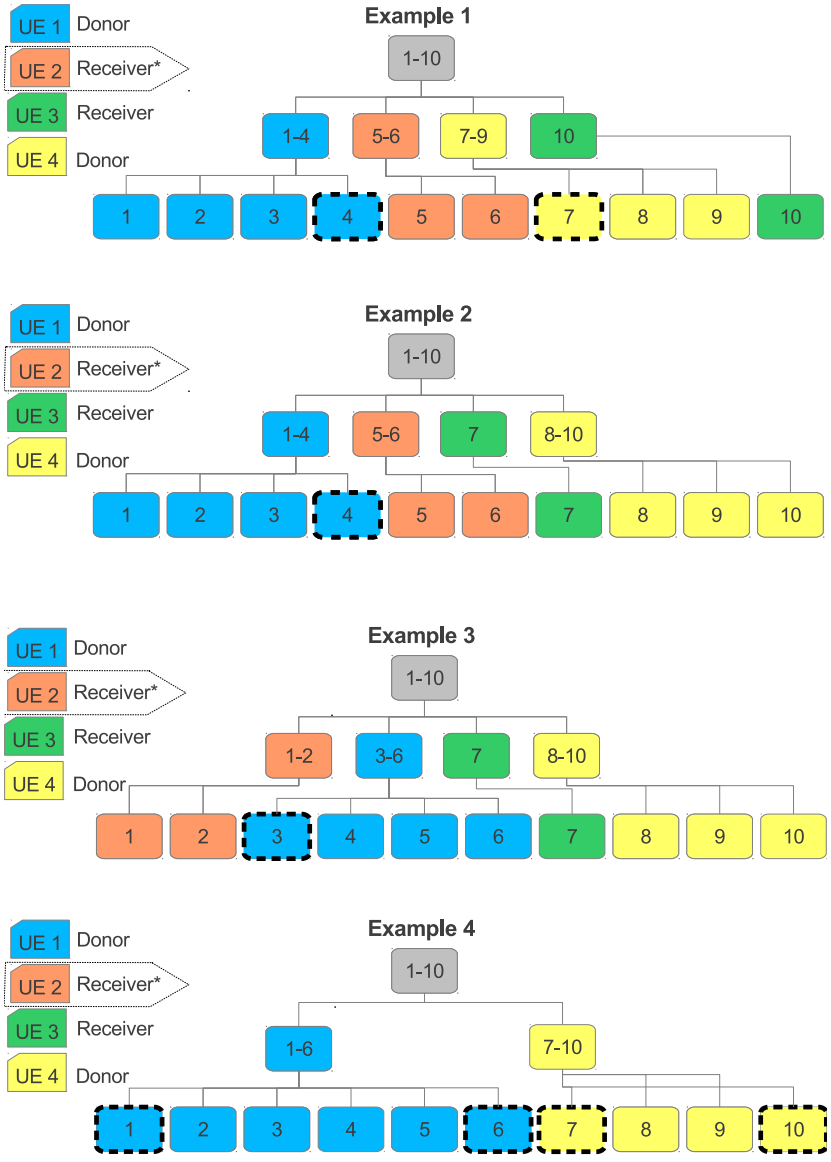

Figure 29 – RB allocation example, for a scenario with 10 RBs and 4 UEs (adapted from (LIMA, 2012)).

possible RB group generate in step (5) will be calculated, as follows:

$$\varphi_a^{\text{CRM UL}} = \left(\frac{1}{\frac{1}{c \cdot (r'' - r' + 1)} \sum_{r=r'}^{r''} \sum_{z=1}^{c} \frac{\gamma_{j^*,z,r}^{\text{UL}}}{\gamma_{j^*,z,r}^{\text{UL}} + 1}} - 1 \right)^{-1}, \tag{4.13}$$

where j^* is the receiver UE index and $\varphi_a^{\text{CRM UL}}$ is the efficiency metric of the ω^{th} RB group. This is the metric for the case where there is no interference in the system, and it represents the effective SNR of all subcarriers in the RB group (LIMA, 2012). Analogously, the metric used

for the case where there is interference in the system is defined as

$$\tilde{\varphi}_a^{\text{CRM UL}} = \left(\frac{1}{\frac{1}{c \cdot (r'' - r' + 1)} \sum_{r=r'}^{r''} \sum_{z=1}^{c} \frac{\tilde{\gamma}_{j^*,z,r}^{\text{UL}}}{\tilde{\gamma}_{j^*,z,r}^{\text{UL}} + 1}} - 1 \right)^{-1} \tag{4.14}$$

In step (9), having the metric calculated in step (8), the RB group with the highest efficiency metric is chosen. Then it is verified, in step (10), if this reassignment would led the donor UE to an unsatisfied state, and in an affirmative case, the metric corresponding to the chosen RB group is deleted (as this same group is ignored) (step (11)), and the next RB group with the highest efficiency metric is chosen. After that, it is necessary to check if the receiver UE will be satisfied when receiving this RB group (step (14)). If the receiver UE is not satisfied after that, variable i is incremented, thus incrementing the number of RBs in a RB group, and the operation is performed again starting from step (5).

When the receiver UE is finally satisfied, the RBs assignment, the receiver and donor sets are updates, as also their respective data rates (step (15)). In step (16) it is checked if the receiver set ($\mathcal{N}$) is empty. If it is not, then the **Reallocation** part is performed from the beginning. If this set is empty, then a feasible solution for the CRM problem was found.

Figure 30 shows the result of the suboptimal algorithm for the example 4 in Figure 29. This figure presents all the possible combinations of RB groups that could be reallocated to UE 2. The RBs assigned to UE 2 are represented in the figure by the boxes with the dotted line.

In the further sections we will present the performance evaluation for the algorithm described above in scenarios subject to interference, as also considering the power constraints mentioned in (WONG *et al.*, 2009).

4.3 Performance Evaluation

This section presents the analyses on the performance of suboptimal solution for the CRM problem for the UL in a scenario with inter-cell interference. We evaluate the UEs' SINRs, outage rates for different values of λ, the MCS usage, since we added SNR/SINR to MCS mapping in our link adaptation and the CDF for the interference power experienced for the UEs. In Section 4.3.1, we present the main simulation assumptions and performance metrics used for comparison. In Section 4.3.2 we show the simulation results.

4.3.1 Simulation Assumptions

In order to evaluate how the interference can impact in the suboptimal solution proposed for the UL case, we performed simulations for different cell loadings (λ parameter). We were also interested in investigating how the power restrictions, mentioned in Section 4.1, can influence the results.

Table 8 summarizes the main simulation parameters.

Table 8 – Main simulation parameters for the uplink scenario.

Parameter	Value	Unit
Cell radius	334	m
Number of subcarriers per RB	12	-
Number of snapshots	3700	-
Number of discarded snapshots [a]	200	-
Antenna configuration $M_R \times M_T$	1×1	SISO
Shadowing standard deviation	8	dB
Path loss	$35.3 + 37.6 \log_{10}(d)$ [b]	dB
Noise spectral density	$3.16 \cdot 10^{-20}$	W/Hz
Total UE power	23	dBm
Number of RBs (α) used to calculate the peak power [c]	5, 15, 25	-
Channel model	Classical IID ZMCSCG	-
Number of services	2	-
Number of UEs per service	8 (Service 1), 6 (Service 2)	
Required number of satisfied UEs per service	7 (Service 1), 5 (Service 2)	
Number of RBs	26	
UEs' required rate	[12 kbps:12 kbps:288 kbps]	
Cell loading (λ)	25%, 50%, 75%, 100%	

We simulated the scenario where there is interference in the system and the suboptimal algorithm is aware of it, and the case where the is interference in the system but the suboptimal algorithm is not aware of it. We also simulated the scenario without interference for comparison purposes. The metrics used during our evaluations are: UEs SNR/SINR, outage rates, MCS usage and inter-cell interference power. An outage event happens when the suboptimal solution to the CRM problem can not manage to find a feasible solution as described in the previous chapter. The MCS usage will be presented in order to show how the UEs behave in the different conditions imposed by our simulations. With those results, we intend to prove that the link adaptation done for the UL is working smoothly.

Finally, increments in the offered load are emulated by increasing the rate requirements of the UEs for all the scenarios described above. We also incremented the cell loading in the system in order to obtain a better view of the simulated scenarios. All the UEs have the same

data rate requirement independently of service type.

4.3.2 Results and Analyses

In this section we will show the results obtained for the suboptimal solution to the CRM problem in the UL in a system subject to inter-cell interference and power restrictions.

We start our analyses by presenting in Figure 31 the CDFs of the SINRs for the scheduled UEs in the system for three scenarios: no interference in the system, interference in the system, but the suboptimal algorithm is not aware of it and interference in the system and the suboptimal algorithm aware of it.

This figure represents the case where the system is subject to 100% of interference, as also with the α parameter set to 5. We can see that the case with the worst condition is the case where the suboptimal algorithm is not aware of interference (green curve). We can also see that, when we give the interference knowledge to the suboptimal algorithm, we increase the system performance, represented in the figure by the red curve. This shift to the right (when compared to the green curve) represents the gain obtained by the algorithm due to the interference knowledge.

As we make the suboptimal algorithm aware of interference, it can use this knowledge in order to perform a more accurate calculation of the efficiency metric (step (8) in the **Reallocation** part of the algorithm) that will be used to select the group of RBs that are going to be assigned to the UEs. It is clear by the figure the system presents the expected behavior: worst case (leftmost curve, green), when the suboptimal algorithm has no knowledge about the interference, better case (rightmost curve, blue), when there is no interference in the system, and between these (red curve), when the suboptimal algorithm is aware of interference.

In order to show the capability of suboptimal algorithm in finding a solution for the CRM problem, Figure 32 presents the outages rates for the three scenarios used during our evaluations, for the case where we have 100% of interference in the system, and with the α parameter set to 5, as we did for the previous figure.

Firstly, we can notice that, as we increase the data rates requirements, the outage rates increase for all the presented scenarios, as expected. Related to the difference presented between the scenarios with and without the interference knowledge, we can see that, for the former case, the outage rates are considerably smaller in comparison to ones in the latter case. Taking the required data rate of 192 kbps as reference, we can see that for the case where the suboptimal algorithm is aware of interference in the system, the outage rate is 9.4%, while for

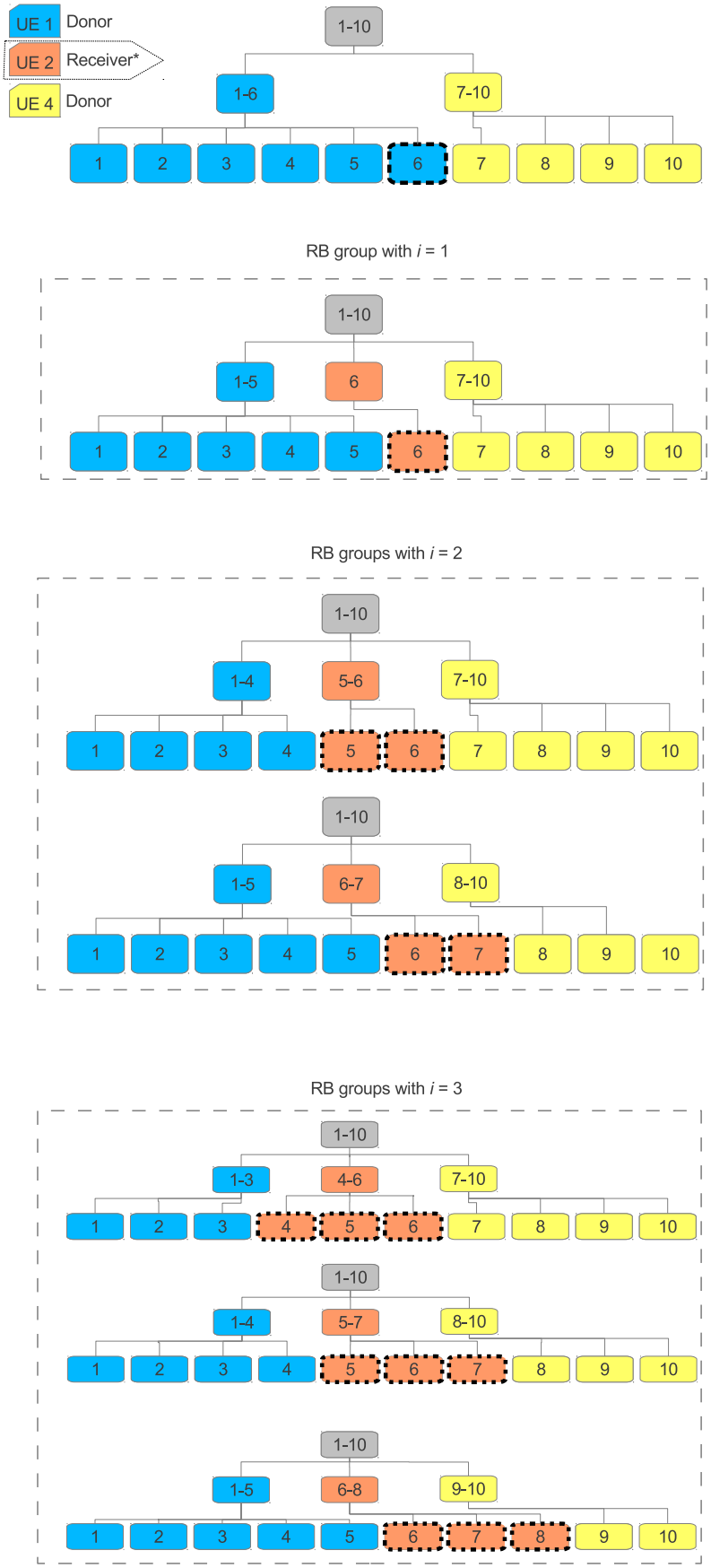

Figure 30 – RB reallocation example, for the example 4 in Figure 29, for different values of *i* variable (adapted from (LIMA, 2012)).

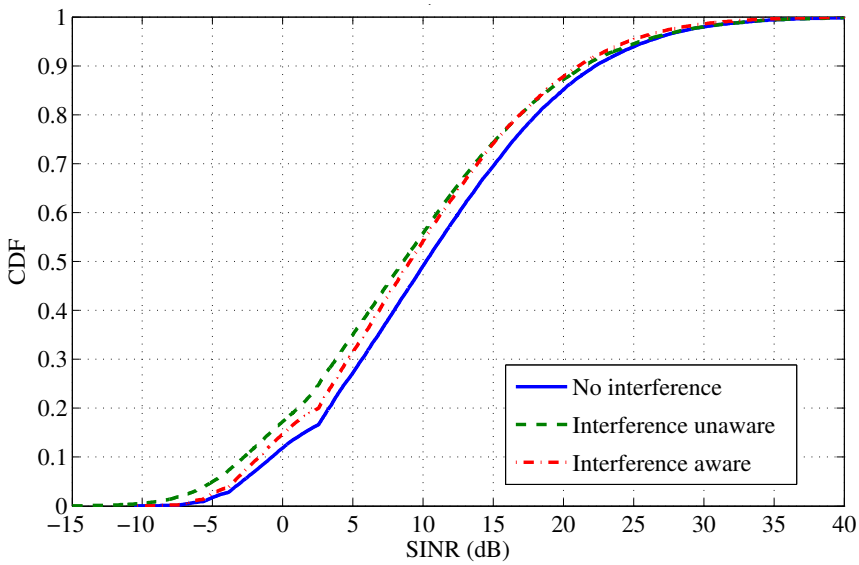

Figure 31 – Comparison of CDFs of the SINRs of the scheduled UEs in the system. Required data rate: 288 kbps, $\lambda = 100\%$, $\alpha = 5$.

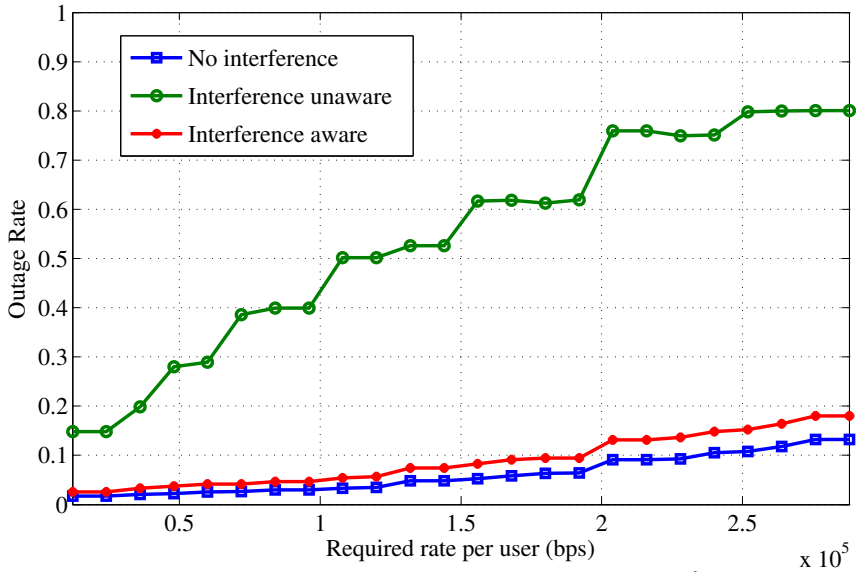

Figure 32 – Comparison of the outage rates for the three scenarios, $\lambda = 100\%$, $\alpha = 5$.

this same rate the for the case where the algorithm is not aware of interference the outage is 62%. We can clearly see that, for this case, the interference knowledge by the algorithm presents a difference of 52.6% in the outage rates, which shows that the suboptimal algorithm can take better decisions when it is aware of interference.

We also wanted to study how the increase in the cell loading could affect our system. Figure 33 presents the SINRs for the case where the suboptimal algorithm **is not aware of interference**, for different values of cell loading. First observation we can do is related the positioning of the curves. We can see the differences between all the evaluated cases. We can also see that the worst case scenario is the one where we have 100% of cell loading, as expected.

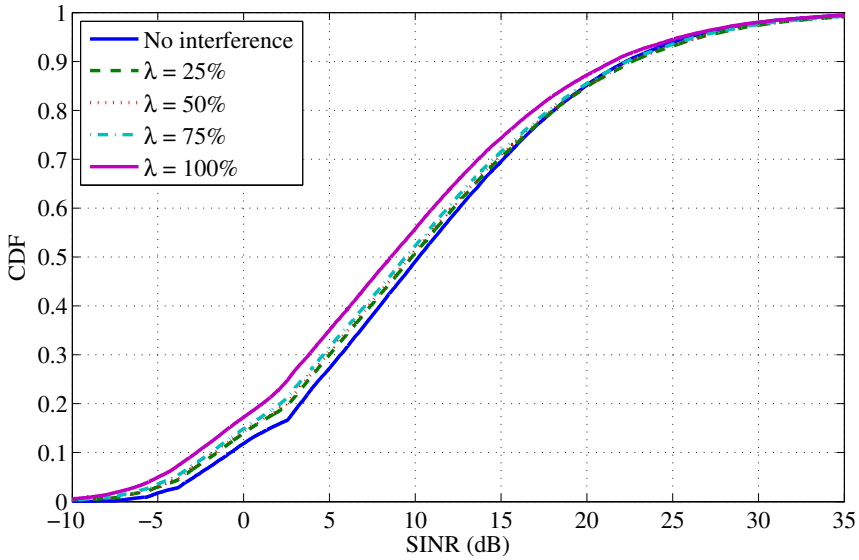

Figure 33 – Comparison of CDFs of the SINRs of the scheduled UEs in the system for the different values of λ when the suboptimal algorithm **is not aware of interference**. Required data rate: 288 kbps, $\alpha = 5$.

Figure 34 presents the SINRs for the case where the suboptimal algorithm **is aware of interference**, for different values of cell loading.

Differently from the previous figure, where we could see the difference between the curves for the intermediary cell loadings (from 25 to 75%), in this case those curves are almost superimposed. This is a result of the interference knowledge by the suboptimal algorithm. However, analogously to the previous case, the worst case scenario is the one where we have 100% of interference. This is quite reasonable, since with the system fully loaded — regarding interference —, the resource allocation becomes a difficult task, thus decreasing the system performance.

In order to show how the suboptimal algorithm deals with different interference

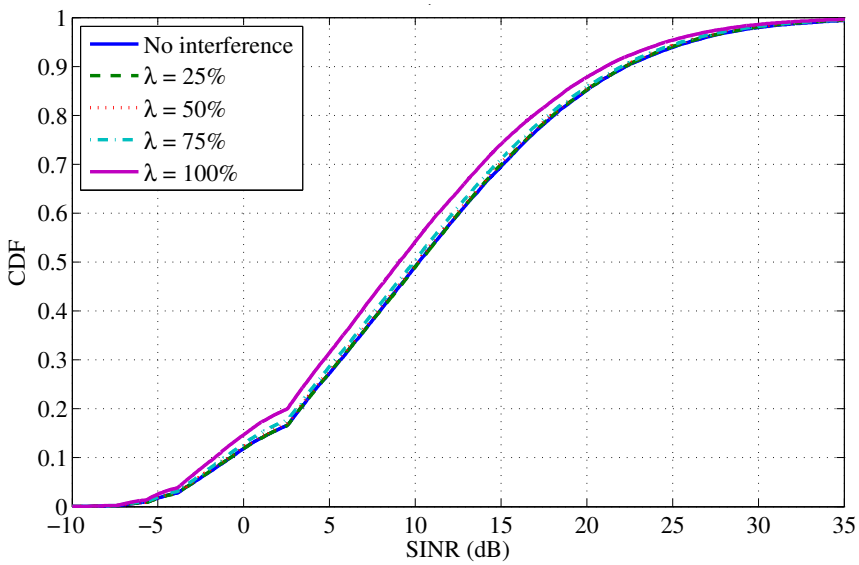

Figure 34 – Comparison of CDFs of the SINRs of the scheduled UEs in the system for the different values of λ when the suboptimal algorithm **is aware of interference**. Required data rate: 288 kbps, $\alpha = 5$.

levels, Figure 35 shows the outage rates for different values cell loading when the suboptimal algorithm **is not aware of interference**. We can notice that the outage rates are considerably high for all the different cell loadings when compared to the scenario without interference, mainly for the highest required rates. For the highest required rate (288 kbps), the outage rate for the case without interference is at approximately 13.5%, while for the case with interference where the cell loading is at 100% we have an outage of 80%, showing a difference of 66.5% between the aforementioned scenarios.

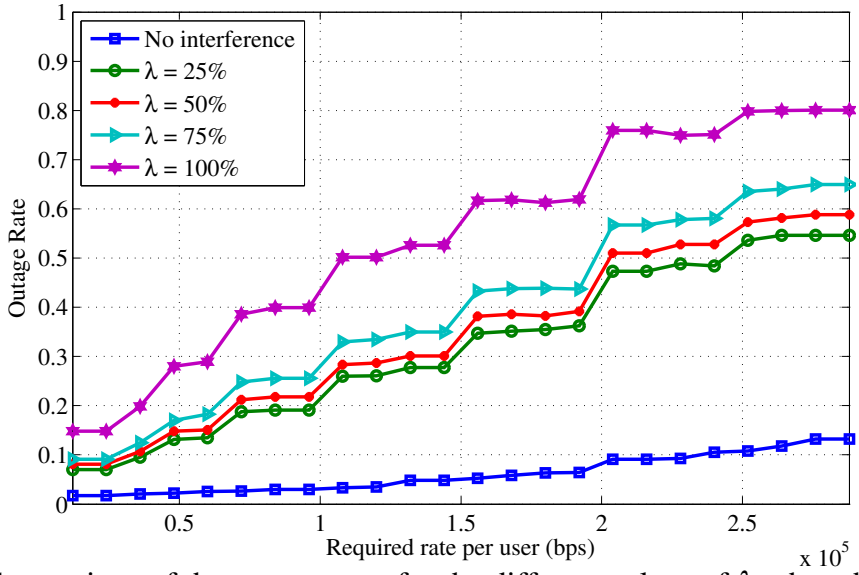

Figure 35 – Comparison of the outage rates for the different values of λ when the suboptimal algorithm **is not aware of interference**, $\alpha = 5$.

Figure 36 shows the outage rates for different values cell loading when the suboptimal algorithm **is aware of interference**. In this figure, differently from the previous one, we can see that for all the different cell loadings, the outage rates remain above 20%. Comparing Figures 35 and 36, we can see that the interference knowledge by the suboptimal algorithm presents a considerable gain to the system performance. If we take the case with 100% of interference in both figures, at the required rate of 288 kbps, we can see that, for the case where the algorithm is aware of interference, the outage rate is approximately 18%, while for the case where the algorithm is not aware of interference the outage rate is 80%, a difference of 62%. From those figures, we can assure that the interference knowledge by the suboptimal algorithm can increase the system performance.

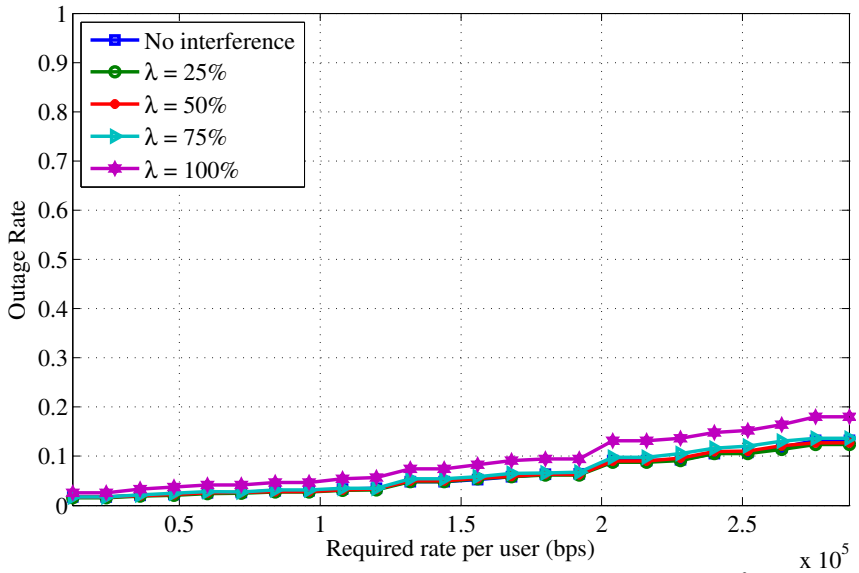

Figure 36 – Comparison of the outage rates for the different values of λ when the suboptimal algorithm **is aware of interference**, $\alpha = 5$.

We also want to evaluate how the power constraints affect our system. All the previous figures showed the case where the α parameter is set to 5, and Figure 37 presents the CDFs of the SINRs for the three studied scenarios, with the cell loading (λ parameter) in 100%, but with $\alpha = 25$. We can see that all the curves are superimposed, which means that, for this case, the system is basically dominated by noise, once the two scenarios with interference present the same behavior as the scenario without interference.

Figure 38 shows the outage rates for the same case described above. Firstly, we can see that the outage rates for all the scenarios start at 30% or above this, which means that the suboptimal algorithm was not able to solve the CRM problem in any case. Once we want to satisfy 12 of 14 UEs, the maximum outage rate possible to occur when the algorithm solves the

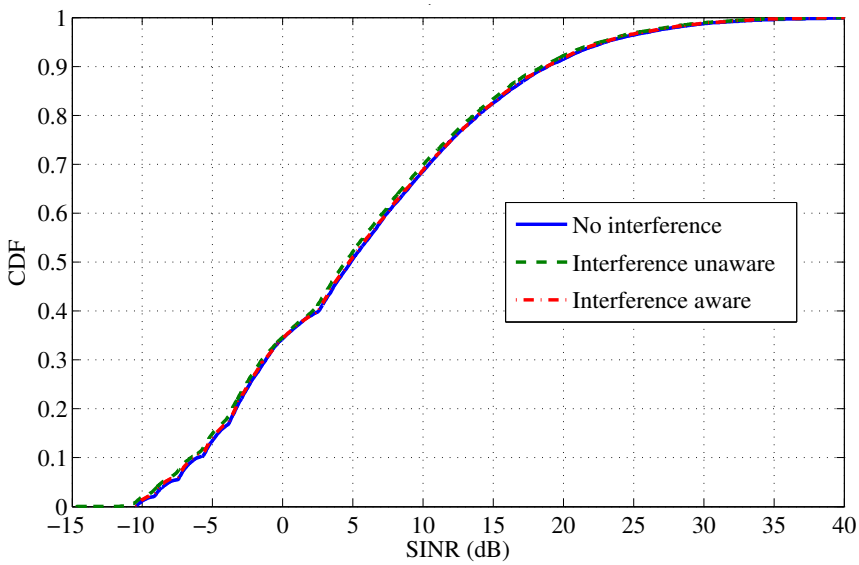

Figure 37 – Comparison of the CDFs of the SINRs of the scheduled UEs for the three scenarios. Required data rate: 288 kbps, $\lambda = 100\%$, $\alpha = 25$.

problem is approximately 14.28%, less than the half of the outage rates presented in the figure. Even with those bad conditions, we can notice that, with the interference knowledge, we have a difference of 4% from the reference scenario (without interference), while the difference from the case where the suboptimal algorithm is not aware of interference to the reference scenario is 16%. Comparing the results in this figure to Figures 35 and 36, which have the α parameter set to 5, we can see that we have a decrease in the overall system performance, due to the reduction in the RBs' subcarriers power. This was expected, since the subcarriers power takes an important part in the SNR/SINR calculation.

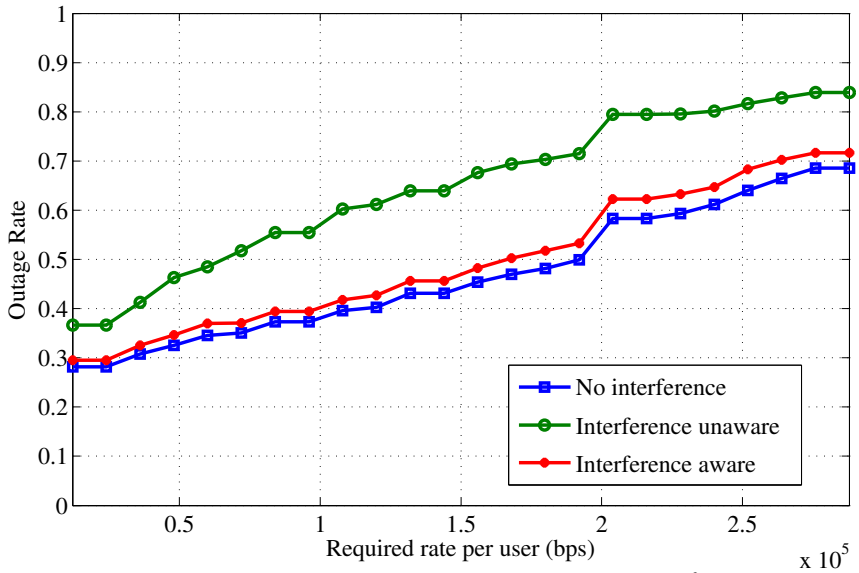

Figure 38 – Comparison of the outage rates for the three scenarios, $\lambda = 100\%$, $\alpha = 25$.

In order to prove that the system is dominated by noise for the case where we set

the α parameter to the highest value, in Figure 39 we show the CDFs of the interference power ($\zeta + \xi$), denominator of (4.6), without the noise) for the scenario where the suboptimal algorithm is aware of interference, for different values of the α parameter. This figure shows that, for the case where $\alpha = 25$, the interference power is considerably lower than the noise power. We can also see that, for this case, in almost 100% of the cases the interference power will be considerably lower than the noise power, while for the case where $\alpha = 5$, approximately in 90% percent of the cases the interference power will be lower than the noise power. However, for the latter case, we can see that the interference power is higher than the values presented for the first case, and this difference is reflected in the SINR and outage curves previously presented for both cases.

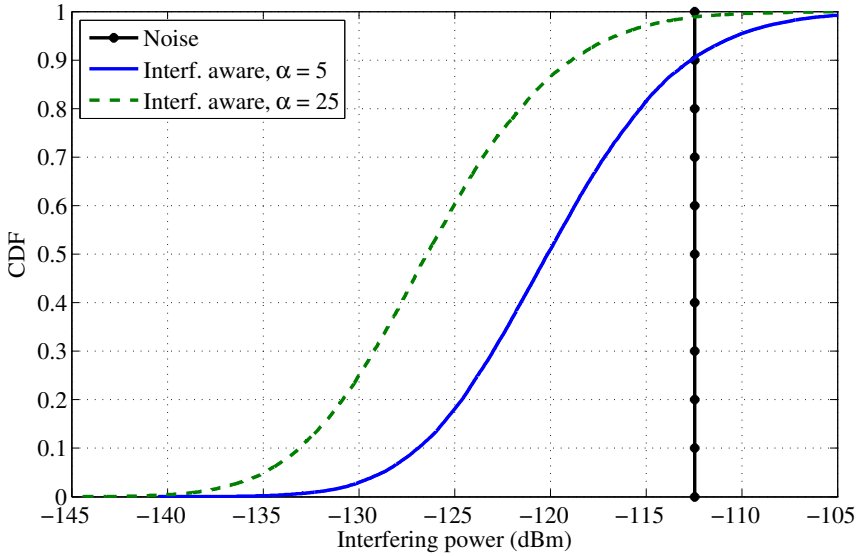

Figure 39 – Comparison of the CDFs of the interference power of the scheduled UEs for the scenario where the algorithm **is aware of interference** for different values of α. Required data rate: 288 kbps, $\lambda = 100\%$.

The other evaluation we performed was related to the MCSs usage. Figures 40 and 41 present the MCSs usage for the three studied scenarios and for cases where the cell loading is at 100% and where $\alpha = 5$ and $\alpha = 25$, respectively.

For the case where $\alpha = 5$, we can see that the highest MCSs are used more often than the lower ones. This was expected, since with more power in the system, higher would be the SNR/SINR values, thus leading the link adaptation function to choose the highest MCSs. Comparing the three scenarios in this case, we can notice that the higher MCS are used more often by the scenarios without interference and the one with interference knowledge, while the lowest MCSs are used more often for the scenario without the knowledge of interference. The

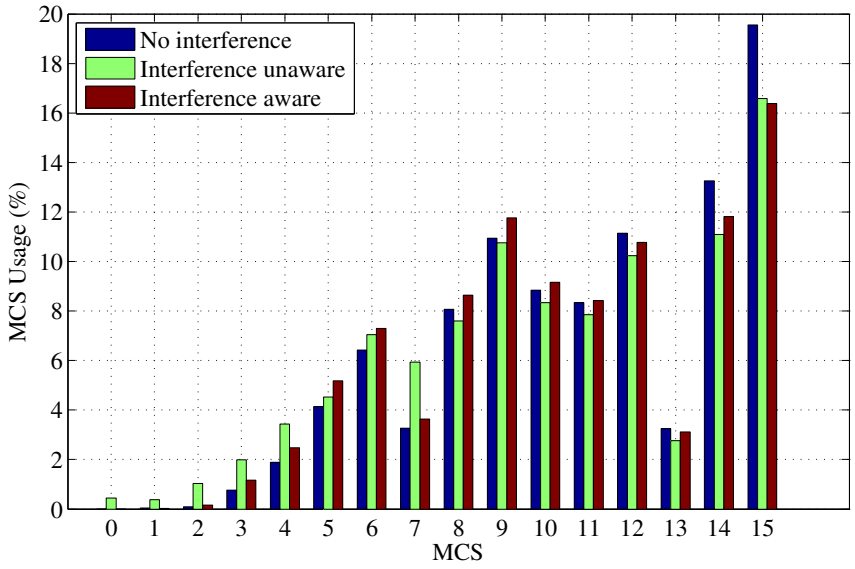

Figure 40 – MCS usage. Required data rate: 288 kbps, $\alpha = 5$, $\lambda = 100\%$.

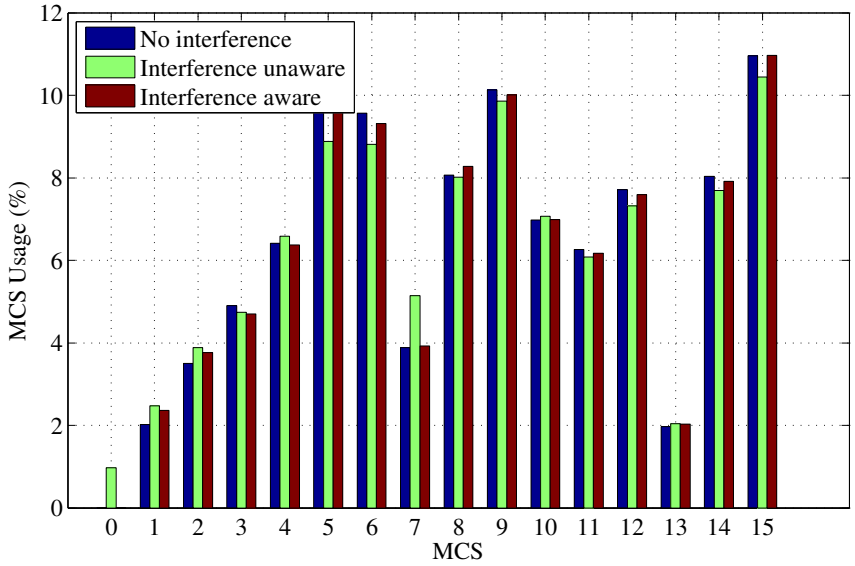

Figure 41 – MCS usage. Required data rate: 288 kbps, $\alpha = 25$, $\lambda = 100\%$.

conclusions to this behavior are analogous to the cases showed before: once the suboptimal algorithm is aware of interference, it can perform a better allocation, which is reflected in the use of the highest MCSs, while for the case where the algorithm is not aware of interference, the allocation is done in a blind way, which is represented in the figure by the choice of the lowest MCSs.

When $\alpha = 25$, we can see that the lowest MCSs are been used more if compared to the previous case. This also happens due to the link adaptation function mapping, but in this case, once we have less power per subcarrier, lower will be the SNR/SINR values, thus contributing to the option for the lower MCSs. We can also notice in this figure a more balanced choice of MCSs, when comparing the three evaluated scenarios. This result reflects the behavior seen in

Figure 37, where the SINR curves were superimposed.

In both figures, we can see the MCS zero. This MCS in fact represents the cases where we had a transmission error. Firstly, we can notice that this MCS happens only for the case where the suboptimal algorithm is not aware of interference. This was expected, since during the allocation phase the suboptimal algorithm is completely blind in relation to interference, which does the algorithm calculate a possible transmit data rate for the UEs, when, in fact, this will not be the real data rate served to those UEs, because of the interference available in the system. Also, we can notice that in Figure 40, the transmission errors (MCS = 0) only occur in 0.44% of the cases, while in Figure 41 we can see that the same errors occur in 1% of the cases — more than the double of the previous case — showing that as lower is the peak power used, as higher are the transmission errors.

4.4 Partial Conclusions

In this chapter we presented the suboptimal solution to the CRM problem to the UL direction, for SU single antenna arrangement, and also its behavior in the presence of interference, as also in the presence of power constraints.

The results showed that, as we increase the cell loading (the amount of interfering links in the cell), the system performance decreases. However, we also could see that we can overcome this issue if the suboptimal algorithm is aware of the interference present in the system. Related to the power constraints, we could see that the better results were acquired when α parameter was set to 5, due to the fact that, with this power level, the RBs could use more power, thus increasing the system performance. However, for the case where the α parameter was set to 25, we could see that the system performance decreased, mainly because the RBs have less power to transmit. We could also see that, for this case, and as we increased the cell loading, we could see that the system was dominated by noise, which resulted in superimposed SINRs curves.

5 CONCLUSIONS AND FUTURE WORK

This thesis presented the evaluation of the RRA suboptimal algorithms for the SU case proposed in (LIMA *et al.*, 2012b; LIMA, 2012) in a scenario subjected to inter-cell interference. We also evaluated the impact of RB aggregation for the DL, and the power limitation for the UL, both in conjunction with interference.

In Chapter 1 we presented the motivation and the important concepts used during this work, as also the state of the art in relation to RRA algorithms in an inter-cell interfering scenario. As we could see in this chapter, this is an aspect that must be considered in the modern wireless cellular systems, as it can cause considerable losses in the system performance.

Chapter 2 was devoted to the system modeling and the description of the suboptimal algorithms. We also presented the CRM problem and the suboptimal framework proposed to solve it, as well as the interference modeling and the RB aggregation.

In Chapter 3 we presented the suboptimal algorithm used to solve the CRM problem for the DL in a scenario subjected to inter-cell interference and RB aggregation. We evaluated three different scenarios: one, with only inter-cell interference in the system, another, with only RB aggregation, and the last one was a combination of the two mentioned before. For the case where there is only inter-cell interference in the system, the results showed that, as we increase the cell loading (the amount of interfering links in the cell), the system performance decreases. However, we also could see that we can overcome this issue if the suboptimal algorithm is aware of the interference present in the system. Related to the RB aggregation, we could see that the worse performance occurs when the RBs are aggregated. For both cases, we also could see that in the presence of multiple antennas in the transmitter and/or receiver, we have an increase in the system performance, which occurs due to the spatial diversity exploited by the multiple antennas. For the case where we combine the effects of inter-cell interference and RB aggregation, we could see that the system performance also tends to decrease. The worst case happens when there is interference and the suboptimal algorithm is not aware of it, together with RB aggregation. But again, if the suboptimal algorithm has knowledge about the interference, and if there is multiple antennas in the transmitter/receiver, then the system performance stays at good levels.

In Chapter 4 we presented the suboptimal algorithm used to solve the CRM problem for the UL in a scenario subjected to inter-cell interference and power constraints. We also presented the algorithm running with link adaptation, where we modeled the use of discrete MCS in order to map the UEs SNR/SINR to the transmit data rate, different from what was

shown in (LIMA, 2012), where the author considered the link adaptation performed based on the upper bound Shannon capacity (CIOFFI, 1991). The results were as expected, showing that if we provide the interference knowledge to the suboptimal algorithm, it will behave better than if did not have this knowledge. We could also see that, when we increased the cell loading, the system performance decreased. Regarding the power constraints, we showed that when we increase the denominator of the peak power function, the system is basically dominated by noise, and we could see that through the superimposed acSNR/SINR curves presented. For the MCSs usage, we showed that when the denominator of the peak power function was set to the smallest value, the higher MCSs where chosen more often, differently from what happened when the denominator of the peak power function was set to the highest value, where we could see the lowest MCSs been chose as often as the highest ones. Also, we could see that, when the suboptimal algorithm is not aware of interference, we could see more transmission error, showed as the MCS 0.

During the development of this work, we noticed that there are some interesting aspects that could be investigated. We list those aspects as follows:

- Since we consider perfect CSI at the receiver and transmitter, we could have a more realistic scenario (or at least something close to it), with the modeling of an error in the SINR estimation performed by the suboptimal algorithm. This would probably decrease the absolute system performance, but otherwise we would have a system modeled more like a real one.
- For the RB aggregation evaluated in Chapter 3, we only evaluated the suboptimal algorithm with aggregation type 0. We could also test the suboptimal solution for the aggregations types 1 and 2, once they are also part of the 3GPP standard for the DL case.
- The use of power control methods for the UL, since nowadays the battery consumption of mobile devices is a concerning matter.
- Allow the use of multi-frequency UEs in the UL, instead of the single 5 Mhz band used for our UL evaluations. With this, we could check if the suboptimal solution proposed would be affected anyhow.
- More traffic models could be used for both DL and UL evaluations. We could evaluate the suboptimal algorithm in a scenario with HyperText Transfer Protocol (HTTP) streaming and subject to interference, for example, since this would be a challenging scenario to which the algorithm should deal.

REFERENCES

3GPP. ***Physical layer aspect for evolved Universal Terrestrial Radio Access (UTRA)***. 2006. Disponível em: <https://www.3gpp.org/ftp/Specs/archive/25_series/25.814/>. Acesso em: 10 mar. 2013.

3GPP. ***Bandwidth saving at Nb interface with IP transport***. 2007. Disponível em: <https://bit.ly/2PVO5VL>. Acesso em: 03 jan. 2013.

3GPP. ***Evolved Universal Terrestrial Radio Access (E-UTRA); Further advancements for E-UTRA physical layer aspects***. 2010. Disponível em: <https://bit.ly/2NH162t>. Acesso em: 11 mar. 2013.

3GPP. ***Evolved Universal Terrestrial Radio Access (E-UTRA); Physical channels and modulation***. 2010. Disponível em: <https://bit.ly/2WJRyIc>. Acesso em: 28 mar. 2013.

3GPP. ***Evolved Universal Terrestrial Radio Access (E-UTRA); Physical layer procedures***. 2010. Disponível em: <https://bit.ly/36yE4n8>. Acesso em: 15 mai. 2013.

3GPP. ***Evolved Universal Terrestrial Radio Access (E-UTRA); Base Station (BS) radio transmission and reception***. 2012. Disponível em: <https://bit.ly/36CUPOb>. Acesso em: 07 nov. 2012.

3GPP. ***Evolved Universal Terrestrial Radio Access (E-UTRA) and Evolved Universal Terrestrial Radio Access Network (E-UTRAN); Overall description; Stage 2***. 2013. Disponível em: <https://bit.ly/33mJOyc>. Acesso em: 18 mar. 2013.

ALMALFOUH, S.; STUBER, G. Interference-Aware Radio Resource Allocation in OFDMA-Based Cognitive Radio Networks. **IEEE Transactions on Vehicular Technology**, IEEE, v. 60, p. 1699–1713, 2011. DOI: 10.1109/TVT.2011.2126613.

BHALERO, R. **3G to 4G Core Network Migration**. 2010. Disponível em: <https://pdfs.semanticscholar.org/f045/c6bec53816bb8343944bb50b2d96c321e399.pdf>. Acesso em: 05 mar. 2013.

BLUMENSTEIN, J.; IKUNO, J. C.; J., P.; RUPP, M. Simulating the Long Term Evolution Uplink Physical Layer. In: **Proceedings of the ELMAR-2011, Zadar, Croatia, 14-16 Sept. 2011**. [S.l.]: IEEE, 2011. p. 141–144.

BOHGE, M.; GROSS, J.; WOLISZ, A.; MEYER, M. Dynamic Resource Allocation in OFDM Systems: An Overview of Cross-Layer Optimization Principles and Techniques. **IEEE Network**, IEEE, v. 21, p. 53–59, 2007. DOI: 10.1109/MNET.2007.314539.

CALABRESE, F. D. **Scheduling and Link Adaptation for Uplink SC-FDMA Systems**. Tese (PhD in Electronic Systems) — Faculty of Engineering, Science and Medicine, Department of Electronic Systems, Aalborg University, Aalborg, 2009.

CIOFFI, J. M. A Multicarrier Primer. **ANSI Contribution T1E1.4/91-157**, ANSI, 1991.

DAHLMAN, E.; PARKVALL, S.; SKOLD, J. **4G: LTE/LTE-Advanced for Mobile Broadband**. 1st. ed. Orlando, FL, USA: Academic Press, Inc., 2011. ISBN 012385489X, 9780123854896.

DECHENE, D. J.; SHAMI, A. Energy Efficient Resource Allocation in SC-FDMA Uplink with Synchronous HARQ Constraints. In: **Proceedings of the 2011 IEEE INTERNATIONAL CONFERENCE ON COMMUNICATIONS (ICC), Kyoto, Japan, 5-9 June 2011**. [S.l.]: IEEE, 2011. p. 1–5. DOI: 10.1109/icc.2011.5962569.

FAN, J.; LI, G. Y.; YIN, Q.; LI, L. Multiuser Pairing and Resource Allocation with Interference Avoidance for SC-FDMA Cellular Systems. In: **Proceedings of the IEEE GLOBAL COMMUNICATIONS CONFERENCE (GLOBECOM), Anaheim, CA, USA, 3-7 Dec. 2012**. [S.l.]: IEEE, 2012. p. 4993–4997. DOI: 10.1109/GLOCOM.2012.6503911.

FRANK, P.; MULLER, A.; DROSTE, H.; SPEIDEL, J. Cooperative Interference-Aware Joint Scheduling for the 3GPP LTE Uplink. In: **Proceedings of the IEEE 21st INTERNATIONAL SYMPOSIUM ON PERSONAL INDOOR AND MOBILE RADIO COMMUNICATIONS (PIMRC), Istanbul, Turkey, 26-30 Sept. 2010**. [S.l.]: IEEE, 2010. p. 2216 – 2221. DOI: 10.1109/PIMRC.2010.5671678.

GHADERI, M.; BOUTABA, R. Towars all-IP Wireless Networks: Architectures and Resource Management Mechanism. **International Journal of Wireless and Mobile Computing**, Inderscience, v. 2, n. 4, p. 263–274, 2007. DOI: 10.1504/IJWMC.2007.016720.

GHOSH, A.; WOLTER, D. R.; ANDREWS, J. G.; CHEN, R. Broadband Wireless Access with WiMax/802.16: Current Performance Benchmarks and Future Potential. **IEEE Communications Magazine**, IEEE, v. 43, n. 2, p. 129 –136, 2005. DOI: 10.1109/MCOM.2005.1391513.

HOLMA, H.; TOSKALA, A.; AHO, K. Ranta; PIRSKANEN, J. High-Speed Packet Access Evolution in 3GPP Release 7. **IEEE Communications Magazine**, IEEE, v. 45, p. 29–35, 2007. DOI: 10.1109/MCOM.2007.4395362.

HOSEIN, P. Uplink Power Control and Interference Management for the support of QoS Applications. In: **Proceedings of the IEEE 21st INTERNATIONAL SYMPOSIUM ON PERSONAL INDOOR AND MOBILE RADIO COMMUNICATIONS (PIMRC), Istanbul, Turkey, 26 - 30 Sept. 2010**. [S.l.]: IEEE, 2010. p. 1390–1394. DOI: 10.1109/PIMRC.2010.5671997.

ITU. **The World in 2013**. 2013. Disponível em: <https://www.itu.int/en/ITU-D/Statistics/Documents/facts/ICTFactsFigures2013-e.pdf>. Acesso em: 12 abr. 2013.

ITU-R. **Requirements Related to Technical Performance for IMT-Advanced Radio Interface(s)**. 2008. Disponível em: <https://www.itu.int/pub/R-REP-M.2134>. Acesso em: 02 fev. 2013.

KOSTA, C.; HUNT, B.; QUDDUS, A. U.; TAFAZOLLI, R. On interference avoidance through inter-cell interference coordination (ICIC) based on OFDMA mobile systems. **IEEE Communications Surveys Tutorials**, IEEE, v. 15, n. 3, p. 973 – 995, 2013. DOI: 10.1109/SURV.2012.121112.00037.

LI, L.; WU, G.; XU, H.; LI, G. Y.; FENG, X. Joint Power Control and Resource Allocation for Interference Mitigation in LTE Uplink Systems. In: **Proceedings of the 45th ANNUAL CONFERENCE ON INFORMATION SCIENCES AND SYSTEMS, Baltimore, MD, USA, 23 - 25 March 2011**. [S.l.]: IEEE, 2011. DOI: 10.1109/CISS.2011.5766211.

LIMA, F. R. M. **Maximizing Spectral Efficiency under Minimum Satisfaction Constraints on Multiservice Wireless Networks**. Tese (Doutorado em Engenharia de Teleinformática) — Centro de Tecnologia, Programa de Pós-Graduação em Engenharia de Teleinformática, Universidade Federal do Ceará, Fortaleza, 2012.

LIMA, F. R. M.; BEZERRA, N. S.; SANTOS, R. B.; MACIEL, T.; FREITAS, W. C.; CAVALCANTI, F. R. P. Maximizing Spectral Efficiency with Acceptable Service Provision in Multiple Antennas Scenarios. In: **Proceedings of the 18th EUROPEAN WIRELESS CONFERENCE 2012, Poznan, Poland, 18-20 April 2012**. [S.l.]: VDE, 2012. p. 1–8.

LIMA, F. R. M.; MACIEL, T. F.; FREITAS, W. C.; CAVALCANTI, F. R. P. Resource Assignment for Rate Maximization with QoS Guarantees in Multiservice Wireless Systems. **IEEE Transactions on Vehicular Technology**, IEEE, v. 61, n. 3, January 2012. DOI: 10.1109/TVT.2012.2183905.

LIU, H.; LI, G. **OFDM-Based Broadband Wireless Networks: Design and Optimization**. 1st. ed. [S.l.]: John Wiley & Sons, 2005.

LÓPEZ-PÉREZ, D.; CHU, X.; VASILAKOS, A. V.; CLAUSSEN, H. On distributed and coordinated resource allocation for interference mitigation in self-organizing lte networks. **IEEE/ACM Transactions on Networking**, IEEE, v. 21, n. 4, p. 1145–1158, 2013. DOI: 10.1109/TNET.2012.2218124.

LÓPEZ-PÉREZ, D.; CHU, X.; ZHANG, J. Dynamic Downlink Frequency and Power Allocation in OFDMA Cellular Networks. **IEEE Transactions on Communications**, IEEE, v. 60, p. 2904–2914, 2012. DOI: 10.1109/TCOMM.2012.081412.110705.

MEHLFÜHRER, C.; WRULICH, M.; IKUNO, J. C.; BOSANSKA, D.; RUPP, M. Simulating the Long Term Evolution Physical Layer. In: **Proceedings of the 2009 17th EUROPEAN SIGNAL PROCESSING CONFERENCE, Glasgow, UK, 24-28 Aug. 2009**. [S.l.]: IEEE, 2009. p. 1471–1478.

MYUNG, H. G.; LIM, J.; GOODMAN, D. J. Single Carrier FDMA for Uplink Wireless Transmission. **IEEE Vehicular Technology Magazine**, IEEE, v. 1, n. 3, p. 30–38, 2006. DOI: 10.1109/MVT.2006.307304.

NEMHAUSER, G.; WOSLEY, L. **Integer and Combinatorial Optimization**. 1st. ed. [S.l.]: John Wiley & Sons, 1999.

NOKIA BELL LABS. **Orthogonal Frequency Division Multiplexing**. 1970. US Patent No. US34884555.

PARKVALL, S.; DAHLMAN, E.; FURUSKÄR, A.; JADING, Y.; OLSSON, M.; S., W.; ZANGI, K. LTE-Advanced - Evolving LTE towars IMT-advanced. In: **Proceedings of the 2008 IEEE 68th VEHICULAR TECHNOLOGY CONFERENCE, Calgary, BC, Canada, 21-24 Sept. 2008**. [S.l.]: IEEE, 2008. p. 1–5. DOI: 10.1109/VETECF.2008.313.

PARKVALL, S.; FURUSKÄR, A.; DAHLMAN, E. Evolution of LTE toward IMT-Advanced. **IEEE Communications Magazine**, IEEE, v. 49, n. 2, p. 84 –91, 2011. ISSN 0163-6804. DOI: 10.1109/MCOM.2011.5706315.

PAULRAJ, A.; BIGLIERI, E.; GOLDSMITH, A. **MIMO Wireless Communications**. 1st. ed. [S.l.]: Cambridge University Press, 2007.

PAULRAJ, A.; NABAR, R.; GORE, D. **Introduction to Space-Time Wireless Communications**. 1st. ed. [S.l.]: Cambridge University Press, 2003.

PAULRAJ, A. J.; KAILATH, T. **Increasing capacity in wireless broadcast systems using distributed transmission/directional reception (DTDR)**. 1994. US Patent No. US5345599A.

RAHMAN, M.; YANIKOMEROGLU, H. Inter-Cell Interference Coordination in OFDMA Networks: A Novel Approach Based on Integer Programming. In: **Proceedings of the 71st IEEE VEHICULAR TECHNOLOGY CONFERENCE SPRING, Taipei, Taiwan, 16 - 19 May 2010**. Taipei, Taiwan: IEEE, 2010. p. 1 – 5. DOI: 10.1109/VETECS.2010.5493662.

SESIA, S.; TOUFIK, I.; BAKER, M. **LTE-The UMTS Long Term Evolution: From Theory to Practice**. 2. ed. [S.l.]: John Wiley & Sons, 2011.

SHI, T.; ZHOU, S.; YAO, Y. Capacity of Single Carrier Systems with Frequency-Domain Equalization. In: **Proceedings of the IEEE CIRCUITS AND SYSTEMS SYMPOSIUM ON EMERGING TECHNOLOGIES CONFERENCE: FRONTIERS OF MOBILE AND WIRELESS COMMUNICATION, Shanghai, China, 31 May-2 June 2004**. [S.l.]: IEEE, 2004. v. 2, p. 429 – 432. DOI: 10.1109/CASSET.2004.1321915.

TSE, D.; VISWANATH, P. **Fundamentals of Wireless Communications**. 1st. ed. [S.l.]: Cambridge University Press, 2005.

TU WIEN. **LTE Uplink Link Level Simulator**. Disponível em: <https://bit.ly/2JP9EmQ>. Acesso em: 22 fev. 2013.

UBISSE, A.; VENTURA, N. Modeling a Link Level Simulator for Long Term Evolution Uplink. In: **Proceedings of the SATNAC, East London, UK, 4-7 September 2011**. [S.l.]: SATNAC, 2011. p. 1–5.

WANNSTROM, J. **LTE-Advanced**. 2013. Disponível em: <https://www.3gpp.org/technologies/keywords-acronyms/97-lte-advanced>. Acesso em: 21 jul. 2013.

WESEMANN, S.; RAVE, W.; FETTWEIS, G. Decentralized Intercell Interference Coordination for Fair Resource Allocation in Large-Scale Networks. In: **Proceedings of the 2012 INTERNATIONAL ITG WORKSHOP ON SMART ANTENNAS (WSA), Dresden, Germany, 7-8 March 2012**. [S.l.]: IEEE, 2012. p. 201–208. DOI: 10.1109/WSA.2012.6181207.

WONG, I. C.; OTERI, O.; MCCOY, W. Optimal Resource Allocation in Uplink SC-FDMA Systems. **IEEE Transactions on Wireless Communications**, IEEE, v. 8, n. 5, p. 2161–2165, 2009. DOI: 10.1109/TWC.2009.061038.

YU, Y.; DUTKIEWICZ, E.; H., X.; MUECK, M. Downlink resource allocation for next generation wireless networks with inter-cell interference. **IEEE Transactions on Wireless Communications**, IEEE, v. 12, n. 4, p. 1783 – 1793, 2013. DOI: 10.1109/TWC.2013.030413.120760.

ZHANG, X.; WANG, Y.; WANG, W. Capacity Analysis of Adaptive Multiuser Frequency-Time Domain Radio Resource Allocation in OFDMA Systems. In: **Proceedings of the IEEE INTERNATIONAL SYMPOSIUM ON CIRCUITS AND SYSTEMS, Island of Kos, Greece, 21-24 May 2006**. [S.l.]: IEEE, 2006. p. 5676–5679.